# *DROSOPHILA* NON-MUSCLE MYOSIN II BIPOLAR FILAMENT FORMATION: IMPORTANCE OF CHARGED RESIDUES AND SPECIFIC DOMAINS FOR SELF-ASSEMBLY

by

DEREK LEE RICKETSON

A DISSERTATION

Presented to the Department of Chemistry
and the Graduate School of the University of Oregon
in partial fulfillment of the requirements
for the degree of
Doctor of Philosophy

June 2009

## University of Oregon Graduate School

## Confirmation of Approval and Acceptance of Dissertation prepared by:

Derek Ricketson

Title:

"Drosophila Non-Muscle Myosin II Bipolar Filament Formation: Importance of Charged Residues and Specific Domains For Self-Assembly"

This dissertation has been accepted and approved in partial fulfillment of the requirements for the Doctor of Philosophy degree in the Department of Chemistry by:

Tom Stevens, Chairperson, Chemistry
Kenneth Prehoda, Advisor, Chemistry
J. Andrew Berglund, Member, Chemistry
Christopher Doe, Member, Biology
Karen Guillemin, Outside Member, Biology

and Richard Linton, Vice President for Research and Graduate Studies/Dean of the Graduate School for the University of Oregon.

June 13, 2009

Original approval signatures are on file with the Graduate School and the University of Oregon Libraries.

An Abstract of the Dissertation of

Derek Lee Ricketson for the degree of Doctor of Philosophy

in the Department of Chemistry to be taken June 2009

Title: *DROSOPHILA* NON-MUSCLE MYOSIN II BIPOLAR FILAMENT FORMATION: IMPORTANCE OF CHARGED RESIDUES AND SPECIFIC DOMAINS FOR SELF-ASSEMBLY

Approved: ______________________________________

Dr. Kenneth Prehoda

Non-muscle myosin II generates contractile forces for processes such as cytokinesis, motility, and polarity. Contractility requires assembly of myosin molecules into bipolar mini-filaments through electrostatic interactions between coiled-coil tail domains of the heavy chains. Analyses of myosin II from various organisms have revealed "assembly domains" within the C-terminal portion of the tail domain that mediate filament formation. However, it has been unclear precisely how assembly domains interact with one another, or otherwise contribute to tail-tail interactions, to form the bipolar mini-filament structure.

To understand tail domain interactions, we first identified a 90-residue region (1849-1940) of the *Drosophila* non-muscle myosin II tail domain that was necessary and sufficient for filament formation, using salt-dependent solubility and a novel fluorescence energy transfer assay. We identified residues within this "assembly domain" that were critical for filament assembly by analyzing the effect of point mutations. We found that single point mutations in specific positively charged regions completely disrupt filament assembly. Surprisingly, none of the negatively charged regions within the assembly domain are required for assembly. Most of the mutations in positively charged residues that disrupted filament assembly clustered within a 15-residue segment (1880-1894) that appears to form a critical interaction surface. Using this information, along with known geometrical constraints and electrostatic calculations, we constructed a structural model of the bipolar mini-filament. This model features one favored anti-parallel tail overlap and multiple slightly less stable alternative overlaps. The ability of the positive segment to interact with multiple negative regions explains the lack of required negatively charged residues in the assembly domain. To our knowledge, this structural model of the non-muscle myosin II bipolar filament is consistent with all physical observations and provides a framework for understanding the detailed mechanism by which this fundamental cellular structure is generated.

This dissertation contains previously published and unpublished co-authored material.

# CURRICULUM VITAE

NAME OF AUTHOR: Derek Lee Ricketson

PLACE OF BIRTH: Hattiesburg, MS

DATE OF BIRTH: July 14, 1980

GRADUATE AND UNDERGRADUATE SCHOOLS ATTENDED:

University of Oregon, Eugene, OR

Mississippi State University, Mississippi State, MS

Jones County Junior College, Ellisville, MS

DEGREES AWARDED:

Doctor of Philosophy, Biochemistry, 2009, University of Oregon

Bachelor of Science, Biochemistry, 2002, Mississippi State University

Associate of Arts, Liberal Arts, 2000, Jones County Junior College

AREAS OF SPECIAL INTEREST:

Cytoskeleton and Motor Proteins

Protein Chemistry

Macromolecular Assemblies

GRANTS, AWARDS AND HONORS:

Molecular Biology and Biophysics Training Grant, NIH, 2005–2009

PUBLICATIONS:

Ricketson D., Frei R., Fewkes N., Prehoda K. E. (2009). Mechanism of *Drosophila* non-muscle myosin II filament formation. Submitted for publication.

Liu, S. L., Fewkes, N., Ricketson, D., Penkert, R. R., and Prehoda, K. E. (2008). Filament-dependent and -independent localization modes of Drosophila non-muscle myosin II. J Biol Chem 283, 380-387.

Ricketson D., Hostick U., Fang L., Yamamoto K. R., Darimont B. D. (2007). A conformational switch in the ligand-binding domain regulates the dependence of the glucocorticoid receptor on Hsp90. J Mol Biol 368, 729-741.

Fang L., Ricketson D., Getubig L., Darimont B. (2006). Unliganded and hormone-bound glucocorticoid receptors interact with distinct hydrophobic sites in the Hsp90 C-terminal domain. Proc Natl Acad Sci U S A 103, 18487-18492.

# ACKNOWLEDGMENTS

First and foremost, I wish to express my sincere gratitude to my advisor, Dr. Ken Prehoda, for his patient guidance and encouragement with the development of both my project and my approach to scientific problems. I would also like to thank my committee members for helpful discussions and support throughout my graduate career. Special thanks go to Dr. Tom Stevens and Dr. Andy Berglund for their insightful career advice and support during my transition between laboratories late in my graduate career. My fellow lab members, both past and current, have been instrumental in the completion of this work and I thank them for providing a great lab environment. A special thanks goes to Dr. Jana Jacobson for a list of things that is too long to include here.

I would be remiss if I didn't give a hardy thanks to all of my friends and family who have supported me throughout my time in graduate school. Mom and Dad, I am truly grateful for your understanding and support. I would also like to thank my sister Melissa, my father and mother-in-law John and Kathy Craig, grandparents all around, aunts, uncles, cousins, and my friend Butch Bailey for all of their support and encouragement. I would also like to thank Dr. Jill Murray and Dr. Dennis Hore specifically for their great friendship and for introducing me to my wife.

Finally, my greatest thanks goes to my wife Dr. Erin Craig Ricketson for listening to complaints, encouraging me, distracting me, and generally getting me through graduate school.

To all of my teachers, professors, and community leaders for being the village.

# TABLE OF CONTENTS

Chapter Page

I. INTRODUCTION ........ 1

Myosin Superfamily ........ 2

Myosin Domain Architecture and Adaptations ........ 5

Regulation of Myosin Activity ........ 10

Non-Muscle Myosin II ........ 15

Remaining Questions ........ 19

II. FILAMENT-DEPENDENT AND -INDEPENDENT LOCALIZATION MODES OF *DROSOPHILA* NON-MUSCLE MYOSIN II ........ 21

Introduction ........ 21

Results ........ 24

The Zipper Tail Domain Contains a 90-Residue Filament "Assembly Domain" ........ 24

The Zipper Tail Domain Specifies Cortical Localization in *Drosophila* S2 Cells ........ 30

The Zipper Filament Assembly Domain Is Not Recruited to the Cortex ........ 32

Interphase Cortical Localization Does Not Require the Assembly Domain ........ 32

Cleavage Furrow Localization Requires the Filament Assembly Domain ........ 35

Chapter Page

Discussion .......... 37

Filament Assembly Determinants .......... 37

Localization Determinants .......... 39

Materials and Methods .......... 41

Molecular Cloning, Protein Expression and Purification .......... 41

Assembly Assays .......... 42

Cell Culture and Transfection .......... 42

Immunofluorescence and Imaging .......... 43

Time-Lapse Imaging .......... 44

Bridge to Chapter III .......... 44

III. MECHANISM OF ASSEMBLY DOMAIN MEDIATED TAIL-TAIL INTERACTIONS IN NON-MUSCLE MYOSIN II FILAMENT ASSEMBLY .......... 45

Introduction .......... 45

Results .......... 48

Identification of Assembly Domain Elements Critical for Filament Assembly .......... 48

Identification of Residues Critical for Bipolar Filament Assembly .......... 52

Role of Negatively Charged Residues in Bipolar Filament Assembly .......... 56

Role of Binary Tail-Tail Interactions in the Formation of Bipolar Minifilaments .......... 63

Chapter Page

Discussion .......... 67

Defining the Critical Elements Within the Assembly Domain That Are Necessary for Filament Assembly .......... 68

Function of the Assembly Domain in Tail-Tail Interactions .......... 69

Full-Length Tail Domain Interactions .......... 72

Three-Dimensional Structural Model of Zipper Filaments .......... 75

Materials and Methods .......... 78

Cloning, Overexpression, and Purification .......... 78

Filament Assembly Assay .......... 78

Electron Microscopy .......... 79

Construction of Zipper Tail Structural Model and Electrostatic Calculations .......... 79

IV. CONCLUDING REMARKS .......... 81

BIBLIOGRAPHY .......... 88

# LIST OF FIGURES

Figure Page

1. Identification of a Zipper Filament Assembly Domain ........ 27
2. The Zipper Filament-Assembly Domain ........ 29
3. Zipper Localization Determinants in *Drosophila* S2 Cells ........ 31
4. An Interphase Cortical-Targeting Domain in the Zipper Tail ........ 33
5. The Zipper Cleavage Furrow-Targeting Domain ........ 36
6. Identification of Conserved Subregions of the Assembly Domain That Are Important for Filament Assembly ........ 51
7. Identification of Residues That Are Important for Zipper Filament Assembly .... 54
8. Structural Model and Electrostatic Calculations of 1744-1968 Interactions ........ 59
9. Identification of Upstream, Negatively Charged Residues that Participate in Filament Assembly ........ 62
10. Model for Full-length Tail Domain Interactions and Implications for Zipper Filament Geometry ........ 66
11. Theoretical Three-Dimensional Model of the Zipper Bipolar Minifilament ........ 74

# CHAPTER I

# INTRODUCTION

The cytoskeleton is a dynamic structure within the cytoplasm of all cells that is the basis for the internal organization, structure, and mechanical properties of the cell. The eukaryotic cytoskeleton is comprised of three major types of protein polymers, which are microfilaments, intermediate filaments, and microtubules. Each of these cytoskeleton systems serves specific functions necessary for the cell to function properly. Microfilaments are polymers of actin subunits that form a dense, crosslinked meshwork of filaments beneath the plasma membrane known as the actin cortex. The actin cortex is responsible for resistive tension, cell shape control, and mechanical support for cell-cell and cell-matrix junctions. These activities not only require the mechanical resistance of actin filaments, but also force production.

Actin based force production occurs via two basic mechanisms. The first is the production of a protrusive force that is generated from the polymerization of the actin filaments. This mode utilizes a Brownian ratchet mechanism of force production, where thermal motion acts on a diffusional object, and the addition of actin subunits biases that diffusion in a directional manner, thus acting as a pawl in a ratchet. The force required for membrane protrusions during endocytosis and cell motility is generated by this mechanism. The other mode of force production involves the movement of motor proteins along actin filaments. Actin based motors, known as myosin, move unidirectionally along actin filaments according to the filaments inherent polarity. The motors can then actively move objects in relation to the actin filaments to produce force. Myosins utilize a power stroke mechanism of force production, in which the ATP hydrolysis cycle is tightly coupled to a deterministic conformational change that drives motion (for review see Howard, 2001; Geeves and Holmes, 1999). Contractile force production necessary for cortical rigidity, morphogenesis, and cytokinesis is generated by class II myosin acting on oppositely polarized actin.

## Myosin superfamily

Myosins constitute a large superfamily of actin-based motor proteins. Motor proteins are so named because they are enzymes that convert chemical energy, in the form of ATP, into force production needed for mechanical work (Sellers, 2000). The superfamily consists of 15–18 classes, many with multiple isoforms, which were identified by the conserved motor domain that has been shown to interact with actin, hydrolyze ATP and produce movement of actin filaments (Sellers, 2000; Berg et al., 2001; Thompson and Langford, 2002).

Much of what is known about myosin enzymatic activity came from the study of class II myosin. Myosin II, the best-characterized myosin, is referred to as conventional myosin since it was the first and only class of myosin known for decades. Prior to recombinant protein technology and other modern molecular techniques, biochemical characterization of proteins was usually reserved for enzymes that could be easily purified from tissue on a large scale. Myosin II was under intense investigation during this period because it could be obtained in large quantities (makes up the majority of cellular protein in muscle), and striated muscle contraction was one of the best-understood physiological processes at this time (Pollard, 2000; Huxley, 2000; Cooke, 2004).

Myosin generated motility involves a cyclic cross-bridging cycle, which is inextricably linked to the ATP hydrolysis cycle in the motor domain. The nucleotide state throughout the ATPase cycle is linked to both the motor domain's affinity for actin and force producing conformational changes (De La Cruz and Ostap, 2004). The ATPase cycle consist of six nucleotide-linked states. Briefly, the cycle starts with low actin affinity, pre-force generating intermediates of ATP bound and hydrolyzed. ATP binding detaches the myosin motor from actin, and hydrolysis of ATP to ADP.Pi results in a conformational change where myosin is "cocked". Upon rebinding actin, the inorganic phosphate resulting from hydrolysis is released, which leads to the force-generating power stroke conformational change. The last portion of the cycle contains high actin affinity, force-bearing intermediates with ADP bound or no nucleotide bound. The absence of nucleotide in the final step allows ATP to bind and begin the cycle once more (De La Cruz and Ostap, 2004).

It is generally accepted that the force production mechanism utilized by myosin comes from a conformational change termed a power stroke, analogous to that of an engine (Cooke, 2004). However, thermally driven models have been suggested as a more appropriate description for motor proteins that act on microtubule tracks (Amos, 2008). Whereas microtubule and actin based molecular motors were thought to work by these different mechanisms, it is now known that they share a common core structure and force transduction mechanisms (Vale and Milligan, 2000). Thus, aspects of both thermally driven and power stroke mechanisms are utilized for motor protein movement, and the debate between the validity of each of these mechanisms is mostly semantic.

Despite the fact that the bulk of the characterization of myosin has occurred on a small number of classes, the incredible diversity of myosin classes suggest a high degree of specialization for specific cellular tasks. All characterized myosins share a common ATPase and force transduction mechanism (Sellers, 2000; Berg et al., 2001). However, now its known that kinetic and equilibrium parameters within the ATPase cycle can be tuned for different mechanical properties that are useful in different contexts (De La Cruz and Ostap, 2004). In a similar manner, the basic myosin domain architecture has evolved in different classes and isoforms for adaptation to different cellular tasks (Sellers, 2000). Finally, regulation of myosin activity to ensure force generation at appropriate cellular sites at the proper time is critical for the execution of complex cellular processes.

Myosin II and myosin V are the best-characterized examples of conventional and unconventional myosins respectively. Each myosin displays three canonical functional domains and serves as good examples for domain architecture adaptation. Myosin II or conventional myosin was discovered for its activity in generating contractile forces in skeletal muscle. A large volume of work has been done on the mechanisms of muscle contraction and the role of myosin II in generating the forces necessary for contraction

(Pollard, 2000; Cooke, 2004). More recently, the non-muscle isoform of myosin II has received increased attention for its role in complex cellular behaviors such as cell migration, organ morphogenesis, wound healing, and cytokinesis (Young et al., 1993; Edwards and Kiehart, 1996; Shelden and Knecht, 1996; Hickson et al., 2006; Pollard, 1981; Warrick and Spudich, 1987; Ridley et al., 2001; Bement et al., 1999; Glotzer, 2005; Robinson and Spudich, 2004). Contractile force production has proven to be critical for these processes as well as general maintenance of cell shape and cortical rigidity (Martens and Radmacher, 2008; Robinson and Spudich, 2004). Myosin V is an unconventional myosin that transports cargo between cellular locations. Myosin V has been implicated in mRNA transport, membrane trafficking, transport and/or tethering of organelles, and cell polarity (Reck-Peterson et al., 2000). Phenotypes associated with loss of function of myosin V demonstrate defects in membrane trafficking and cell polarity (Mercer et al., 1991; Johnston et al., 1991).

## Myosin domain architecture and adaptations

In general myosin heavy chains contain three functional domains termed the head, neck, and tail domains. The head and neck domains are responsible for ATP-dependent force production. The tail domain is highly variable between classes and is specialized for different functions (Sellers, 2000; Berg et al., 2001).

The head domain or motor domain is the domain that binds actin and hydrolyzes ATP. The motor domains of myosin and the resulting ATPase cycle mechanism linked to the myosin-actin binding cycle, is conserved for all myosin classes (De La Cruz and

Ostap, 2004). Detailed topology and mechanistic insight into the function of the motor domain have been gained through structural studies of myosin II (Rayment et al., 1993; Dominguez et al., 1998; Houdusse et al., 1999). The motor domain structure consists of four subdomains connected by flexible linkers. The four subdomains are an SH3-like motif common to myosin II, an upper and lower 50 kDa subdomains, and a converter subdomain. The upper and lower 50 kDa subdomains comprise most of the actin binding interface. The active site where ATP binds and is hydrolyzed is located in the interface between the upstream SH3-like motif and the 50kDa subdomains (Houdusse et al., 1999). The converter domain is the pivot point for the movement of the motor domain that is controlled by conformational changes that are intimately linked to the ATPase active site. This domain is primarily responsible for the chemo-mechanical coupling of the ATPase activity to force production. Small changes in the conformation of the converter domain resulting from different steps of the ATPase cycle are amplified by the attached stiff neck domain (Rayment et al., 1993; Houdusse et al., 1999). For extensive review of the motor domain structure and enzymatic activity, please see Rayment et al., 1996 and Geeves and Holmes, 1999.

The neck domain of myosin acts as a rigid lever arm that translates small conformational changes of the motor domain into large displacements of the actin track (Houdusse et al., 1999). The neck domain of myosin is an extended helix that usually contains binding sites for light chains or calmodulin. These binding sites are comprised of an IQ motif that has a consensus sequence of IQXXXRGXXXR (Cheney and Mooseker, 1992; Rhoads and Friedberg, 1997). The number of IQ motifs present in different myosins is variable. For instance, myosin II contains one consensus and one degenerate IQ motif that bind specifically to the essential light chain (ELC) and the regulatory light chain (RLC) respectively (Houdusse et al., 1999). Myosin V on the other hand contains six IQ motifs, the most of any class, that bind calmodulin and in some cases a related myosin light chain (Wang et al., 2000; Espindola et al., 2000; Koide et al., 2006). The primary function of calmodulin and light chain binding to this extended helix that makes up the neck domain is to stabilize and stiffen the helix into a lever arm (Rayment et al., 1993; Trybus, 1994; Dominguez et al., 1998; Howard and Spudich, 1996; Vilfan, 2005). The number of IQ motifs and correlative lever arm length is linearly related to the step size and actin sliding velocity properties of a given myosin (Uyeda et al., 1996; Schott et al., 2002; Sakamoto et al., 2005). The other main function of having these EF hand proteins bind to the neck domain is regulation of myosin activity (Trybus, 1994; Sellers and Knight, 2007; Taylor 2007).

A common feature of myosin motors is the ability to sense tension (Kee and Robinson, 2008). This mechanosensation ability is utilized differently between myosin classes. Myosin V utilizes intramolecular strain to inhibit actin release by the leading head, which coordinates the two heads for processive, directional hand-over-hand walking along the actin filament (Purcell et al., 2005). Similarly, resistive force slows the ADP release of myosin II, thereby turning it into a high-duty-ratio motor for energy-efficient tension maintenance (Kovacs et al., 2007). This property also allows more heads of large myosin II ensembles to bind under load, thus progressively allowing the contractile force to overcome the resistive force until maximum stall force is achieved.

The head and neck domains of the myosin heavy chain are sufficient for nucleotide dependent force generation and actin sliding (Sellers, 2000). The tail domain of different myosin classes is highly variable with specialized functions for each class. However, a conserved function of the tail domain in most myosin classes is to function as a dimerization interface for the heavy chains. The heavy chains of both myosin II and myosin V dimerize through parallel coiled-coil structural motifs yielding two-headed functional molecules with associated light chains and/or calmodulin (Sellers, 2000). Coiled-coil proteins are characterized by amphipathic $\alpha$-helices, with hydrophobic residues lining one side of the helix. Two helices coil around each other as the hydrophobic seam is buried. This creates the dimerization interface (Lupas, 1996; Burkhard et al., 2001).

Both myosin II and myosin V, having dimerized heavy chains, contain two motor domains per functional molecule. However, the two motor domains are utilized differently in these two classes. Myosin V uses each of its motor domains to bind the actin filament in an alternating fashion resulting in a hand-over-hand walking motion that moves the motor along the filament. Conversely, only one myosin II head is attached at any one time rendering it functionally similar to a single headed, non-dimerized myosin similar to class I myosin (Sellers, 2000). The ADP release step is rate limiting for myosin V, which means that it is predominantly strongly bound to actin at steady state. Being a high-duty-ratio motor (spends a large fraction of the ATPase cycle time attached to its track), allows myosin V to be highly processive for long distant transport of cargo (Mehta et al., 1999; Rief et al., 2000). In comparison myosin II has a low duty ratio, but works in ensembles of motors yielding a higher effective duty ratio. A fast ATPase cycle lifetime allows myosin II to rapidly contract upon activation and the high effective duty ratio allows for continuous sliding (De La Cruz and Ostap, 2004). Even different myosin II isoforms have developed important differences in biochemical parameters. For instance, smooth muscle myosin II has a longer duty ratio and lifetime of strong-binding states than skeletal muscle, which results in a slower rate of contraction, but the ability to produce higher forces (Guilford et al., 1997; Marston and Taylor, 1980). Also, mammalian non-muscle myosin IIb has a higher duty ratio than non-muscle myosin IIa, which seems to have adapted this isoform for tension maintenance as opposed to rapid contraction (Wang et al., 2003; Rosenfeld et al., 2003).

Tail domains also appear to play a regulatory role, potentially in conjunction with the light chains and/or calmodulin, which could be a conserved regulatory mechanism across all motor proteins (Sellers and Knight, 2007). The myosin II tail domain is a long coiled-coil rod that displays an alternating charge repeat that is important for electrostatic self-association (Parry, 1981; McLachlan and Karn, 1982). Myosin II forms bipolar filaments with multiple subunits through parallel and anti-parallel tail-tail interactions (Craig and Woodhead, 2006). The formation of these filaments with oppositely oriented motor domains is a prerequisite for contractile force generation (Warwick and Spudich, 1987). The myosin V tail domain is comprised of a coiled-coil rod region and a globular tail region that functions in cargo binding and regulation of myosin V activity. Myosin V uses its tail to bind cargo via cargo-specific receptors that it then transports along actin tracks to targeted cellular sites (Trybus, 2008).

### Regulation of myosin activity

Until now I have primarily discussed the important features of myosin for producing actin-based force generation. Arguably more interesting is the link that myosin provides between signaling pathways and regulation of the cytoskeleton. In the following section I will be talking at length about the regulation of myosin activity.

The ability of myosins to be activated only at the correct cellular site, at the appropriate time is critical for complex cellular processes. For instance, during cell division myosin II is inactivated at the polar cortex, while contraction results in an elongated cell shape that is necessary to allow for anaphase extension of the mitotic spindle, thus aiding in chromosome segregation. Myosin II then concentrates at the cell equator after chromosome segregation, where it aids in the division of cytoplasm between the resulting daughter cells, known as cytokinesis (Robinson and Spudich, 2004). The tight spatio-temporal regulation of myosin II activity during this process, and the signaling pathways that control it has been the subject of intense investigation in cell biology for many decades now (Glotzer, 2005).

The ability of myosin to achieve an inhibited or off state is critical for the ability of signaling pathways to regulate motor activity. As stated above, the neck domain, with light chains and/or calmodulin bound, and the tail domain are responsible for the regulation of myosin activity of many isoforms. Though both myosin II and myosin V utilize these two domains for regulation, the mechanism of regulation is quite different between these two classes.

Myosin V activity is regulated in two basic fashions. One mode of regulation is by calcium binding to calmodulin or related light chain, whereas the other mode involves the molecule adopting a compact off state. The regulation of myosin V by calcium is complex. Calcium has been shown to increase ATPase activity of myosin V, but interestingly there is decreased actin motility (Cheney et al., 1993; Krementsov et al., 2004; Li et al., 2004; Wang et al., 2004). Myosin V is an unusual substrate for calmodulin due to the fact that calmodulin binds the IQ motifs in the absence of calcium, which usually activates calmodulin ligand binding. Unexpectedly, in the presence of calcium, myosin V is activated, but calmodulin dissociates from one of the IQ motifs (Nguyen and Higuchi, 2005; Krementsov et al., 2004; Koide et al., 2006; Trybus et al., 2007). The dissociated calmodulin molecule renders the lever arm flexible, resulting in an inability to transmit force and decreased actin motility (Veigel et al., 2005; Lu et al., 2006). The extent that this mode of regulation occurs *in vivo* is not known.

The second mode of regulation of myosin V activity is the ability to reversibly change conformation into a compact inhibited state. Hydrodynamic data shows that active myosin V exists in an elongated state (11S), while the inhibited state is in a compact folded conformation (14S) (Krementsov et al., 2004; Li et al., 2004; Wang et al., 2004). A similar conformational change has been observed for smooth muscle myosin II and kinesin, suggesting that this is a common mechanism of motor protein inhibition (Trybus et al., 1982; Trybus and Lowey, 1984; Hackney et al., 1992). The three-dimensional structure of the myosin V inhibited state has been determined by electron microscopic approaches (Liu et al., 2006; Thirumurugan et al., 2006). Myosin V bends at the lever arm to rod junction so that the globular tail interacts with the motor domain near the active site. In this fashion, the globular tail domain inhibits the ATPase activity, thus achieving an "off" state (Li et al., 2006). The heads in this compact inhibited state are in a post-power stroke conformation, and the globular tail domain does not occlude the actin-binding region (Liu et a., 2006; Thirumurugan et al., 2006). The 14S conformation of myosin V is able to bind to actin with high affinity but is restricted from binding with both heads simultaneously (Olivares et al., 2006). A low concentration of calcium unfolds the inhibited state and activates the myosin molecule through rearrangements of the bound calmodulins in the neck domain (Trybus et al., 2007). Another mode of activation could involve cargo competing with the heads for binding to the globular tail domain. Whereas this model is attractive since myosin V activity is needed presumably only for transporting cargo, it has yet to be demonstrated convincingly.

The control of myosin II activity is complex, and involves isoform specific mechanisms of regulation. The activity of myosin II isoforms is regulated according to their function. For instance, muscle isoforms of myosin II are regulated by calcium fluxes, which are activated by the nervous system. Non-muscle myosin on the other hand is regulated by signal transduction pathways in non-muscle cells.

Myosin II isoforms from striated muscle, such as skeletal and cardiac muscle, are constitutively active in the presence of actin. The activity of these myosin II isoforms is regulated by calcium binding to the actin-associated troponin-tropomyosin regulatory complex. Muscle contraction occurs when the muscle cell is excited by a motor neuron, leading to a release of calcium from the sarcoplasmic reticulum. Calcium binding to the troponin-tropomyosin complex causes a conformation change that results in actin no longer being occluded from myosin interaction (Gordon et al., 2000). Actin then stimulates myosin activity leading to muscle contraction.

Smooth muscle myosin II can be regulated through neural input, but also can be independently or synergistically regulated by paracrine, metabolic, and physical stimuli. The integrative nature of smooth muscle myosin II is important for its physiological tasks. For instance, smooth muscle myosin II controls the amount of blood flow to different tissues depending on their metabolic states or in response to epinephrine/ norepinephrine (adrenaline/ noradrenaline) release during short-term stress. The effects of inputs on smooth muscle myosin II depends on the characteristics of the specific receptor activated as several types of input can have an excitatory (contraction) or inhibitory (relaxing) effect. For example, in response to stress, epinephrine causes dilation of blood vessels within skeletal muscle, but constriction in skin and the gastrointestinal tract.

Smooth muscle myosin II activation is linked with the phosphorylation state of its regulatory light chain (RLC). Neural stimulation results in calcium influx that activates myosin light chain kinase (MLCK). Activated MLCK phosphorylates RLC on activating residues that lead to contraction (Ding et al., 2009). Thus, smooth muscle myosin II is activated by calcium, despite the absence of troponins in smooth muscle. Other pathways to excitation also result in RLC phosphorylation by MLCK, whereas inhibitory pathways activate myosin light chain phosphatase or kinases that inhibit MLCK (Ganitkevich et al., 2002). Sarcomeric myosins that are present in striated muscle can also be phosphorylated on their respective RLCs, but the effect is only modulatory to enzymatic activity and mechanical properties (Sweeney and Stull, 1990).

The ATPase activity of smooth muscle myosin II is greatly reduced when RLC is not phosphorylated (Trybus and Lowey, 1989; Trybus, 1989). A proteolytic fragment that contains the head and neck domain with associated light chains displays high ATPase activity in the absence of RLC phosphorylation (Greene et al., 1983). A larger fragment that contains part of the coiled-coil tail, allowing for dimerization, is regulated by phosphorylation of RLC, suggesting that two heads are necessary for regulation (Sellers et al., 1981; Cremo et al., 2001; Sweeney et al., 2000; Konishi et al., 2001). However, it appears that dimerization alone is not sufficient to restore regulation. A stretch of native tail sequence approximately the length of a head domain is required for achieve complete inhibition in the unphosphorylated state (Trybus et al., 1997). Electron microscopic studies have clarified the requirement of two heads, as well as the role of the tail domain in smooth muscle myosin II regulation (Wendt et al., 1999; Wendt et al., 2001; Liu et al., 2003). The inhibited state is achieved through an asymmetric interaction between head domains of a single molecule. The two heads also bend back and interact with the beginning of the tail domain, suggesting that this sequence is specific to bind the inhibited head domains and that this interaction is necessary for complete inhibition (Trybus et al., 1997; Wendt et al., 2001). Even lower ATPase activity is achieved in the full-length molecule suggesting that the entire tail domain may stabilize the inhibited state (Trybus 1989; Cross et al., 1988).

Similar to class V myosin, smooth muscle myosin adopts a compact off state (10S) when inhibited, and adopts an elongated state (6S) when activated (Trybus et al., 1982; Onishi and Wakabayashi, 1982; Trybus and Lowey, 1984). The inhibited state is marked by a folded-back tail domain with two acute bends, giving rise to three elongated segments (Trybus and Lowey, 1984; Burgess et al., 2007). The transition from the 10S to 6S state is a prerequisite of filament formation; therefore RLC phosphorylation regulates both enzymatic activity and the state of assembly of smooth muscle myosin II (Trybus and Lowey, 1984). However, the role of the 10S form of myosin in smooth muscle is controversial. Smooth muscle myosin filaments are present in relaxed smooth muscle, and there is no known role for depolymerization in smooth muscle regulation (Somlyo et al., 1981; Horowitz et al., 1994; Seow 2005).

The regulation mechanisms of vertebrate non-muscle myosin II is remarkably similar to that of smooth muscle myosin II. Several kinases have been shown to phosphorylate its respective RLC, coupling it to several signal transduction pathways independent of calcium (Tan et al., 1992; Yamakita et al., 1994; Jordan and Karess, 1997; Kamatsu et al., 2000). Unlike smooth muscle myosin II, the ability to regulate the assembly state of non-muscle myosin II seems to be vitally important for the physiological role of this myosin II isoform.

## Non-muscle myosin II

The non-muscle myosin II isoform is of great interest due to its roles in fundamental cell biological processes in all eukaryotic cell types and organisms. Muscle isoforms of myosin II were evolved for complex systems in multi-cellular organisms, such as the gastrointestinal tract, circulatory system, and locomotion. The specialized structures that these isoforms operate within are dynamic in their activity, but there construction is more static in nature. When activated, muscle isoforms lead to the contraction of the entire muscle cell. On the other hand, non-muscle myosin II must dynamically localize and assembly into filaments at cellular sites where contractile force production is needed locally.

Non-muscle myosin II generates the contractile force for controlling cortical rigidity, cell shape, cell-cell and cell-matrix adhesion, cell migration, and the ability to divide during proliferation (Young et al., 1993; Edwards and Kiehart, 1996; Shelden and Knecht, 1996; Hickson et al., 2006; Martens and Radmacher, 2008; Pollard, 1981; Warrick and Spudich, 1987; Ridley et al., 2001; Bement et al., 1999; Glotzer, 2005; Robinson and Spudich, 2004). This makes non-muscle myosin II essential for life of eukaryotic organisms. The ability of non-muscle myosin II to organize and alter the mechanical properties of the actin cortex when activated provides a direct link between signaling pathways and the regulation of cell mechanics. This activity also makes non-muscle myosin II unique among the myosin superfamily, in that it is a motor protein that is acting as a regulator of the actin cytoskeleton system.

Much of what is known about myosin II function in non-muscle cells comes from studies in the cellular slime mold *Dictyostelium discoideum*. Surprisingly, cells lacking non-muscle myosin II are viable if grown on a surface where cell division occurs through a unique traction-mediated cytofission (De Lozanne and Spudich, 1987; Spudich, 1989;

Pasternak et al., 1989). However, in suspension, ablated myosin II results in large multinucleated cells, similar to all other known eukaryotes (De Lozanne and Spudich, 1987; Knecht and Loomis, 1987; Manstein et al., 1989). In normal cytokinesis, cells round up then elongate during anaphase extension with myosin II concentrating in a contractile ring that constricts to form two cells (Zang et al., 1997). In myosin II null cells, elongation and cytokinesis is inhibited, but traction forces from polar ruffling in the presence of a surface is sufficient to constrict the midzone (Zang et al., 1997). This interesting adaptation has allowed the role of myosin II in cell shape changes during cytokinesis, cell migration, development, surface receptor capping, and cortical tension to be studied (Zang et al., 1997; Xu et al., 1996; Knecht and Loomis, 1988; Peters et al., 1988; Pasternak et al., 1989; Aguado-Velasco et al., 1997). Also, myosin II null cells can serve as a host for reintroduced myosin mutants, allowing physiological characterization and purification for biochemical assays (Egelhoff et al., 1993; Kubalek et al., 1996; Shu et al., 1999; Manstein et al., 1989; Manstein et al., 1995). This advance has allowed identification of localization signals, domains responsible for filament assembly, and mechanisms of regulation. Unfortunately, non-muscle myosin II from *Dictyostelium discoideum* has a divergent sequence, and is regulated by myosin heavy chain phosphorylation, while myosin II from higher organisms is regulated through RLC phosphorylation (Tan et al., 1992). Despite this, knowledge garnered from these studies has been invaluable for understanding cell mechanics and upstream cytoskeleton regulation, which is conserved with other eukaryotes (Clarke and Spudich, 1977; Egelhoff and Spudich, 1991; Robinson and Spudich, 2004).

Studies of non-muscle myosin II in *Drosophila melangaster* and mammalian tissue culture have revealed similar roles for myosin in these physiological processes as those studied in *Dictyostelium discoidium*. Zipper, the *Drosophila* non-muscle myosin II heavy chain, was the first motor protein shown to be involved in morphogenesis (Young et al., 1993; Edwards and Kiehart, 1996). *Drosophila* has proven to be a useful model for understanding the role of non-muscle myosin II and its regulation through RLC, in tissue architecture and development of multi-cellular organisms (Franke et al., 2005; Edwards and Kiehart, 1996).

As mentioned above, non-muscle myosin II from *Dictyostelium* and higher organisms are regulated in different manners to achieve localized activity. In *Dictyostelium* a portion of the heavy chain tail domain, which is responsible for tail-tail interactions within bipolar filaments, is phosphorylated. This phosphorylation interferes with inter-tail domain interactions, thereby disrupting filament assembly (Sabry et al., 1997; Nock et al., 2000; Nagasaki et al., 2002). In higher organisms, non-muscle myosin II is regulated by a number of mechanisms, with RLC phosphorylation being the most common mechanism (Bresnick, 1999). How phosphorylation of the RLC, near the head domains, alters the ability of tail domains to interact is poorly understood. However, the common theme of non-muscle myosin II regulation is that, in contrast to muscle isoforms, the assembly state is the property that is primarily regulated (Egelhoff et al., 1993; Breckenridge et al., 2009; Sellers and Knight, 2007). It is perhaps easy to imagine that non-muscle cells would like to restrict the assembly of this contractile apparatus to localized regions where contraction is needed, as opposed to primarily regulating the activity of static assemblies.

## Remaining questions

Currently, it is well understood how non-muscle myosin II from *Dictyostelium discoidium* self-associates to form bipolar filaments and how this interaction is regulated by signaling pathways (Zang et al., 1997; O'Halloran et al., 1990; Hostetter et al., 2004). However, the mechanism of bipolar filament formation, the regulation of filament assembly, and the localization mechanisms of non-muscle myosin II from multi-cellular organisms are poorly understood. Despite our limited knowledge of these basic activities of non-muscle myosin II, the signal transduction pathways that regulate its function during complex physiological processes have been under intense investigation (Warrick and Spudich, 1997; Young et al., 1993; Bement et al., 1999; Robinson and Spudich, 2004).

In the following chapters the role of the tail domain in the formation of bipolar filaments and targeting of the *Drosophila* non-muscle myosin II molecule to specific cellular sites is discussed. Chapter II will show the identification of subdomains within the tail domain that are responsible for bipolar filament formation and distinctive localization patterns that occur in a cell cycle-dependent manner. This work has been previously published with Dr. Su-Ling Liu, Natasha Fewkes, Rhiannon Penkert, and Dr. Ken Prehoda. Chapter III will demonstrate how assembly domains contribute to tail-tail interactions that form the basis for bipolar filament formation. Also, analysis of inter-tail domain interactions has lead to the first structural model for non-muscle myosin II bipolar filament. Natasha Fewkes and Ryan Frei carried out filament assembly assays on several mutant constructs used in this study. Finally, chapter IV will outline the progress that has been made to understanding non-muscle myosin II function, and outline some future investigations that have been started due to this work.

# CHAPTER II

## FILAMENT-DEPENDENT AND -INDEPENDENT LOCALIZATION MODES OF *DROSOPHILA* NON-MUSCLE MYOSIN II

Reproduced with permission from Su-Ling Liu, Natasha Fewkes, Derek Ricketson, Rhiannon R. Penkert, Kenneth E. Prehoda. 2008, *Journal of Biological Chemistry,* 283(1):380-7. Copyright 2008. The American Society for Biochemistry and Molecular Biology, Inc.

### Introduction

The motor protein myosin II assembles into bipolar filaments, which, through interactions with F-actin, generate contractile forces that are important for many cellular processes. In non-muscle cells, myosin II accumulates at the cytokinetic cleavage furrow with a band of F-actin, which together constricts the midzone of the cell to produce two daughter cells (1,2). Myosin II is also important for organization of the cell cortex in processes such as cell movement (3,4), cell polarity and asymmetric cell division (5-9). In this study, we investigate the requirements for assembly of *Drosophila* myosin II and its targeting to the cortex and cleavage furrow.

Actomyosin contraction requires the assembly of individual myosin II hexamers (containing two heavy chains, and two pairs of distinct light chains) into bipolar filaments that drive actin filaments in opposite directions. Bipolar filament assembly is mediated by a large coiled-coil tail domain present in the heavy chain. In myosin IIs from several organisms, only a small region of the tail domain is required to confer the ability to assemble into filaments (10-16). However, the best-studied examples of filament assembly, myosin II tail domain from *Acanthamoeba* and *Dictyostelium*, show little sequence homology (~10% identity, ~19% homology) to zipper, the *Drosophila* myosin II heavy chain. Furthermore, the tail domain of zipper displays uniform conservation (~ 52% identity, ~74% homology) with those of vertebrate non-muscle myosin IIs, which leaves the precise determinants of filament assembly unclear.

As filament assembly is a prerequisite for contractile force generation, modulation of filament stability can be used to regulate actomyosin contraction. Filament stability can be regulated by covalent modification of the tail domain, regulatory light chain, or by ligand binding to the tail domain. In *Dictyostelium*, myosin heavy chain kinase (MHCK) phosphorylates three threonine residues in the tail domain, which leads to inhibition of filament assembly (17,18). However, MHCKs do not exist in higher organisms and the mechanism of filament assembly regulation is less clear. Although other kinases can phosphorylate the heavy chain, these phosphorylation events appear to be functionally distinct from the MHCK regulation of *Dictyostelium* myosin II. For example, although protein kinase C (PKC) phosphorylates zipper, phosphorylation does not appear to alter filament stability and is not required for viability (19). In cultured mammalian cells however, atypical PKC phosphorylates myosin II, which leads to slower filament assembly and delocalized myosin II (20).

Proper myosin II function also requires recruitment of filaments to specific cellular sites. Myosin II localizes to the F-actin rich cell cortex where it alters cellular mechanical properties and actively organizes the molecular composition of the cortex (8). For example, in *C. elegans*, cortical flows of myosin II are required for the segregation of cell fate determinants in the early embryo (21-23). In the *C. elegans* one-cell embryo cortical myosin II forms a dynamic cortical network of contractility that is destabilized near the point of sperm entry. The resulting asymmetry induces cortical flow of myosin II, F-actin, and Par proteins toward the opposite pole. Myosin II localization is also important during mitosis where it is depleted at the polar cortex and becomes highly concentrated around a narrow band of the cell surrounding the central spindle that ultimately forms the contractile ring (1). Interestingly, in *Dictyostelium* localization to the cleavage furrow does not require myosin II's actin-binding motor domain as myosins in which the motor domain has been replaced by green fluorescent protein (GFP) correctly localize to the cleavage furrow (24). However, the role of the motor domain in the localization of myosin II in higher organisms is unknown.

In order to further understand myosin II filament assembly and localization, we have investigated these properties using the *Drosophila* non-muscle myosin II heavy chain, zipper. Zipper function is important for diverse developmental processes including border cell migration (25), nuclear migration in the syncytial preblastoderm (26), cellularization, and dorsal closure (27-29). During embryonic cellularization the plasma membrane invaginates in the syncytial blastoderm around cortically positioned nuclei to simultaneously form 6000 columnar epithelial cells. Contraction of an actin array by myosin II is required for the basal closure of the membrane around the nuclei (28).

In *Drosophila* neuroblasts, precursors of the central nervous system, zipper function is required for correct partitioning of cell fate determinants in a similar but mechanistically distinct manner as occurs in *C. elegans* (7,8,22). Myosin II is initially restricted to the apical cortex by the tumor suppressor Lethal (2) giant larvae (Lgl) (7). During anaphase and telophase myosin II localization expands basally and this correlates with the basal restriction of cell fate determinants. Although myosin II function at the cell cortex is important in many different contexts, the determinants for its cortical localization are unknown. Here we examine the determinants of zipper filament assembly and localization with the goal of understanding myosin II function at the cell cortex.

## Results

### *The zipper tail domain contains a 90-residue filament "assembly domain"*

We first defined the precise requirements for oligomerization of the coiled-coil tail so that we could compare the zipper elements that specify filament assembly with those that target it to the cell cortex. The *Drosophila* myosin II heavy chain, zipper, consists of an 800 residue motor domain and a 1000-residue tail domain (Fig. 1A). The tail domain contains approximately 800 residues with a heptad repeat, consistent with its ability to formed coiled-coils, followed by a short section known as the tailpiece that lacks the heptad repeat. Interactions between coiled-coils are responsible for higher order oligomerization of myosin II intobipolar filaments.

Which elements of the zipper tail sequence are necessary for tail domain assembly? The so-called "assembly domain" (AD) for several non-muscle myosin heavy chain tail domains have been determined (13-16), but the homology among tail domains is distributed uniformly and in some cases is very low such that it is not yet possible to predict the AD of myosin II tail domains. The zipper AD is known to occur in the COOH-terminal 300 residues (19) and we tested regions of the tail domain for the ability to form filaments using salt-dependent assembly assays to identify the AD to higher resolution. Filaments and paracrystals efficiently sediment upon centrifugation, whereas unassembled coiled-coil dimers remain in solution (13). Zipper tail domain regions exhibited different propensities to sediment in a salt-dependent manner (Fig. 1B). Oligomerization of *Dictyostelium* myosin II is highly salt-dependent (13), only assembling at intermediate salt concentrations (25-100 mM NaCl) and this is the case for certain zipper tail regions (Fig. 1C). Other tail domain regions remained soluble over the entire salt concentration range indicating that they fail to oligomerize into structures that sediment under these conditions. Circular dichroism spectroscopy and analytical ultracentrifugation analysis (data not shown) of the tail region 1550-1810 shows that it forms a coiled-coil dimer, so the failure of oligomerization is not due to the disruption of secondary and tertiary structure.

In order to measure the extent of filament assembly in solution, we developed an assay based on fluorescence resonance energy transfer (FRET) between $NH_2$-terminally attached fluorescent proteins. We predicted that the close proximity of the $NH_2$-terminal regions of the tail when polymerized would allow for energy transfer between fluorescent proteins at this position (Fig. 1D). A solution of cyan and yellow fluorescent protein (CFP and YFP, respectively) fusions of zipper show a salt-dependent ratio of donor (CFP) to acceptor (YFP) fluorescence, indicative of energy transfer in the filament state (Fig. 1D,E).

The FRET and pelleting assays yielded qualitatively similar results indicating that the separation between soluble and insoluble phases that occurs in the pelleting assay did not significantly perturb the equilibrium between individual coiled-coils and higher order oligomers. It should be noted that placing fluorescent "heads" on *Dictyostelium* myosin II restores the bipolar mini-filament nature of the oligomers formed by tail domain truncations (13), thus the FRET assay likely represents filaments that are in a native form. Furthermore, identical pelleting results were obtained using fluorescent protein tagged or non-tagged tail fragments (Fig. 1B). The only exception occurred when the CFP and YFP were placed directly adjacent to the assembly domain (see below) where they inhibited filament assembly, presumably for steric reasons. The FRET assay did allow for observation of subtle differences between zipper tail regions in their ability to form filaments. For example oligomers of the tail domain regions 1744-2011 and 1570-1969 oligomers are maximally stable at different salt concentrations indicating that regions outside the AD can influence filament stability. We expect that this assay will also be useful for measuring other filament assembly parameters, including assembly kinetics.

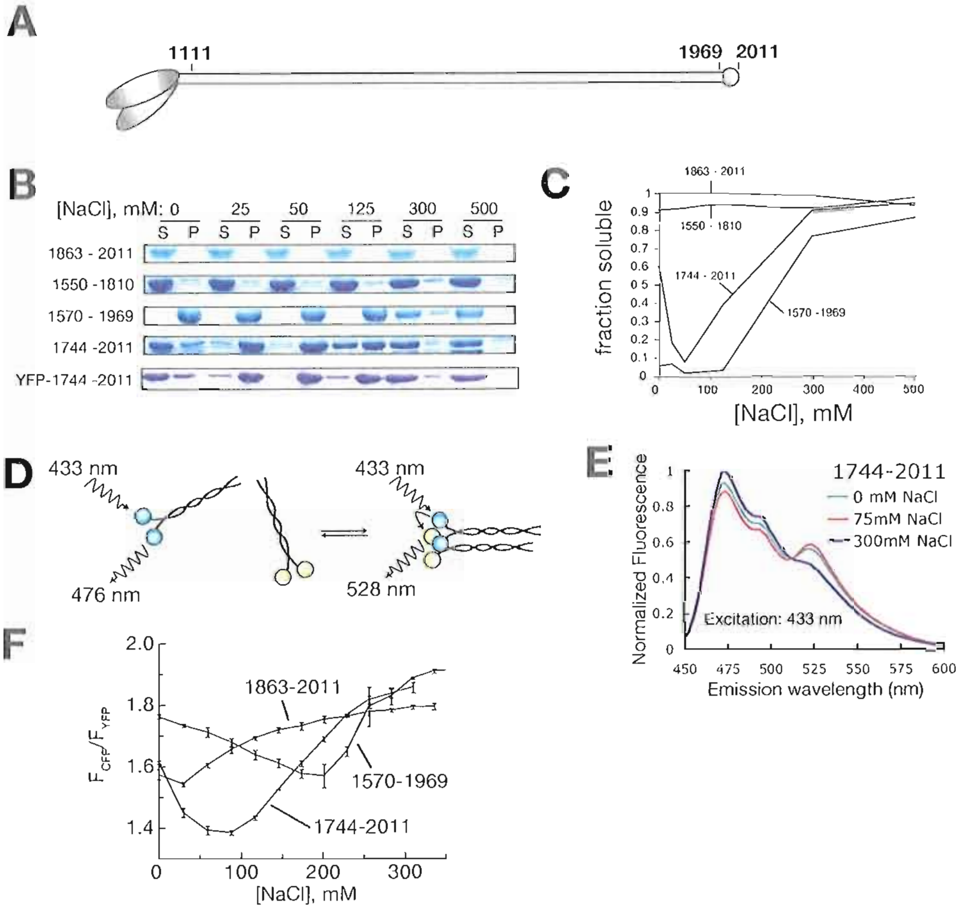

Figure 1. **Identification of a zipper filament assembly domain. A. Zipper domain structure.** A schematic of a zipper dimer is shown with motor domains (ovals), coiled-coil tail domain (rod; amino acid residue 1111-1969) and non-helical tailpiece (circle). Non-tagged zipper tail domain proteins were used on B and C, except where indicated, and fluorescent protein-tagged tail domain proteins were used on E and F. B. Pelleting assay for filament assembly for several tail domain regions. S stands for supernatant fraction and P sands for pelleted fraction. C. Quantification of solubility for tail domain regions shown in (B). D. Scheme for fluorescence resonance energy transfer (FRET)-based assay for filament assembly. E. Fluorescence emission spectra of an assembly domain-containing zipper tail domain at low, medium, and high salt concentrations. Energy transfer is observed at 75 mM salt where the tail domain is expected to form filaments. F. Salt dependence of FRET signal for several tail fragments. Error bars represent standard deviations from three independent measurements.

Comparison of the ability of different regions of the zipper tail to assemble reveals that residues 1849-1940 comprise a minimal assembly domain (AD) that is both necessary and sufficient to robustly assemble into filaments (Fig. 2A). Sequence comparison shows that the zipper AD partially overlaps the 39-residue second assembly competence domain identified in human non-muscle myosin (15) and encompasses the 29-residue AD found in sarcomeric myosin II (16). The zipper AD does not include the globular tailpiece, which is required for filament assembly in *Acanthamoeba* but not *Dictyostelium* myosin IIs (13,14), vertebrate smooth muscle and non-muscle myosin II (31). Unlike the *Dictyostelium* AD, which is far away from the tip of coiled-coil rod, the zipper AD is close to the end of rod and does not have "ala-rich" flanking segments that contain alanines in the core 'a' and 'd' heptad repeat positions (13).

What are the unique features of the zipper tail assembly domain that allow it to oligomerize? The ability of other segments of the tail domain, such as 1550-1810, to form coiled-coils suggests that a trigger sequence necessary for coiled-coil formation (32) is not the unique feature of the AD. Like other myosin II tail domains, the zipper tail domain contains a repeating charge structure that may be important for specifying the structure of the filament (Fig. 2C)(13,33). Figure 2C shows the overall charge of 15 and 29 residue windows of the zipper tail. Although this repeat occurs throughout the tail domain, including in regions that do not assemble into filaments, the assembly domain is the region in which the repeat is most evenly distributed among alternating 15-residue positive and negative charged sequences. Further study will be needed to establish the role of the specific charge repeat in stabilizing the filament structure.

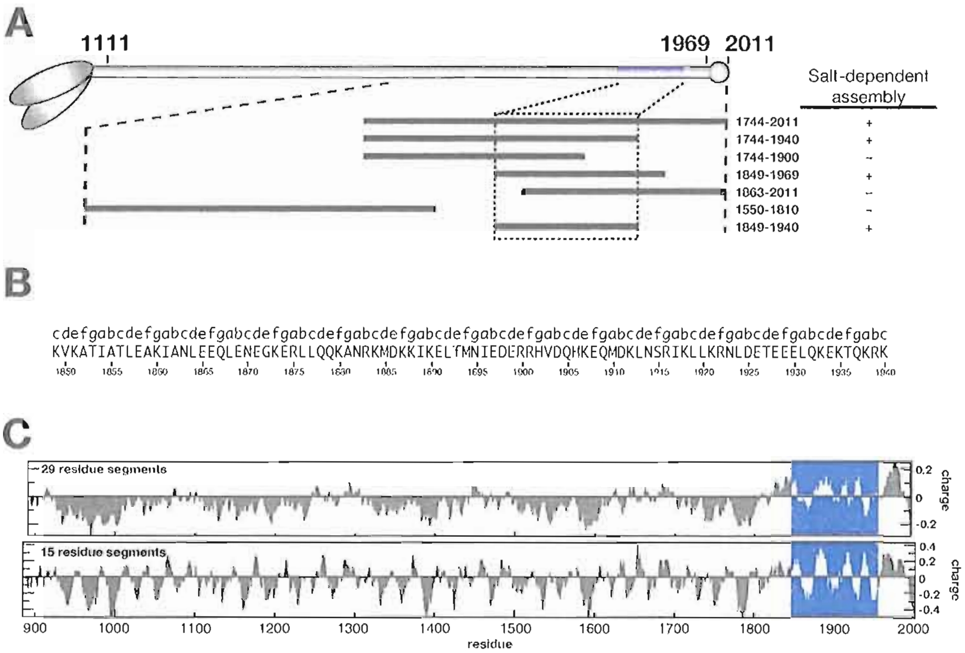
A
1111
1969
2011
Salt-dependent assembly
1744-2011 +
1744-1940 +
1744-1900 -
1849-1969 +
1863-2011 -
1550-1810 -
1849-1940 +
B
cdefgabcdefgabcdefgabcdefgabcdefgabcdefgabcdefgabcdefgabcdefgabcdefgabcdefgabcdefgabcdefgabc
KVKATIATLEAKIANLEEQLENEGKERLLQQKANRKMDKKIKELTMNIEDERRHVDQHKEQMDKLNSRIKLLKRNLDETEEELQKEKTQKRK
1850
1855
1860
1865
1870
1875
1880
1885
1890
1895
1900
1905
1910
1915
1920
1925
1930
1935
1940
C
~29 residue segments
15 residue segments
0.2
0
-0.2
0.4
0.2
0
-0.2
-0.4
charge
charge
900
1000
1100
1200
1300
1400
1500
1600
1700
1800
1900
2000
residue

Figure 2. **The zipper filament-assembly domain.** A. Deletion analysis of zipper tail domain. B. Sequence of the zipper assembly domain showing heptad repeat. C. Charge repeat structure of zipper tail domain calculated with 15 and 29 residue windows.

### *The zipper tail domain specifies cortical localization in Drosophila S2 cells*

We next examined the localization of myosin II in *Drosophila* S2 cells to delineate the structural requirements for localization. Myosin II exhibits a complex localization pattern in S2 cells (Fig. 3A) that is similar to many other cell types: during interphase, myosin II exists both in the cytoplasm and at the cortex; during mitosis, it is depleted from the cortex until anaphase at which point it forms cortical patches; in late anaphase and telophase myosin II concentrates in a narrow band around the central spindle ultimately forming the cytokinetic ring. Thus cortical localization occurs in interphase, anaphase, and telophase, but is inhibited in early mitosis.

We expressed both the motor and tail domains in S2 cells to determine which elements of the heavy chain are required for localization. As shown in Figure 3B, full-length zipper transfected into S2 cells under the control of an inducible copper promoter exhibits a localization pattern like endogenous zipper. However, the motor domain remains in the cytoplasm throughout the cell cycle (Fig. 3C) indicating that it is not sufficient for targeting to the interphase cortex or cleavage furrow. In contrast, the tail domain does specify cortical localization in both of these contexts (Fig. 3D). As the tail domain is responsible for zipper dimerization, we cannot rule out interactions with endogenous zipper to form mixed coiled-coils as the localization mechanism of the full tail domain based on this data alone. However, several large tail domain regions with many heptad repeats are unable to localize (see below) suggesting that coiled-coil interactions with endogenous zipper cannot lead to targeting of tail domain regions on their own.

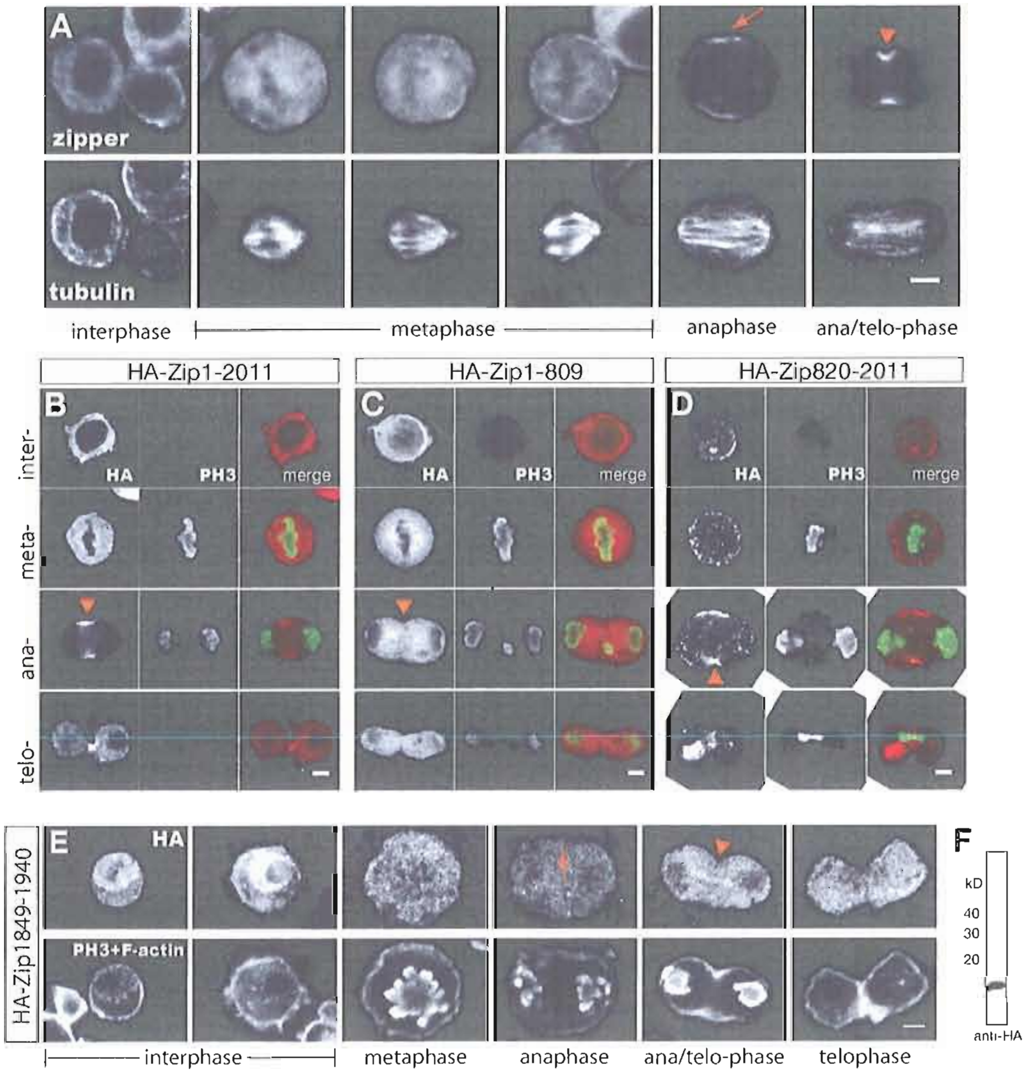
A
zipper
tubulin
interphase
metaphase
anaphase
ana/telo-phase
HA-Zip1-2011
HA-Zip1-809
HA-Zip820-2011
B
C
D
HA
PH3
merge
inter-
meta-
ana-
telo-
E
HA
PH3+F-actin
HA-Zip1849-1940
interphase
metaphase
anaphase
ana/telo-phase
telophase
F
kD
40
30
20
anti-HA

Figure 3. **Zipper localization determinants in *Drosophila* S2 cells.** A. Localization of endogenous zipper in S2 cells. Zipper and tubulin, visualized by anti-zipper and anti-alpha-tubulin antibody staining, are shown in cells at different cell cycle stages. Zipper is recruited to equatorial cortex (indicated by an arrow) and cleavage furrow (arrowhead) at anaphase and telophase. B. Localization of transiently transfected full-length zipper. Zipper localization is shown by anti-Hemoagglutinin (HA) epitope antibody staining; mitotic marker is by anti-phospho-histone H3 (PH3) antibody. C. Localization of the zipper motor domain. D. Localization of the zipper tail domain. E. The zipper filament assembly domain (AD; amino acid residue 1849-1940) is not recruited to the cortex. F-actin is shown by FITC-phalloidin staining to highlight the cell cortex area. F. Expression of the assembly domain in S2 cells. The scale bar represents 3 μm.

### *The zipper filament assembly domain is not recruited to the cortex*

In order to determine the elements of the tail domain required for cortical targeting, we first examined the localization properties of the AD as it is recruited to the cleavage furrow in *Dictyostelium*. Interestingly, we find that the AD (1849-1940) is unable to be targeted to either the interphase cortex or the cytokinetic cleavage furrow in S2 cells but instead remains in the cytoplasm throughout the cell cycle (Fig. 3E), although it is expressed properly, as assayed by anti-HA western blotting (Fig. 3F). The inability of the filament AD to localize indicates that either it doesn't form filaments in the cell or AD filaments cannot target to the cortex.

### *Interphase cortical localization does not require the assembly domain*

As the assembly domain is not recruited to the cell cortex, we examined other tail domain regions for their ability to localize to the interphase cortex and the cytokinetic cleavage furrow. Analysis of a series of tail domain regions reveals an interphase cortical targeting domain (iCTD) that is almost entirely distinct from the filament assembly domain. Whereas many tail domain regions remained in the cytoplasm, those that contain residues 1350-1865 efficiently localized to the cell cortex during interphase (Fig. 4A). The iCTD only partially overlaps with the AD indicating that the AD, and presumably the ability to form filaments, is dispensable for localization to the interphase cortex.

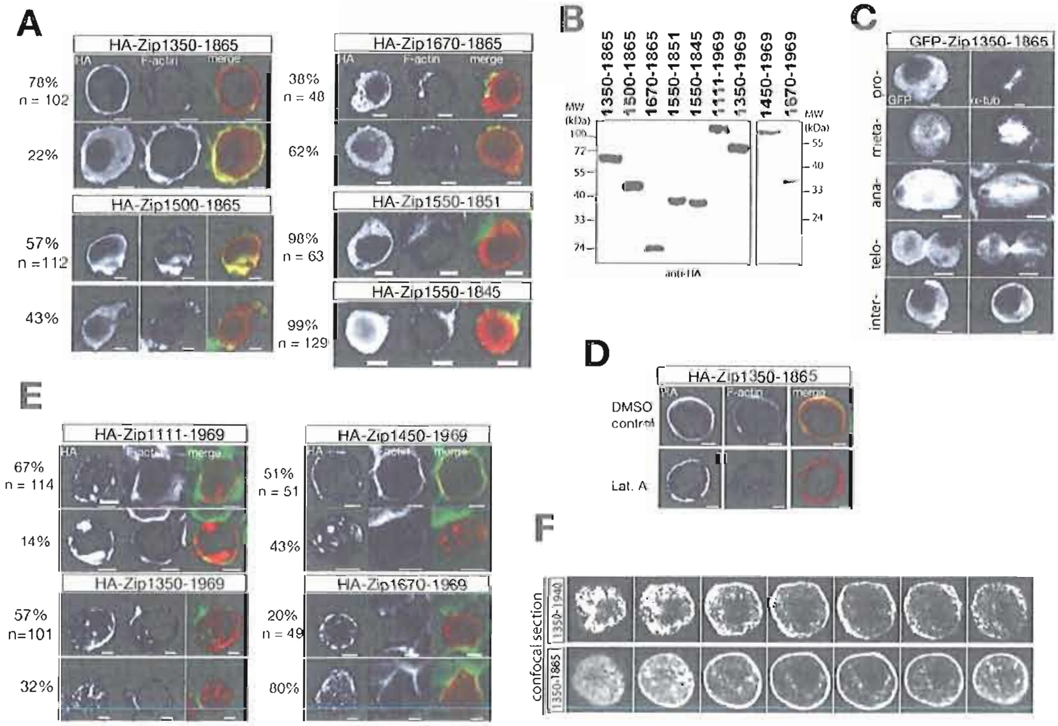
A
HA-Zip1350-1865
HA
F-actin
merge
78%
n = 102
22%
HA-Zip1500-1865
57%
n = 112
43%
HA-Zip1670-1865
38%
n = 48
62%
HA-Zip1550-1851
98%
n = 63
HA-Zip1550-1845
99%
n = 129
B
MW (kDa)
100
72
55
40
33
24
1350-1865
1500-1865
1670-1865
1550-1851
1550-1845
1111-1969
1350-1969
1450-1969
1670-1969
MW (kDa)
55
40
33
24
anti-HA
C
GFP-Zip1350-1865
GFP
α-tub
pro-
meta-
ana-
telo-
inter-
D
HA-Zip1350-1865
HA
F-actin
merge
DMSO control
Lat. A
E
HA-Zip1111-1969
HA
F-actin
merge
67%
n = 114
14%
HA-Zip1450-1969
51%
n = 51
43%
HA-Zip1350-1969
57%
n=101
32%
HA-Zip1670-1969
20%
n = 49
80%
F
confocal section
1350-1940
1350-1865

Figure 4. **An interphase cortical-targeting domain in the zipper tail.** A. The zipper interphase cortical targeting domain (iCTD) encompasses residues 1350-1865. Transiently transfected zipper tail region localization is shown by anti-hemoagglutinin (HA) epitope antibody staining; F-actin is by FITC-phalloidin. B. Expression of several tail domain regions as assayed by anti-HA western blotting. Expression levels reflect the transfection efficiency of ~17% for 1111-1969 and 1350-1969 but lower to ~9% for 1450-1969 and 1670-1969. C. The iCTD localizes to the cytoplasm during mitosis. Transiently transfected zipper and endogenous alpha-tubulin, visualized by GFP tag and anti-alpha-tubulin antibody staining, are shown in cells at different cell cycle stages. D. F-actin is not required for iCTD localization. Cells treated with latrunculin A (Lat A) or solvent alone (DMSO), are shown with anti-HA (zipper) and FITC-phalloidin staining. E. Inclusion of the assembly domain leads to the formation of cortical aggregates. F. Confocal sections of the iCTD (1350-1865) and iCTD+AD (1350-1940). The scale bar represents 3 μm.

Truncation of the iCTD at the $NH_2$-terminus causes the tail domain to localize less efficiently such that by residue 1670 it is predominantly cytoplasmic (1670-1865), however intermediate length tail domain regions such as 1500-1865 still show partial cortical localization (Fig. 4A) when each is transfected at ~20% efficiency and expressed at roughly equivalent levels (Fig. 4B). The COOH-terminal iCTD boundary is more defined such that truncation from residue 1865 to residue 1851 is sufficient to abolish cortical localization. As large regions of the tail domain were unable to localize to the cortex, we conclude that interaction with endogenous zipper (through mixed coiled coils) is not sufficient to specify localization.

Although the iCTD region of the zipper tail domain efficiently localizes to the cortex during interphase, it is not recruited to and enriched at the cleavage furrow during cytokinesis (Fig. 4C and movie S1). Early in mitosis, the strong cortical localization of the iCTD is lost (movie S2) and becomes predominantly cytoplasmic where it remains until the end of cytokinesis.

A hallmark of the cell cortex is the presence of dense meshwork of F-actin below the cell membrane. To test if cortical F-actin is required for iCTD localization, we treated S2 cells with Latrunculin A (Lat A). As shown in Figure 4D, treatment with Lat A leads to loss of cortical F-actin as assayed by a loss of FITC-phalloidin staining. However, Zipper iCTD proteins are still targeted to the cortex despite the loss of F-actin. Thus, the zipper iCTD cortical anchor is not F-actin and is not dependent on the presence of F-actin.

When the ability to form filaments is restored to the iCTD by adding the AD, localization occurs predominantly to the cortex, but rather than the uniform distribution observed with the iCTD alone, localization is in cortical patches (Fig. 4E,F). As the patches correlate with the presence of the AD these discrete structures may result from assembly of the tail region into filaments. In addition, they appear similar to the cortical patches of the *C. elegans* heavy chain NMY-2 in the early embryo.

### *Cleavage furrow localization requires the filament assembly domain*

We next asked what region of the tail domain is sufficient for cleavage furrow localization as the iCTD becomes cytoplasmic during mitosis. As expected, the tail domain fragment 1350-1940 (iCTD + AD) localizes to the cleavage furrow like the full-length zipper during mitosis (Fig. 5A). Truncation of the zipper tail domain at the N-terminus does not inhibit furrow-targeting ability until residue 1744 (Fig. 5E). Regions that encompass the AD, and approximately 100 more residues (1744-1969), which constitute a furrow-targeting domain (FTD) (Fig. 5D), efficiently localize to the cleavage furrow during cytokinesis (Fig. 5 & movie S3). As this region lacks the complete iCTD, it fails to target to the cortex during interphase but does form cytoplasmic aggregates, consistent with its ability to form filaments (Fig. 5B). Interestingly, a region of the tail that includes the FTD and the non-helical tailpiece (1744-2011) localizes to the cytoplasm but fails to form aggregates indicating that this region may be involved in filament assembly regulation (Fig. 5C).

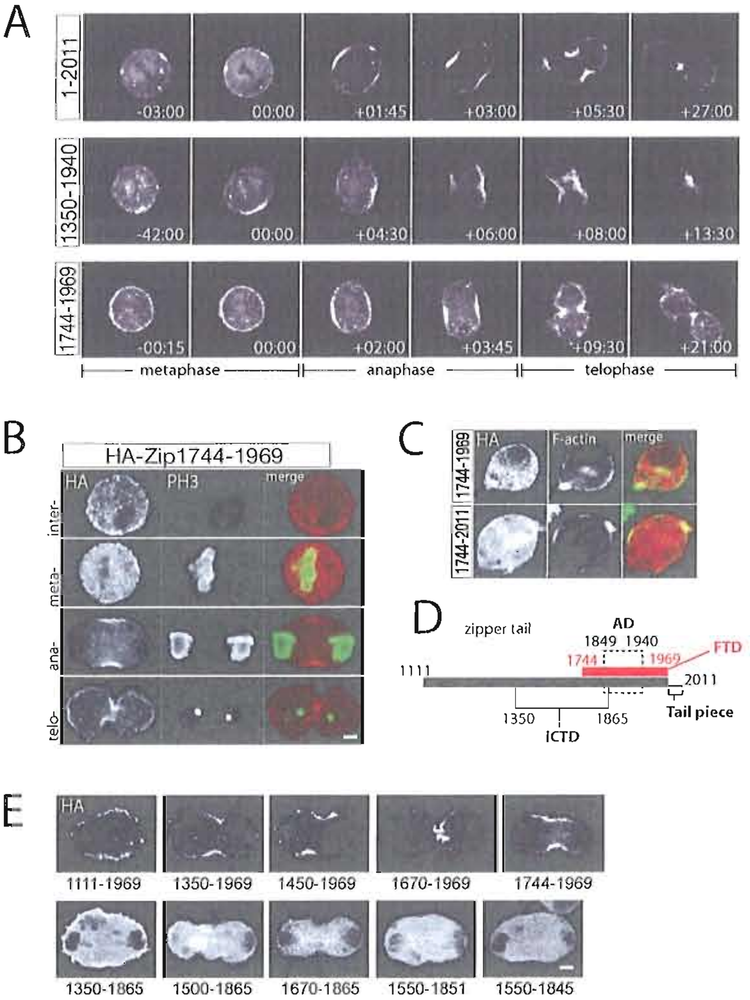
A
1-2011
-03:00
00:00
+01:45
+03:00
+05:30
+27:00
1350-1940
-42:00
00:00
+04:30
+06:00
+08:00
+13:30
1744-1969
-00:15
00:00
+02:00
+03:45
+09:30
+21:00
metaphase
anaphase
telophase
B
HA-Zip1744-1969
HA
PH3
merge
inter-
meta-
ana-
telo-
C
1744-1969
1744-2011
HA
F-actin
merge
D
zipper tail
AD
1849 1940
1744
1969
FTD
1111
2011
1350
1865
Tail piece
ICTD
E
HA
1111-1969
1350-1969
1450-1969
1670-1969
1744-1969
1350-1865
1500-1865
1670-1865
1550-1851
1550-1845

Figure 5. **The zipper cleavage furrow-targeting domain.** A. Selected time point of time-lapse imaging of GFP-tagged full-length zipper 1-2011, tail domain 1350-1940 and 1744-1969. The time is shown as min:sec and zero time point is the onset of DNA segregation (movies S3-5). B. A region of the zipper tail that includes the filament assembly domain specifies cleavage furrow targeting. Transiently transfected zipper 1744-1969 and mitotic marker, visualized by anti-HA and anti-phospho-histone H3 (PH3) antibody staining respectively, are shown in cells at different cell cycle stages. C. The non-helical tailpiece disrupts cytoplasmic aggregation of the cleavage furrow-targeting domain. The tail domain region 1744-1969 forms cytoplasmic aggregates, but the same region that also includes the non-helical tailpiece (1744-2011) does not. Zipper tail domains and F-actin are shown with anti-HA and FITC-phalloidin staining. D. The relative position of interphase cortical targeting domain (iCTD), assembly domain (AD) and furrow targeting domain (FTD) locate in zipper tail region. E. Cleavage furrow targeting requires AD. Anaphase cellular localization of different tail domain constructs is shown by anti-HA staining. The mitotic marker PH3 staining is not displayed, but the spindle poles are clear in cells in lower panel. The scale bar represents 3 μm.

We observed cortical puncta of fragment 1350-1940 (iCTD + AD) throughout the cell cycle (Fig. 4E & 5A), rather than only at late metaphase and anaphase like endogenous myosin II (Fig. 3A & 5B) either because of increased protein levels, or misregulation due to the presence of the iCTD but lack of head and light chain binding domains.

## Discussion

Myosin II undergoes dynamic filament assembly and localization during cell division and other processes. While the molecular mechanism of these dynamics is fairly well understood in *Dictyostelium,* it is less clear in higher organisms that lack myosin heavy chain kinase (MHCK). To contribute to our understanding of myosin II filament assembly and localization in higher organisms, we have examined the filament assembly and localization properties of the *Drosophila* non-muscle myosin II.

### *Filament assembly determinants*

Of the greater than 1000-residue zipper tail domain, only a 90-residue segment is required to assemble into oligomers that are disrupted by high salt, similar to filament assembly domains from various organisms (11,13-15,31). The 90-residue zipper AD does not include the non-helical tailpiece and is close to the end of coiled-coil rod (Fig. 2A). Based on sequence comparison, the zipper AD encompasses the assembly competence domain (AD) of sarcomeric myosin II and overlaps the second assembly competence domain of human non-muscle myosin IIb, but is distinct from the region that is critical for assembly of vertebrate smooth muscle myosin II (31). There is low sequence homology between zipper and *Acanthamoeba* or *Dictyostelium* myosin II heavy chain tail domain beyond the presence of a heptad repeat.

Different models have been proposed to illustrate the specific domain associated with filament assembly. *Acanthamoeba* myosin II heavy chain required the C-terminal 14 heptads repeats plus the tailpiece to initiate bipolar filament assembly through hydrophobic as well as electrostatic interactions (14). The AD of *Dictyostelium* myosin II heavy chain is a 35-residue region within an extended assembly domain flanked by two regions containing alanines in core “a” and “d” heptad positions, with phosphorylation of three threonine residues controling filament formation by folding back the tail (11,13). The 29-residue AD of vertebrate sarcomeric myosin II has the characteristic of clustered negatively charged residues in the center, flanked by positively charged residues on each side (16). Negatively charged and positively charged assembly competence domains from human non-muscle myosin IIB are located 100 residues apart, and antiparallel electrostatic interactions between these domains are essential for filament nucleation (15). The *Drosophila* zipper AD identified in this study possesses an evenly distributed alternating charge repeat, and is necessary and sufficient to oligomerize *in vitro* (Fig. 2).

The lack of a consensus filament assembly model among different myosin IIs may be due to the considerable diversity in filament properties essential for the wide range of cellular activities within various cell types. However, investigation of the interaction between identified assembly domains and other interacting sites should reveal the general principles of filament assembly. The zipper tail domain possesses an alternating charge repeat that is thought to be important for filament assembly. This charge repeat is more evenly distributed in the AD than the rest of the tail, which fails to assemble into filaments (Fig. 2C). We are currently undertaking a mutational analysis to test the importance of the charge repeat in filament stability.

### *Localization determinants*

We have found that interphase and mitotic cortical localization in S2 cells require distinct tail domain elements. In interphase S2 cells, myosin II partitions between cortical and cytoplasmic pools, but the targeting domain that we have identified (iCTD) is biased towards cortical localization (Fig. 3A,B & 4A,C). This suggests that cortical targeting is regulated during interphase. The iCTD does not contain the filament AD so we expect that it does not form filaments in the cell. Thus, at least one mode of interphase cortical targeting utilizes a mechanism that does not require filament assembly. However, when the iCTD is combined with the filament AD, the localization becomes punctate rather than the even distribution observed with the iCTD alone (Fig. 4A,F). It has been observed that deletion of the AD of α-cardiac MYH expressed in COS cells abolished the formation of a needle-shaped structure (16). Surprisingly, inclusion of the non-helical tailpiece causes this punctate localization to be lost, although we observed no effect of the tailpiece on the *in vitro* filament assembly characteristics (Fig. 1B & 5C). If punctate localization represents filament assembly, which is supported by the correlation of punctate localization with the presence of the AD, then the tailpiece may be involved in regulating filament assembly.

Myosin II localization becomes very dynamic during mitosis, and these dynamics appear to be important for function. For example, photobleaching experiments in *Dictyostelium* have shown that myosin II dynamically cycles between the cytoplasm and furrow, and that this cycling requires filament assembly and disassembly (34). In S2 cells myosin II is highly regulated (35) and is not detected on the cortex early in mitosis, but forms dynamic cortical aggregates at the metaphase to anaphase transition and ultimately forms a concentrated band around the central spindle that becomes the cleavage furrow (Fig. 3A & 5A). The initial recruitment of myosin II to the F-actin rich equatorial cortex requires myosin regulatory light chain phosphorylation through Rho1 signaling (35, 36). Since the recruitment of myosin to the equatorial cortex during mitosis is independent of F-actin, it is likely that the role of regulatory light chain is to regulate myosin II filament assembly rather than its actin-dependent ATPase activity. Our data shows that non-muscle myosin II filament formation is essential for cleavage furrow localization and requires the zipper AD, but localization to the interphase actin cortex is independent of filament assembly (Fig. 4 & 5). Consistent with this, the AD of vertebrate smooth muscle and human non-muscle myosin IIa is required for furrow localization in COS cells (31).

Surprisingly the minimum filament AD (1849-1940) that forms filaments *in vitro* fails to localize to the cortex at any stage of the cell cycle (Fig. 3E). However, a slightly larger region (1744-1969), the furrow-targeting domain (FTD), efficiently localizes to the cleavage furrow (Fig. 5A,B). It is unlikely that these tail fragments localize to the cleavage furrow through mixed coiled-coils with endogenous myosin since several long tail domain fragments including the iCTD were not recruited to the cleavage furrow.

However, based on our data, we cannot rule out the possibility that these tail fragments are recruited to the cleavage furrow through oligomerization with endogenous myosin II.

What is the cortical anchor that recruits myosin II? Few proteins have been identified that bind the heavy chain tail domain. Possible cortical anchors include membrane phospholipids as the tail domain of mammalian non-muscle myosin IIs have been shown to bind phosphatidyl serine containing liposomes (37). Another candidate is the tumor suppressor Lethal (2) giant larvae (Lgl), which binds the myosin II tail domain and is cortically associated with the cytoskeleton (38). Given that we have observed different requirements for interphase and mitotic cortical localization, it is likely that cortical recruitment in these two contexts utilizes distinct anchoring mechanisms. Future work will be directed at the identification of the cortical anchoring factors, and possible filament regulatory mechanisms. The reagents described here should be useful in this regard.

## Materials and methods

### *Molecular cloning, protein expression and purification*

Zipper regions were subcloned using a plasmid containing the full-length Zipper B sequence that was kindly provided by Dan Kiehart (19). Zipper regions were expressed in *E. coli* using the pET-19b derivative pBH which places a hexahistidine purification tag followed by a tobacco etch virus (TEV) protease cleavage site at the $NH_2$-terminus of the expressed protein (30). Hexahistidine fusion proteins were purified using Ni-NTA resin and standard protocols. Ion-exchange chromatography was used to further purify proteins if necessary. Purified proteins were dialyzed extensively against salt-free buffer (10 mM Tris, pH 8.0; 1 mM DTT; 1 mM EDTA) at 4°C. Purity was established using SDS-PAGE and/or MALDI-TOF mass spectrometry.

### *Assembly assays*

For the solubility assay, we incubated zipper tail regions at 20 μM at a range of salt concentrations in 10 mM Tris, pH 8.0; 1 mM DTT; 1 mM EDTA for 30 minutes at 4°C followed by centrifugation at 100,000 x *g* for 30 minutes. We then separated the soluble and insoluble phases and loaded equal volumes for analysis by SDS-PAGE. We used ImageJ (NIH) to determine relative protein amounts from scanned, coomassie brilliant blue stained gels.

For the fluorescence resonance energy transfer (FRET) assay, we expressed and purified CFP and YFP $NH_2$-terminal zipper fusions separately and mixed them in equal molar proportions to a total fluorescent protein-zipper fusion concentration of 20 μM. We then acquired fluorescence emission spectra at a range of salt concentrations on an ISS PC1 spectrofluorometer with an excitation wavelength of 433 nm and a slit width of 0.5 nm. The sample temperature was maintained at 20°C using a circulating water bath.

### *Cell culture and transfection*

We transiently transfected *Drosophila* S2 cells grown in Schneider's insect medium supplemented with 10% fetal bovine serum with the pMT/V5-HisA vector (Invitrogen) containing hemagglutin (HA) or enhanced green fluorescent protein (EGFP)

$NH_2$-terminal fusions to zipper regions. The *Drosophila* embryo derived Schneider cell line (S2) was maintained in Schneider's insect medium supplemented with 10% heat-inactivated fetal bovine serum at room temperature. For transient expression of zipper fragments, between 1 and 3.5 million cells at fast growing stage were transfected with 0.8 ug of plasmid DNA using Effectene reagent (Qiagen) in 6-well plate. After 16 hours recovery cells were induced with 0.5 mM $CuSO_4$ for 16-24 hours and subject to detecting proteins expression by Western blot or fixing and immunofluorescence staining.

### *Immunofluorescence and imaging*

To determine localization of endogenous and ectopic Zipper, S2 cells were settled down on No.1.5 coverslip and fixed with 4% paraformaldehye for 10 minutes. After fixing, cells were permeabilized and blocked in blocking solution (1X PBS, 0.1% Triton-X, 1% BSA, 10 mM Glycine and 0.02% $NaN_3$), followed by incubations with primary and then secondary antibodies diluted in the blocking solution. Phalloidin-FITC (Invitrogen-Molecular Probes) was added to stain F-actin. All procedures were performed at room temperature. The stained cells were mounted in Vectashield with DAPI (Vector Laboratories). For drug treatment, cells were transferred to medium containing 20 uM Latrunculin A (Sigma) or the parallel DMSO control for 30 minutes before fixation. The primary antibodies used include rabbit polyclonal anti-Zipper (raised against a.a. 1670-1851) at 1:2500, anti-phosphohistone H3 (Upstate) at 1:500, mouse monoclonal anti-HA (Covance) at 1:1000 and anti-α-tubulin (DM1A, Sigma-Aldrich) at 1:500. The secondary antibodies used include goat anti-rabbit IgG-Cy3, donkey anti-mouse IgG-Cy3 (Jackson

ImmunoResearch) and goat ant-rabbit IgG-AlexaFluo594 (Invitrogen-Molecular Probes). Images were taken using a Nikon D-Eclipse C1 inverted confocal microscope using either a 40X air or 60X oil immersion objective.

### *Time-lapse imaging*

For following localization of GFP tagged zipper tail domain, transfected S2 cells were imaged using a Perkin Elmer spinning disk confocal mounting on a Nikon Eclipse TE2000-U inverted microscope. A 60X oil immersion objective was used to collect 3-5 z steps at 1 μm intervals every 15-60 seconds using Metamorph software. All data were processed by Image J and reconstructed into Quicktime movies.

## Bridge to Chapter III

Chapter II discussed the identification of subdomains within the *Drosophila* non-muscle myosin II, zipper, coiled-coil tail domain that mediates distinct functions of this domain. A 90-residue region (1849-1940) of the tail domain was found to be necessary and sufficient for filament formation. Another region (1350-1865) mediates localization of zipper to the interphase cortex. However, a distinct domain (1744-1969) mediates the targeting of zipper to the cleavage furrow during cytokinesis. The ability of zipper to form filaments is thought to be important for targeting to the cleavage furrow. Thus, its not surprising that this furrow targeting domain encompasses the assembly domain. It is unclear how assembly domains interact to form filaments. Chapter III will go on to discuss the role of assembly domains in tail-tail interactions during filament assembly.

# CHAPTER III

# MECHANISM OF ASSEMBLY DOMAIN MEDIATED TAIL-TAIL INTERACTIONS IN NON-MUSCLE MYOSIN II FILAMENT ASSEMBLY

The testing of mutant zipper fragments was carried out by a number of lab members, including Natasha Fewkes, Ryan Frei, and myself. Natasha Fewkes and Ryan Frei contributed substantially to this work by verifying results collected for several mutant zipper fragments. I was the primary contributor to the testing of the ability of mutant zipper fragments to form filaments *in vitro*.

## Introduction

Myosin is a superfamily of actin-based molecular motors that convert the chemical energy of ATP hydrolysis into mechanical work. Myosin II or conventional myosin, one of the best-studied members of the superfamily, is unique in its ability to generate contractile forces that are important for processes such as muscle movement. In non-muscle cells, dynamic myosin II activity is important for regulating cell shape, cortical rigidity, cell migration, and cytokinesis (Young et al., 1993; Shelden and Knecht, 1996; Hickson et al., 2006; Martens and Radmacher, 2008; Pollard, 1981; Ridley et al., 2001; Glotzer, 2005; Robinson and Spudich, 2004). Although myosin IIs contain an actin binding motor domain that is very similar to other myosins, its ability to generate contractile forces arises from the assembly of individual myosin II monomers into bipolar filaments with the motor domains arranged in opposite orientations (such that actin filaments are moved in opposite directions by the set of heads at each end).

Myosin II molecules are hexamers containing two heavy chains, two essential light chains, and two regulatory light chains. The myosin heavy chain is comprised of a head region (actin binding, ATPase, force generation), a neck region (light chain binding), and a large coiled-coil tail domain that mediates both dimerization of the heavy chains and is sufficient for bipolar filament assembly (Lowey et al., 1969). Spontaneous and rapid filament assembly of the tail domain suggests that all the information needed to form this important cellular structure is contained within the tail itself. Assembly of myosin molecules into bipolar filaments is salt dependent, which is consistent with electrostatic interactions between tail domains being the principle driving force for filament assembly. The sequence of the tail domain reveals a heptad repeat that is characteristic of coiled-coils, and a 28 residue charge repeat with alternating zones of negatively and positively charged residues that is thought to be important for the packing of the tail domains into the filament backbone (Parry, 1981; McLachlan and Karn, 1982; Atkinson and Stewart, 1992). Indeed the widely reported molecular staggers of approximately 14.3 nm and 43 nm found in filaments from various myosin isoforms correspond to favorable overlaps of this charge repeat (Lowey et al., 1969; Kendrick-Jones et al., 1971; Niederman and Pollard, 1975; Trybus and Lowey 1984; Trybus and Lowey, 1987; Cross et al., 1991; Atkinson and Stewart, 1992).

Despite the conserved charge repeat along the entire tail, most tail segments are not competent to form filaments. In all myosin II isoforms studied, a small region of the tail domain (assembly domain), usually near the C-terminus, is required and often sufficient for filament assembly (Nakasawa et al., 2005; Sohn et al., 1997; Nyitray et al., 1983; Cross and Vandekerckhove, 1986; Atkinson and Stewart, 1991; Cohen and Parry 1998; Ikebe et al., 2001; Rosenburg et al., 2008; Liu et al., 2008). Assembly domains are unique due to an even charge distribution and an overall more positive charge than the rest of the tail (Rosenberg et al., 2008; Liu et al., 2008). Our understanding of how assembly domains interact to form filaments is relatively advanced in *Dictyostelium* and *Acanthamoeba* (O'Halloran et al., 1990; Lee et al., 1994 Hostetter et al., 2004; Shoffner and De Lozanne, 1996; Sinard et al., 1989; Sinard et al., 1990; Turbedsky and Pollard, 2005). However, these protozoan myosins have little sequence homology to invertebrate and vertebrate myosins (Hodge and Cope, 2000; Liu et al., 2008). Nakasawa et al. recently proposed an interesting structural model for binary parallel and anti-parallel interactions of short C-terminal fragments. In this model positively charged residues in a region that corresponds to an assembly domain interacts with negatively charged residues upstream, forming a second complementary assembly domain (Nakasawa et al., 2005). However, the precise residues within the assembly domain that are required for filament formation have not been identified for any myosin II. Such information would indicate the tail-tail interactions that are critical for assembly, which could lead to a complete structural model of the filament, as the base structure of individual monomers is known to be a coiled-coil.

We previously identified the filament assembly domain (1849-1940) of *Drosophila* non-muscle myosin II heavy chain, zipper. Here we have undertaken a comprehensive mutagenesis study of the zipper assembly domain to identify residues required for filament assembly. We have combined the results of these experiments with electrostatic calculations of the tail domain to determine how assembly domains interact, identify critical interactions in important binary tail-tail interactions, and explain the multiplicity of interactions that occur in a myosin bipolar filament. Based on these studies we propose a model in which multiple stable overlaps of the tail are possible. These overlaps are determined by the position of a specific positively charged region within the assembly domain relative to the interacting filament. By examining which of these overlaps are possible within the context of a minifilament, we have been able to construct a three-dimensional structural model of the non-muscle myosin bipolar minifilament that, to our knowledge, is consistent with all physical observations and provides a framework for understanding the detailed mechanism by which this contractile force-generating machine is constructed.

## Results

### *Identification of assembly domain elements critical for filament assembly*

We previously identified a 90-residue region (1849-1940) of the *Drosophila* non-muscle myosin II tail domain that was both necessary and sufficient for filament assembly (Liu et al., 2008). The length of the assembly domain (AD) corresponds to approximately one superhelical coiled-coil turn and we hypothesized that shorter segments may have unstable coiled-coils. Thus, regions within the assembly domain may only serve to stabilize the coiled-coil dimer and not contribute significantly to tail-tail interactions.

To determine if the entire assembly domain (AD) is required for filament assembly we made several tail domain constructs that lack short sections of the assembly domain but in the context of a larger tail fragment (1744-2011) that forms robust coiled-coils (Liu et al., 2008). We deleted regions of the assembly domain, with windows of 28 residues to preserve the heptad repeat and the 28-residue charge repeat, to narrow down specific sequences that are critical for filament formation (Figure 1A). We tested these tail domain fragments that form coiled-coils but lack portions of the assembly domain for their ability to form filaments using a salt-dependent filament assembly assay that exploits the fact that filaments and paracrystals sediment upon centrifugation, but unassembled coiled-coil dimers remain soluble (Hostetter et al., 2004; Liu et al., 2008). For these experiments we used proteins containing fluorescent protein “heads” that restore the bipolar filament nature of assembled tail fragments, but do not occlude filament formation of fragments of this length (Hostetter et al., 2004; Liu et al., 2008) (Figure 1, B and C). For the tail fragment 1744-2011, filament formation is highly salt dependent, only assembling at intermediate salt concentrations (Figure 1, B and C). Deletion of the first 1/3 of the assembly domain (Δ1850-1877) does not alter the ability of this fragment to sediment in a salt-dependent manner. Deletion of residues (1913-1940), which corresponds to the sarcomeric myosin assembly competence domain (Sohn et al., 1997) and most of the second assembly competence domain of human non-muscle myosin IIb (Nakasawa et al., 2005), resulted in solubility throughout the salt concentration range, indicating a loss of filament assembly. Also, deletion of a segment upstream (1878-1905) completely disrupted filament assembly (Figure 1, B and C).

It has been suggested that a region c-terminal to the assembly domain could be important for filament formation (Ikebe et al., 2001). We found that c-terminal truncation up to the assembly domain does not greatly disrupt filament assembly (Figure 1, B and C). However, the salt-dependent characteristics of filament assembly are slightly altered, such that at physiological salt concentrations, few filaments would form (Figure 1, B and C). Thus, it appears the C-terminal 2/3 of the assembly domain (1878-1940) appears to be critical for filament assembly whereas the remainder is dispensable. Interestingly, this region corresponds to conserved assembly domains discovered in previous studies, suggesting that the assembly domain function in the formation of different types of filaments is conserved across myosin II isoforms and species (Figure 1D)(Sohn et al., 1997; Nakasawa et al., 2005; Ikebe et al., 2001).

Although the entire tail domain displays a repeating charge pattern, it displays an overall negative charge (Liu et al., 2008). Rosenburg et al. found that the entire C-terminal segment of human non-muscle myosin IIb tail, that displayed a net positive charge, was necessary for filament assembly (Rosenburg et al., 2008). Similarly, we have identified a sub-region within the assembly domain of *Drosophila* non-muscle myosin that occurs in the most positively charged region of the tail domain. This supports the idea that the unique charge profile of this segment of the tail is important for filament assembly.

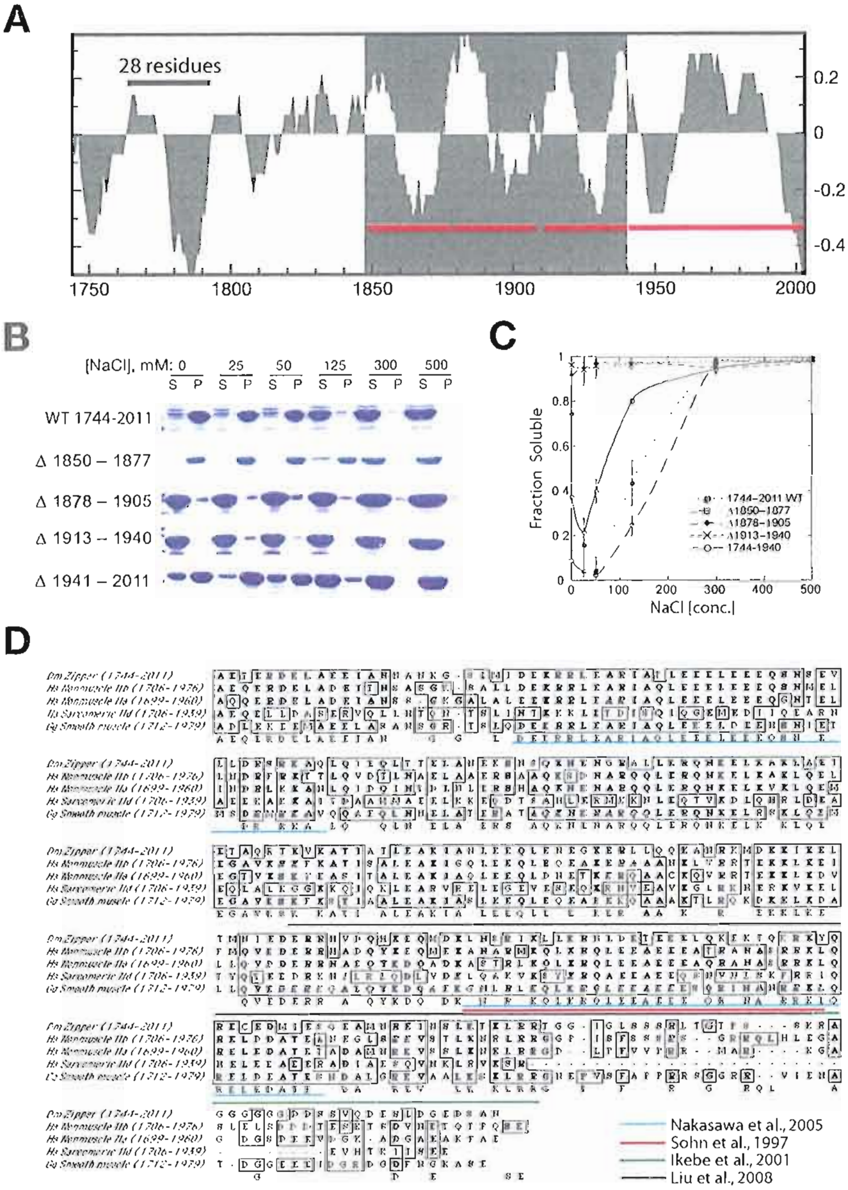

Figure 6. **Identification of conserved subregions of the assembly domain that are important for filament assembly.** A, Charge repeat structure of zipper tail fragment-1744-2011calculated with a 15-residue window. Regions targeted for deletion are marked by red lines. B, Filament pelleting assay of tail fragments with various deletions. S, supernatant fraction; P, pellet fraction. C, Quantification of solubility of deletion constructs shown in panel B. Error bars represent S.D. from three independent experiments. D, Sequence alignment of zipper tail fragment-1744-2011 with analogous regions from other myosin II isoforms from different organisms. Regions indispensible for filament assembly from other studies are outlined.

### *Identification of residues critical for bipolar filament assembly*

The assembly domain has been identified in a large number of myosin tail domains from a variety of organisms (Nakasawa et al., 2005; Sohn et al., 1997; Nyitray et al., 1983; Cross and Vandekerckhove, 1986; Atkinson and Stewart, 1991; Cohen and Parry 1998; Ikebe et al., 2001; Rosenburg et al., 2008; Liu et al., 2008; O'Halloran et al., 1990; Lee et al., 1994 Hostetter et al., 2004; Shoffner and De Lozanne, 1996; Sinard et al., 1989; Sinard et al., 1990; Turbedsky and Pollard, 2005). However, our understanding of how tail domains interact with one another to form highly ordered assemblies is rudimentary. To better understand the interactions of these unique tail fragments, we decided to define the determinants of filament assembly down to the amino acid level. To do this we used site-directed mutagenesis to reverse the charge of individual or clusters of residues within the previously described tail fragment (1744-2011) that robustly forms filaments *in vitro*.

Like other coiled-coils, the tail domain contains a heptad repeat pattern of residues (a, b, c, d, e, f, g). Residues in the a and d positions of the amphipathic α-helices constitute a buried hydrophobic seam that forms the dimer interface (Figure 2A). The rest of the positions are generally polar or charged, and likely form interaction surfaces that are utilized during filament assembly (Figure 2, A and B). It is thought that residues in the e and g positions stabilize the coiled-coil through electrostatic interactions (Lupas, 1996; Burkhard et al., 2001), thus we have mostly focused on the remaining b, c, and f positions for site-directed mutagenesis (Figure 2B). It should be noted however, that given the multitude of interactions a tail must make within a filament, the e and g positions also likely participate in tail-tail interactions. Predicting the heptad repeat positions that each residue occupies is important for our directed mutagenesis strategy (Figure 2B). One prediction places a number of charged residues in core a and d positions of this myosin II tail fragment, which has also been observed in other long parallel two-stranded coiled-coil containing proteins, cortexillin I and tropomyosin (Burkhard et al., 2000; McLachlan and Stewart, 1975). In support of this prediction, no skip residues have been predicted or identified within the assembly domain (Offer et al., 1990; Straussman et al., 2005). Fortunately, coiled-coil prediction that places skips in the heptad repeat to avoid charged residues in core positions does not significantly alter the identity of residues in the b, c, and f positions, thus we are confident in the identification of potential interacting residues (Figure 2B). Since tail domains bind through electrostatic interactions, we reversed the charge of residues at these positions to potentially disrupt filament assembly.

We tested the ability of 1744-2011 WT and various mutants to form filaments using the salt-dependent filament assembly assay previously described (Figure 2, C–G). The concentration of myosin or tail fragment it takes to begin to form filaments is called the critical concentration for polymerization. The critical concentration for WT tail fragments is very low. As the tail-tail interactions are weakened, by alteration of the electrostatic pattern of the tail, the critical concentration becomes higher. By using a concentration of 1744-2011 that was several-fold higher than the critical concentration, we were able to classify charge mutations based on their ability to form filaments in a salt-dependent fashion as well as the degree of the disruption (Figure 2, C–G).

Figure 7. **Identification of residues that are important for zipper filament assembly.** A, Model of the coiled-coil folding motif, with spatial organization of residues within the heptad repeat. Adapted from 1D7M (Burkhard et al., 2000). B, Prediction of amino acid identities of heptad repeat positions within the coiled-coil tail fragment-1744-2011. b, c and f positions of the heptad repeat are in spatial locations available for tail-tail interactions, and are targeted for site-directed mutagenesis. C, Pelleting assay for mutation-containing tail fragments. Examples of wild-type and mutations that have no effect, intermediate effect and strong effects on the ability to form filaments are shown. D–G, Quantification of solubility properties of mutation-containing tail fragments organized by location of mutation in distinct tail regions. Error bars represent S.D. from three independent measurements. H, Schematic of the location, within the charge repeat structure of 1744-2011, of mutations that disrupt filament assembly.

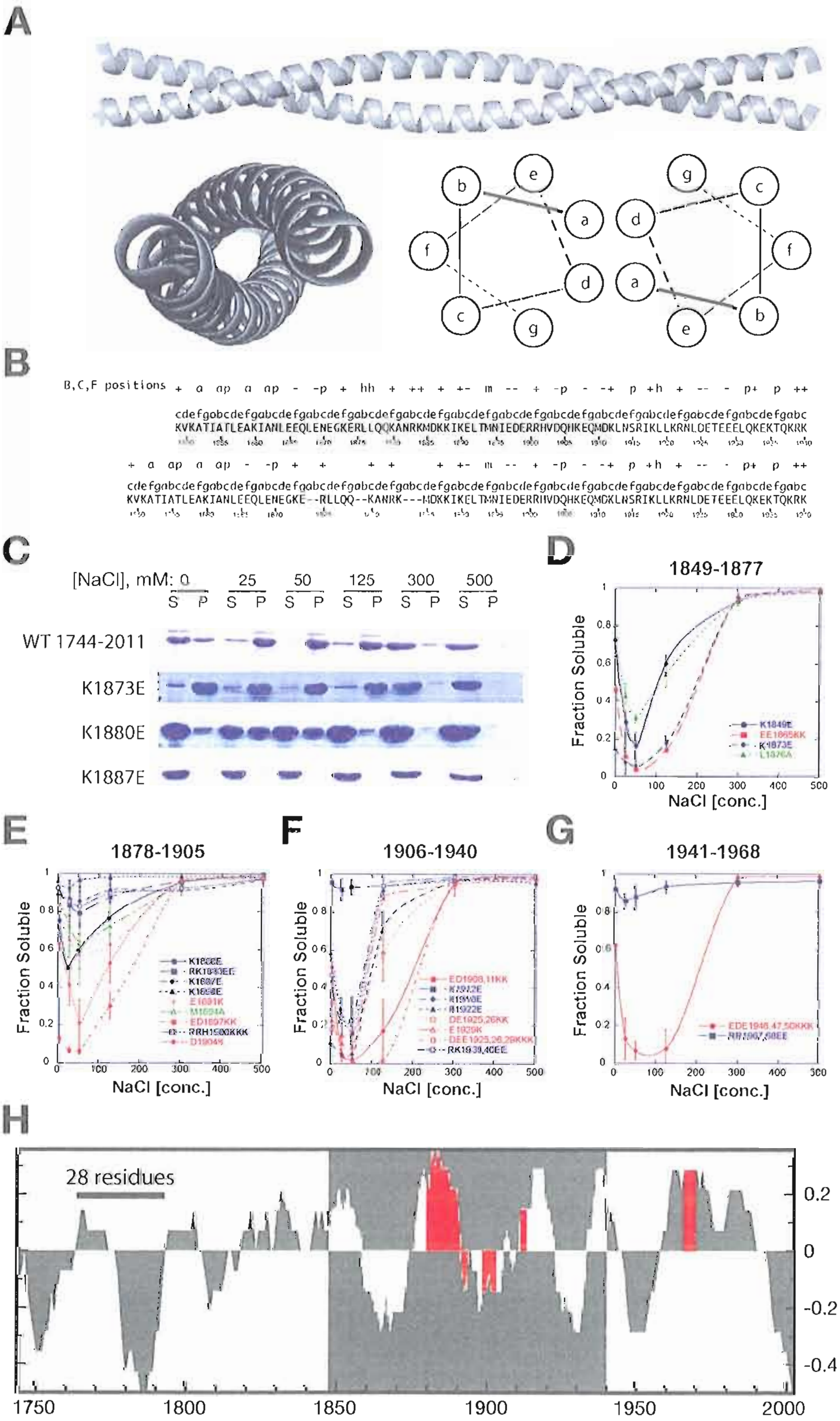
A
b
e
a
d
f
c
g
g
c
d
f
a
b
e
B
B,C,F positions + a ap a ap - -p + hh + ++ + +- m -- + -p - -+ p +h + -- - p+ p ++
cdefgabcdefgabcdefgabcdefgabcdefgabcdefgabcdefgabcdefgabcdefgabcdefgabcdefgabcdefgabcdefgabcdefgabcdefgabc
KVKATIATLEAKIANLEEQLENEGKERLLQQKANRKMDKKIKELTMNIEDERRHVDQHKEQMDKLNSRIKLLKRNLDETEEELQKEKTQKRK
+ a ap a ap - -p + + + + + +- m -- + -p - -+ p +h + -- - p+ p ++
cdefgabcdefgabcdefgabcdefgabcdefgabcdefgabcdefgabcdefgabcdefgabcdefgabcdefgabcdefgabcdefgabcdefgabcdefgabc
KVKATIATLEAKIANLEEQLENEGKE--RLLQQ--KANRK---MDKKIKELTMNIEDERRHVDQHKEQMDKLNSRIKLLKRNLDETEEELQKEKTQKRK
C
[NaCl], mM: 0 25 50 125 300 500
S P S P S P S P S P S P
WT 1744-2011
K1873E
K1880E
K1887E
D
1849-1877
Fraction Soluble
NaCl [conc.]
K1849E
EE1865KK
K1873E
L1876A
E
1878-1905
Fraction Soluble
NaCl [conc.]
K1880E
RK1883EE
K1887E
K1890E
E1891K
M1894A
ED1897KK
RRH1900KKK
D1904K
F
1906-1940
Fraction Soluble
NaCl [conc.]
ED1908,11KK
K1912E
R1918E
R1922E
DE1925,26KK
E1929K
DEE1925,26,29KKK
RK1939,40EE
G
1941-1968
Fraction Soluble
NaCl [conc.]
EDE1946,47,50KKK
RR1967,68EE
H
28 residues
0.2
0
-0.2
-0.4
1750
1800
1850
1900
1950
2000

Mutations were made throughout the region previously tested with deletion analysis. With the exception of RR1967,68EE, all mutations that significantly disrupted filament assembly occurred within the last 2/3 of the assembly domain (1878-1940), which was identified as important in the previous section (Figure 2, E and F). The RR1967,68EE mutation likely makes an energetically costly electrostatic clash within the filament, though these residues are dispensable for filament assembly (Figure 1, B and C). Most of the mutations that disrupt filament assembly cluster within a 15-residue segment (1880-1894) that has an overall positive charge (Figure 1A and 2E). We confirmed that alteration of residues that disrupted filament assembly did not prevent coiled-coil formation by examining the circular dichroism spectra (data not shown).

### *Role of negatively charged residues in bipolar filament assembly*

The electrostatic interaction of positively charged residues with negatively charged residues provides the energy that causes myosin molecules to spontaneously and rapidly assemble into bipolar filaments with tightly packed tail domains in the filament backbone. It is not surprising that mutation or deletion of positively charged residues and regions disrupts filament assembly since the concentration of positive charge is the unique feature of the assembly domain. However, negatively charged residues that are complementary to these critical regions are necessary to accomplish filament assembly.

To better understand how the critical positively charged residues are contributing to important binary tail-tail interactions we made a structural model of the 1744-1968-tail fragment. There is no structural information for the folding of the non-helical tailpiece;

therefore we omitted it from our model for simplicity. Despite structural similarities, we could not base our model on the structure of tropomyosin, due to the bending of the coiled-coil that allows it to wind around the actin helix (Brown et al., 2001). Instead, we used a coiled-coil segment derived from the structure of the parallel two-stranded coiled-coil trigger site of the actin crosslinker cortexillin I from *Dictyostelium discoideum* to build a coiled-coil backbone (Burkhard et al., 2000; 1D7M). This coiled-coil structure can yield a subunit that can be repeated to build a long, straight coiled-coil backbone (Figure 2A). We then used a mutate function to change the sequence to the 1744-1968 fragment with residues in their appropriate heptad positions and energy-minimized the sidechains (Figure 3A). A skip residue was removed from the sequence prior to mutating to keep the heptad repeat in register (Offer et al., 1990; Straussman et al., 2005).

The energy of electrostatic contacts between two interacting fragments at a center-center spacing of 20Å (Niederman and Pollard, 1975) was calculated using the Poisson-Boltzmann equation. The energy of binary electrostatic interactions was calculated from completely overlapped to non-overlapped molecules in 5Å increments, with sidechain positions energy-minimized at each increment (Figure 3B). The resulting energy profile was normalized against positions of the two tails not interacting in solution to render the excess energy of interaction. The energy of interaction between two tails displays an oscillatory pattern resulting from alternating favorable and non-favorable overlaps of the 28-residue charge repeat (Figure 3B). In both orientations, tail-tail interactions are particularly favorable at certain molecular staggers. In contrast to the parallel orientation, anti-parallel tails display unique interactions as the tails are offset in two different directions. The anti-parallel interaction is characterized by one favorable overlap, and several less stable alternative overlaps (Figure 3B). The parallel interaction is also characterized by one favorable stagger, and a couple of less stable alternative staggers (Figure 3B). The most favorable parallel and anti-parallel offsets is close to the observed 14.3nm and 43nm molecular staggers reported in electron microscopy studies of myosin II (Figure 3, B and C)(Lowey et al., 1969; Kendrick-Jones et al., 1971; Niederman and Pollard, 1975; Trybus and Lowey 1984; Trybus and Lowey, 1987; Cross et al., 1991; Atkinson and Stewart, 1992).

Interestingly, in both the most favorable parallel and anti-parallel interacting staggers, assembly domains do not interact with each other (Figure 3C). Instead, the assembly domain makes contact with a conserved negatively charged segment upstream in the tail domain, reminiscent of the model for tail domain interaction proposed by Nakasawa et al., 2005. Though the parallel offset we describe here is nearly identical to this model, the anti-parallel overlap is shifted by several nanometers (Figure 3C)(Nakasawa et al., 2005). When truncated, the assembly domain alone must self-interact to form filaments using one or more of the less stable alternative overlaps. This could explain our inability to identify negatively charged residues within the assembly domain that are critical for filament assembly.

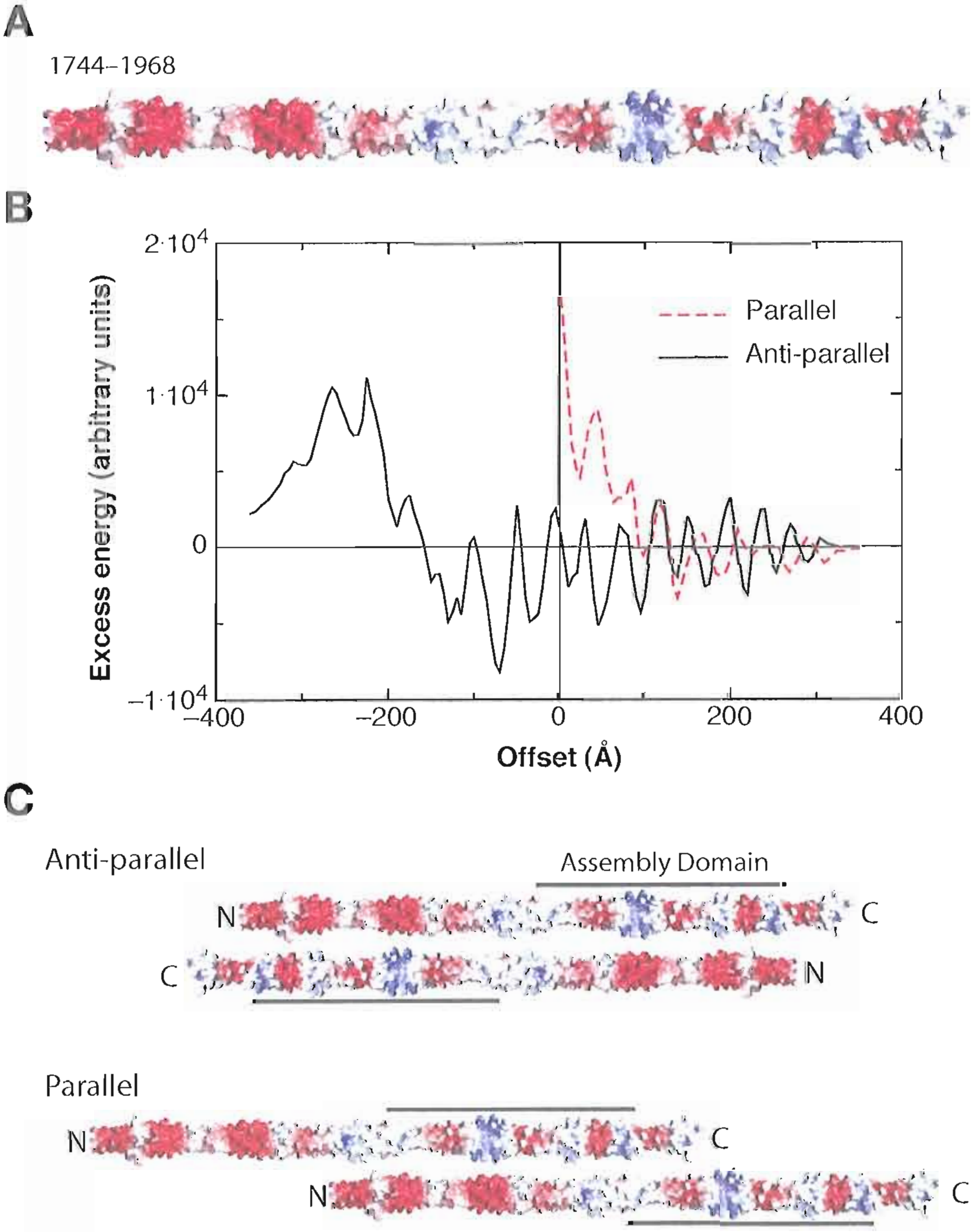

Figure 8. **Structural model and electrostatic calculations of 1744-1968 interactions.** A, Structural model of the 1744-1968 tail fragment based on the coiled-coil strucutre of cortexillin I trigger site (1D7M)(Burkhard et al., 2000). The skip residue, K1849 was removed to keep the heptad repeat in register. B, Interaction energy of electrostatic contacts by two tail fragments in parallel and anti-parallel orientations. These calculations were performed using the Poisson-Boltzmann equation. C, Structural models of stable binary tail fragment interactions in the parallel and anti-parallel orientations.

A conserved negative charge region upstream of the assembly domain was previously found to be important for filament formation (Nakasawa et al., 2005). In contrast, we found that a tail fragment (1800-2011), that is missing the complementary, negatively charged region, is still able to form filaments (Figure 4A). Mutation of either of the negatively charged residue clusters (1749-1750; 1780-1792) also had no effect on filament assembly (Figure 4A). This is consistent with the assembly domain being sufficient for filament assembly. Electrostatic calculations suggest that multiple negatively charged residue clusters could form alternative complementary interaction surfaces to the critical, positively charged regions identified within the assembly domain. Thus, we investigated the structure of a tail fragment containing a mutation in one of the negatively charged regions (Figure 4B).

Like full-length myosin II, tail fragments form ordered aggregates with repeats of 14.3 nm and 43 nm in low-salt buffers (Lowey et al., 1969; Bennett, 1981). Native tail-tail interactions are important for paracrystal formation and packing (Bennett, 1981; Chowrashi and Pepe, 1977). Unfortunately, paracrystals formed by 1744-2011 WT did not grow large, uniform paracrystals (data not shown). The length of the tail fragment impacts its ability to form large, ordered paracrystals (Sohn et al., 1997). Thus we analyzed mutants in the context of a larger fragment (1550-2011) that forms large, ordered paracrystals (Figure 4B). The wild type tail fragment formed paracrystals with a uniform 14.3 nm periodicity (Figure 4B). Tail fragment containing mutations in the n-terminal negative charge region (DEE1749, 50, 53KKK) formed large aggregates robustly (Figure 4A), but the aggregates were not well ordered like wild type (Figure 4B).

The tangled paracrystalline structures formed by this mutant displayed an altered periodicity of approximately 45 nm, suggesting that the mutation altered molecular packing of tail fragments, but did not disrupt assembly (Figure 4B).

Electrostatic calculations suggested that the critical, positively charged region (1880-1894) interacts with a negatively charged upstream region (1780-1792) in both the parallel and anti-parallel oriented interactions, albeit with different residue contacts in each orientation (Figure 3C). Also, another positively charged residue (R1912E) contacts a second negative charge region (1749-1753) in the anti-parallel oriented interaction, but doesn't seem to make a significant electrostatic contact in the parallel oriented interaction (Figure 3C). To confirm these contacts, deleterious mutations within the assembly domain were complemented with oppositely charged mutations in the upstream interacting elements. Mutation of negatively charged residues 1749, 50, 53 to positive residues, completely complemented the mutation of R1912 to a negative residue (Figure 4C). Since these residues only contact each other in the anti-parallel orientation, it seems that the deleterious effect of mutating R1912 occurs during anti-parallel interactions, which likely inhibits filament nucleation (Cross et al., 1991). Interestingly, two types of paracrystalline structures are formed by this double mutant tail fragment (Figure 4D). Both large well-ordered paracrystals displaying a uniform 14.3 periodicity, and tangled paracrystals displaying the altered 45 nm periodicity are observed at low salt (Figure 4D). This suggest that co-mutation of these residues can restore wild-type molecular packing, but that this packing is less stable, leading to a distribution of different molecular arrangements.

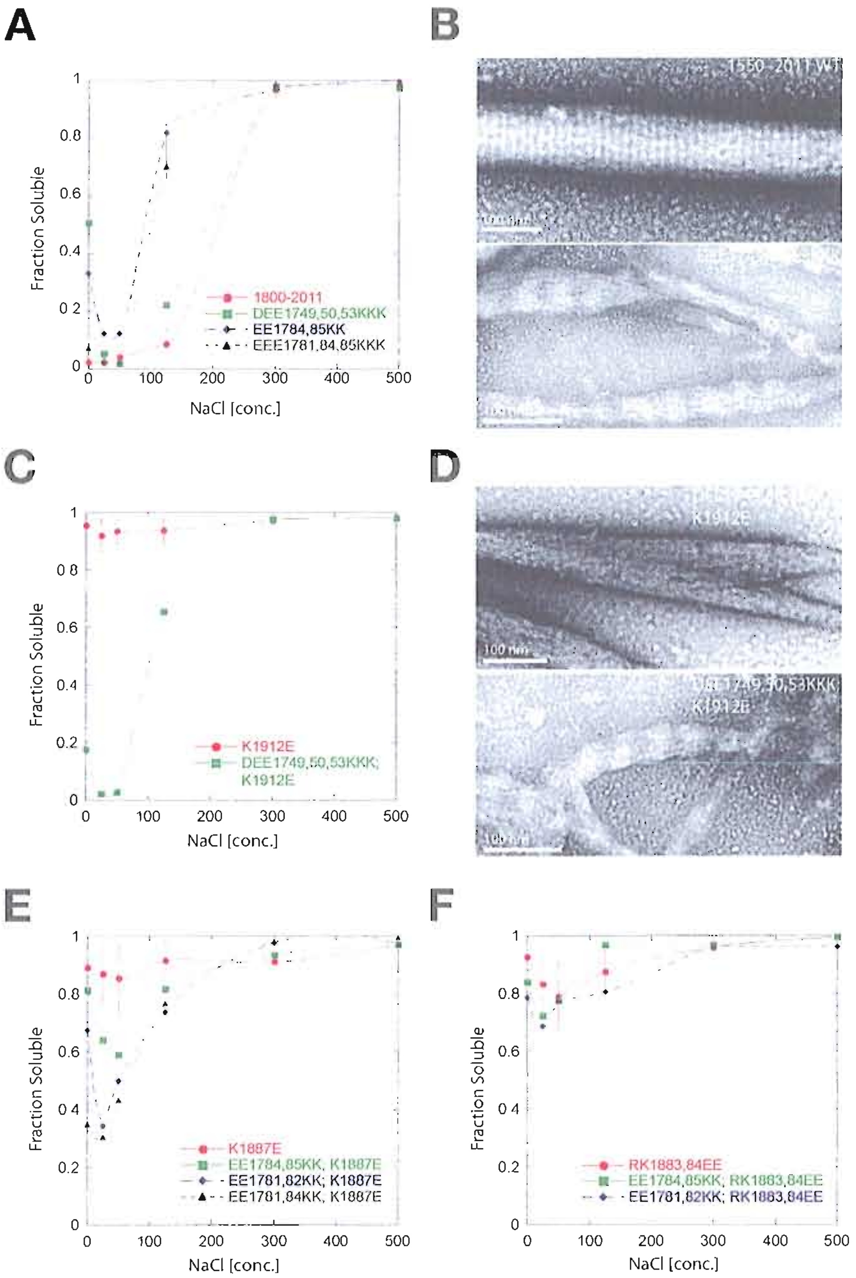

Figure 9. **Identification of upstream, negatively charged residues that participate in filament assembly.** A, Filament solubility assay of tail fragments containing deletion or mutation of upstream residues. B, Electron micrographs of tail fragment assemblies, negatively stained with 1-2% uranyl acetate. C-F, Filament solubility assays and electron micrographs of the restoration of filament assembly with complementary mutations that restore disrupted tail-tail interactions.

K1887 makes important contacts in both the parallel (E1784, E1785) and anti-parallel (E1781, E1782, and potentially E1784) interactions of tail domains. Mutation of K1887 completely disrupts filament assembly, but co-mutation of residues involved in the parallel interaction partially restores filament assembly (Figure 4E). Co-mutation of anti-parallel interacting residues (E1781, E1782, and potentially E1784) with K1887 leads to greater complementation (Figure 3E). Interestingly, co-mutation of upstream residues with another inhibiting mutation (R1883, K1884) does not restore filament assembly (Figure 3F). Perhaps both parallel and anti-parallel interacting residues must be mutated to a complementary charge to restore filament assembly. Another possibility is that two mutated residues (R1883, K1884) are harder to complement due to a larger interaction surface that is disrupted. Taken together, these results suggest that we have accurately predicted the contacts made between two tail fragments in the binary parallel and anti-parallel interactions.

### *Role of binary tail-tail interactions in the formation of bipolar minifilaments*

We have described two important binary tail-tail interactions, oriented in a parallel and anti-parallel fashion, and the role of the assembly domain in mediating these interactions. However, it is still unknown how inter-tail domain interactions are organized into a bipolar minifilament structure. Also, it is likely that there are multiple interactions with neighboring molecules that occur within the native minifilament. Thus we extended our structural model to the entire tail domain (1111-1968), which must pack tightly into the bipolar filament backbone. We used the same method as before to extend our coiled-coil structural model to represent the full-length tail domain with skip residues removed to keep the heptad repeat in register (Figure 5A).

Electrostatic interaction between entire tail domains was carried out as described above. The electrostatic interaction of two full-length tail domains displays some similar features to that described for the shorter tail fragment 1744-1968 (Figure 5, B and C; Figure 3B). The energy of interaction oscillates according to the previously described 28-residue charge repeat (Figure 5, B and C)(Parry, 1981; McLachlan and Karn, 1982; Atkinson and Stewart, 1992). In addition to this 28-residue oscillation, there appears to be a longer periodicity present of approximately 286Å in both parallel and anti-parallel orientations (Figure 5, B and C). This longer periodicity has previously been suggested to be important for filament formation (Straussman et al., 2005), and would favor parallel and anti-parallel molecular staggers of odd multiples of 143Å, which have been observed in filaments and paracrystals (Lowey et al., 1969; Kendrick-Jones et al., 1971; Niederman and Pollard, 1975; Trybus and Lowey 1984; Trybus and Lowey, 1987; Cross et al., 1991; Atkinson and Stewart, 1992). Similar to the tail fragment 1744-1968, one particularly favorable anti-parallel overlap of approximately 395Å is present with other less favorable alternative overlaps (Figure 5B).

In contrast, calculation of the interaction of parallel tail domains is remarkably different than the shorter tail fragment (Figure 3B; Figure 5C). It appears that the interaction of parallel full-length tails is generally unfavorable, though energy minima are observed at regular intervals (Figure 5C). Significant parallel packing of tail domains has been observed in myosin II filaments (Niederman and Pollard, 1975, Woodhead et a., 2005; Zoghbi et al., 2008). Within the head-zones there is exclusively parallel packing of molecules with a 14.3nm axial stagger and a 43nm helical repeat observed in many myosin IIs (Craig and Woodhead, 2006) that corresponds to electrostatic interaction energy minima (Figure 5C). In the shorter tail fragment 1744-1968, parallel interactions are energetically favorable (Figure 3B). One possible explanation is that interactions involving the n-terminal portion of the tail domain are less favorable than the c-terminal portion. It has been suggested that parallel interactions are less stable than anti-parallel interactions, which causes "flaring" of the head regions away from the filament backbone in smooth muscle myosin II (Cross et al., 1991). Taken together, these results explain the unique role of the tail domain c-terminus in filament formation.

These electrostatic calculations lead to certain implications for molecular packing within the non-muscle myosin II bipolar minifilament. Our results are consistent with anti-parallel interactions being the most stable type of interaction within the filament, and likely serves as the principal driving force for filament nucleation and elongation (Figure 5B)(Cross et al., 1991). The prevailing non-muscle myosin II bipolar minifilament model explained the geometry of the filament by suggesting that multiple anti-parallel overlaps led to the progressive shortening of anti-parallel dimers within the filament (Figure 5D). This leads to the observed lengths of head-zones, bare-zones, and the 14.3nm axial staggers of myosin heads in the filament (Niederman and Pollard, 1975). Our results show that there is one preferred favorable anti-parallel interaction that is close to the widely reported anti-parallel overlap in other myosin IIs (Kendrick-Jones et al., 1971; Onishi and Wakabayashi, 1984; Barylko et al., 1989; Trybus and Lowey, 1987).

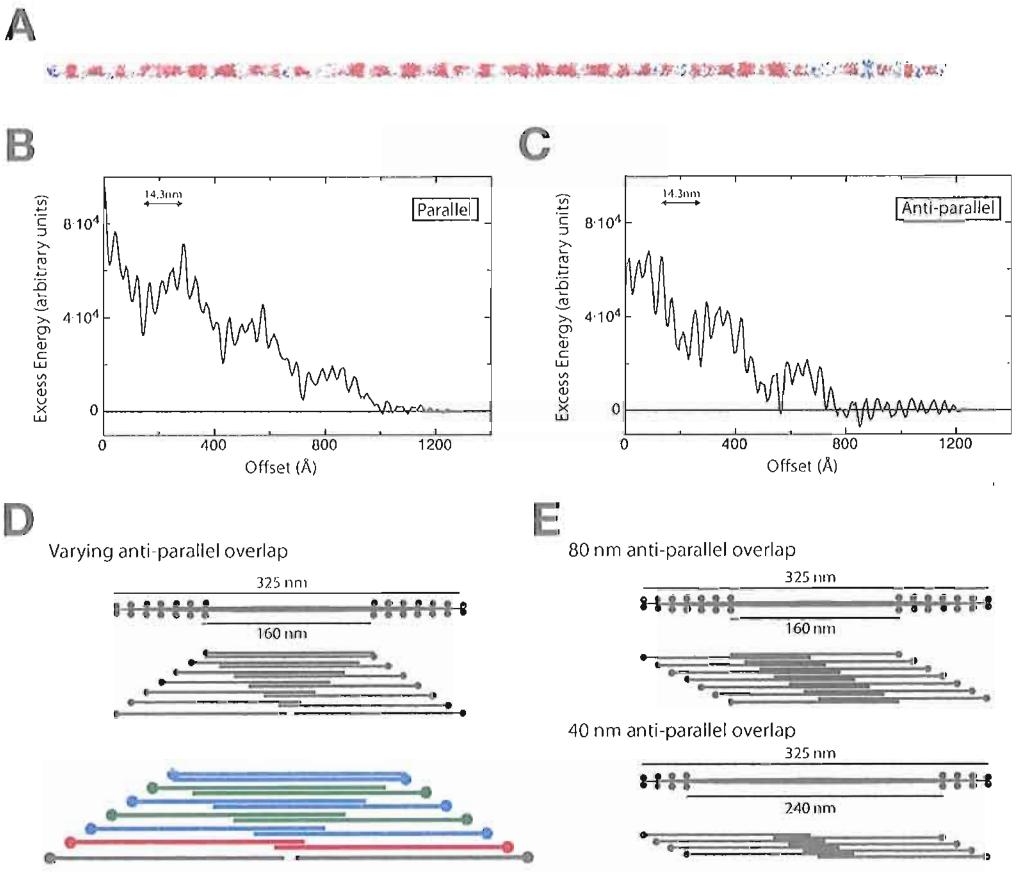

Figure 10. **Model of full-length tail domain interactions and implications for zipper filament geometry.** A, Strucutral model for the full-length tail domain of zipper (1111-1968) generated by extension of the 1744-1968 model to the entire tail domain sequence. Skip residues were removed to keep the heptad repeat in register. Electrostatic potential mapping onto the structure reveals the relative concentration of negative and positive charge along the tail. B and C, Interaction energy of electrostatic contacts by two fulllength tail domains in parallel and anti-parallel orientations. These calculations were performed using the Poisson-Boltzmann equation. D, Filament model explaining head domain staggers along the bipolar filament using multiple anti-parallel overlaps (adapted from Niederman and Pollard, 1975). Represented anti-parallel dimers are color coded according to potential tail-tail interactions; red - reference dimer, blue - dimers that could interact with reference dimer using only parallel interactions, green - dimers that could interact with reference dimer using only anti-parallel interactions. The reference dimer cannot interact with another dimer using both types of interactions. E, Filament models that contain one stable anti-parallel interaction that translates along the filament backbone to generate staggered zones of head domains along the filament.

A filament model with one stable anti-parallel dimer that is translated along the filament to yield the staggered myosin heads in the filament would better fit our results (Figure 5, B and C). However, to generate a minifilament with 28 molecules with the reported lengths of head-zones, bare-zones, and axial head staggers, with one stable anti-parallel overlap, would require that overlap to be approximately 80nm (Figure 5E)(Niederman and Pollard, 1975). An anti-parallel overlap of this length is electrostatically unfavorable (Figure 5B). An anti-parallel overlap of approximately 40nm would yield a bipolar filament with a bare-zone of 1.5 times longer, head-zones 0.5 shorter, and 16 molecules per filament (Figure 5E). Zipper forms filaments with this geometry and approximate number of monomers (Kiehart and Feghali, 1986).

## Discussion

Non-muscle myosin II dynamically assembles into bipolar minifilaments and associates with actin to produce contractile forces necessary for processes such as cytokinesis (Robinson and Spudich, 2004). The mechanisms of filament assembly are relatively well understood for myosin II from protozoa (O'Halloran et al., 1990; Lee et al., 1994 Hostetter et al., 2004; Shoffner and De Lozanne, 1996; Sinard et al., 1989; Sinard et al., 1990; Turbedsky and Pollard, 2005), but it remains unclear how myosin II assembles into force-generating filaments in higher eukaryotes. To date, assembly domains have been identified within the c-terminus of the tail domain in myosin II from a variety of higher organisms (Figure 1D)(Nyitray et al., 1983; Cross and Vandekerckhove, 1986; Atkinson and Stewart, 1991; Sohn et al., 1997; Cohen and Parry 1998; Ikebe et al., 2001; Nakasawa et al., 2005; Rosenburg et al., 2008; Liu et al., 2008). However, the precise role of assembly domains in the formation of bipolar minifilaments has yet to be defined. In this study, we examined the role of the *Drosophila* non-muscle myosin II assembly domain in mediating tail-tail interactions, and how these interactions lead to the assembly of the bipolar minifilament.

### *Defining the critical elements within the assembly domain that are necessary for filament assembly*

In order to understand the function of the assembly domain, we identified elements within the assembly domain that were indispensable for filament formation. The assembly domain of *Drosophila* non-muscle myosin II, zipper, was identified as a short tail fragment (1849-1940) that was necessary and sufficient for filament assembly (Liu et al., 2008). We found that the last 2/3 of the assembly domain contain sequences that are indispensable for filament assembly (Figure 1). This subregion within the zipper assembly domain overlaps with assembly competence domains previously described (Figure 1D)(Sohn et al., 1997; Nakasawa et al., 2005). However, we did not find the c-terminal 28 residues of the coiled-coil tail or the non-helical tailpiece to be important for filament assembly as previously suggested (Figure 1)(Ikebe et al., 2001; Hodge et al., 1992). This is consistent with our previous findings that regions outside the assembly domain are dispensable for filament assembly (Liu et al., 2008). Alignment of the 1744-2011-tail fragment with comparable regions in other myosin IIs shows a remarkable amount of sequence conservation, beyond the conservation of the heptad repeat for coiled-coil folding (Figure 1D). The larger tail domain is also highly conserved, suggesting that conservation may be important for generating the stereotypical molecular staggers observed in different types of myosin II filaments (Niederman and Pollard, 1975; Trybus and Lowey 1984; Trybus and Lowey, 1987; Cross et al., 1991). Unfortunately, widespread sequence conservation is not useful for understanding the functional elements of the assembly domain that are important for filament assembly.

We further characterized critical assembly elements, down to the amino acid level, using site directed mutagenesis to alter the charge of clusters and single residues that occur in positions that could make inter-tail domain contacts during filament assembly (Figure 2). Consistent with previous work, we only found positively charged regions that were critical for filament assembly (Figure 2)(Rosenburg et al., 2008). This supports the idea that the positive charged nature of the assembly domain is the unique feature that is critical for filament formation. Interestingly, we found mutation of a negatively charged residue (E1891) and an apolar residue (M1894) that occurs in an especially positively charged region significantly disrupts filament assembly (Figure 2E). This would be consistent with sequence-specific interactions between tail domains, rather than gross charge, being important for filament assembly.

### *Function of the assembly domain in tail-tail interactions*

The majority of the mutations that disrupt filament assembly cluster within a 15-residue segment (1880-1894), which forms a positively charged interaction surface (Figure 2, E and H). This segment corresponds to the positive charge cluster P1, which was suggested as being important for tail-tail interactions (Nakasawa et al., 2005). In this model, positive charge clusters P1 and P2 interact with a conserved negative charge cluster N1 in the parallel and anti-parallel oriented tail-tail interactions respectively (Nakasawa et al., 2005). This model yields molecular staggers that are close to the reported values for each interaction (Nakasawa et al., 2005; Kendrick-Jones et al., 1971; Barylko et al., 1989; Trybus and Lowey, 1987; Small and Squire, 1972). Using structural modeling and electrostatic calculations, we found similar energetically favorable molecular staggers (Figure 3). Whereas the parallel interaction was indistinguishable from the previously reported model, the anti-parallel interaction was shifted such that the P1 cluster was interacting with the N1 cluster in both interactions (Figure 3, B and C). The discrepancy could be due to the slightly longer fragment we used, that contained a second negative charge cluster that paired up with P2 in the anti-parallel interaction (Figure 3C). This also explains why mutation of residues in P1, but not P2, strongly disrupted filament assembly (Figure 2, E and F).

Interestingly, deletion of the region containing both negative charge clusters does not inhibit filament assembly (Figure 4A). Mutation of either of the negative charge clusters also does not disrupt filament assembly (Figure 4A). It was previously reported that the 90-residue assembly domain was sufficient for filament assembly (Liu et al., 2008). Also, calculations of the energy of electrostatic interactions between tail domains show that multiple, albeit less stable, alternative molecular staggers can occur during tail-tail interaction (Figure 3B). This suggests that less stable filaments, with altered molecular staggers, could be formed when this upstream negatively charged domain is deleted or mutated. Structural analysis of paracrystalline aggregates formed by one of these mutants displays structures that appear to be less stable and have altered molecular packing (Figure 4B).

In further experimental support of these tail-tail interactions, filament assembly of tail fragments containing inhibitory mutations within the assembly domain could be restored to varying degrees with complementary mutations in a negatively charged, upstream region (Figure 4, C, E and F). Complementation of anti-parallel interactions seems to be more effective in restoring filament assembly than parallel interactions (Figure 4, C and E). In fact, complementation of R1912E mutation with DEE1749,50,53KKK mutation not only restored filament assembly, but also led to partial restoration of ordered molecular packing within paracrystalline aggregates (Figure 4D).

### *Full-length tail domain interactions*

Structural modeling and electrostatic calculations of the tail fragment 1744-1968 was useful for understanding how two fragments interact with one another (Figure 3). To understand how full length tail domains would pack into a bipolar minifilament, we extended our modeling to the entire tail domain (1111-1968)(Figure 5). Our modeling displays an electrostatic argument for the appearance of parallel and anti-parallel molecular staggers found within filaments (Figure 5, B and C). Our data also explains the observed relative affinities of tail-tail interactions that are oriented in a parallel and anti-parallel fashion (Cross et al., 1991).

Our understanding of the formation of the minifilament structure has not progressed much since early electron microscopy studies, due to the lack of three-dimensional, structural information and the shift of interest to identifying tail segments that confer competence to form filaments. The prevailing model for human platelet non-muscle myosin filament structure consists of multiple anti-parallel overlaps that progressively shorten to yield the 14.3 nm offset increment observed between head domains in the filament (Niederman and Pollard, 1975). We found that one anti-parallel stagger is more energetically favorable that several other, shorter alternative staggers. After this favorable overlap, the longer the tail overlap becomes the less energetically favorable the interaction between the two tail domains (Figure 5C). However, energy minima do occur at intervals corresponding to the varying overlaps suggested in this filament model (Figure 5, C and D)(Niederman and Pollard, 1975). A tail domain makes contact with multiple neighboring tails within filaments. Thus, it may be possible that multiple interactions between tails within the filament could stabilize these less favorable anti-parallel overlaps. In light of our electrostatic calculations, it is interesting to consider how different anti-parallel dimers could interact with each another, while the center of mass of each dimer doesn't change relative position along the filament. A particular anti-parallel dimer would be able to interact with a subset of other dimers using anti-parallel contacts, but would only be able to interact with a distinct subset of dimers using parallel contacts (Figure 5D).

We have found evidence that seems to confirm the notion that anti-parallel interactions are more stable than parallel interactions, and likely drive the formation of filaments (Figure 5, B and C)(Cross et al., 1991). Thus we propose a filament model that utilizes one stable anti-parallel interaction that is translated along the filament backbone, which creates staggered head domains in the filament (Figure 5C). A similar filament model, containing 8 molecules, has been proposed for *Acanthamoeba* myosin II, which is a well-understood model for bipolar filament formation (Sinard et al., 1989; Sinard et al., 1990; Turbedsky et al., 2005). Despite the lack of sequence conservation, we propose that myosin II from higher eukaryotes form filaments by a similar mechanism. Using one stable anti-parallel overlap (approximately 40 nm) as a building block, a bipolar filament that is twice as long as the myosin monomer would contain 16 molecules (Figure 5, C and E). The anti-parallel overlap needed to generate a filament with 28 molecules would be approximately 80 nm, which is energetically unfavorable (Figure 5, C and E). This model of the filament would contain different lengths of head zones and bare zone than reported for platelet myosin II (Figure 5E)(Niederman and Pollard, 1975). However, electron microscopic analysis of zipper has yielded bipolar filaments that fit closely to the model we propose here (Figure 5E)(Kiehart and Feghali, 1986).

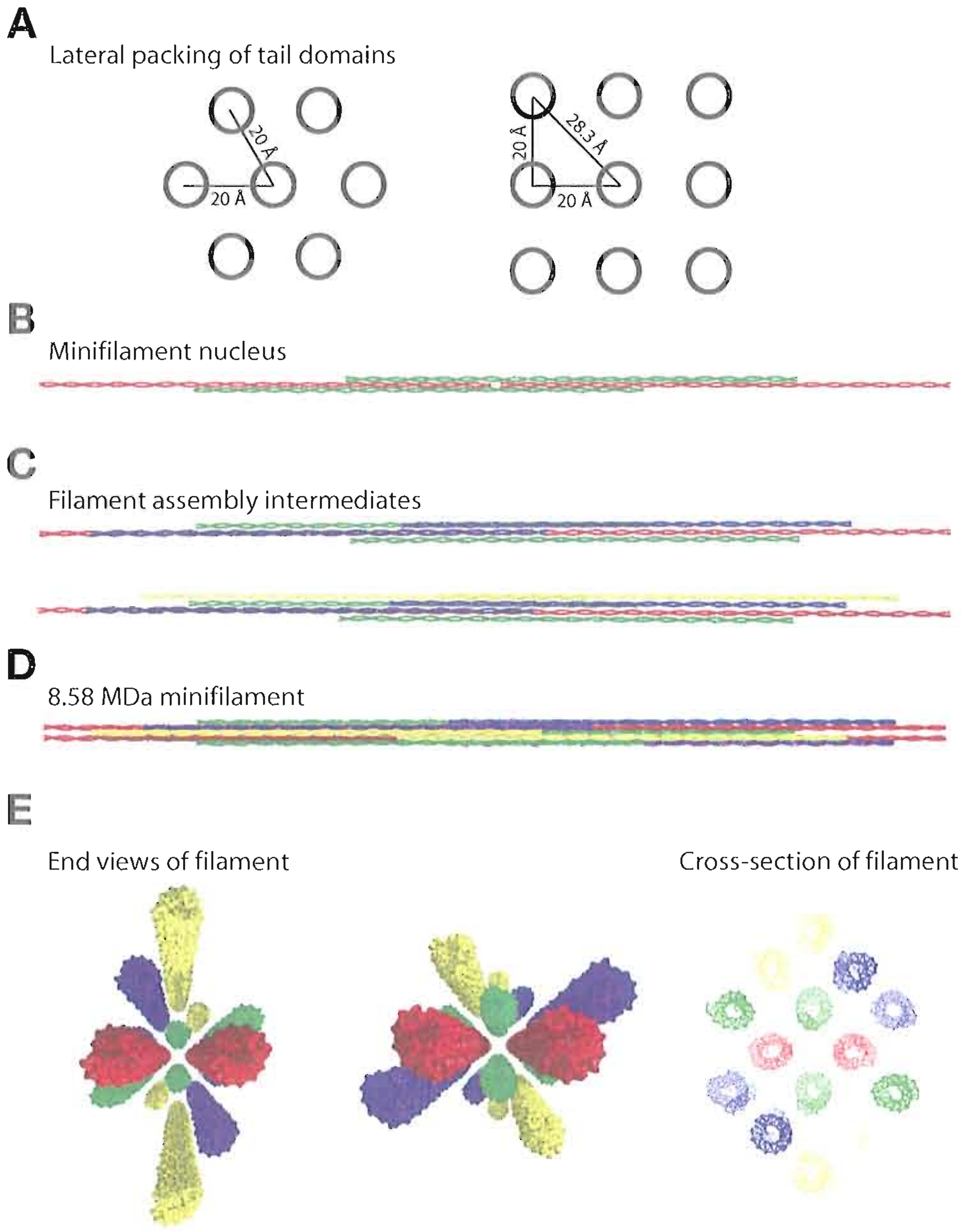
A
Lateral packing of tail domains
20 Å
20 Å
20 Å
28.3 Å
20 Å
B
Minifilament nucleus
C
Filament assembly intermediates
D
8.58 MDa minifilament
E
End views of filament
Cross-section of filament

Figure 11. **Theoretical three-dimensional model of the zipper bipolar minifilament.** A, Lateral packing geometries, hexagonal and tetragonal, of coiled-coil tail domains. B, Early interactions within the minifilament that stabilzes end-on-end tail domains. These interactions set the barezone length, the overall length of the minifilament, and consequently the number of myosin molecules per minifilament. C, Strucutral intermediates of filament formation. D and E, Structural model of the fully-assembled zipper minifilament. Three anti-parallel interactions (1 x 14.3 nm, 3 x 14.3 nm, 5 x 14.3 nm equivalent) and two parallel interactions (1 x 14.3 nm and 3 x 14.3 nm) form the building blocks for zipper bipolar minifilament formation.

### *Three-dimensional structural model of zipper filaments*

Our understanding of the structure of non-muscle myosin minifilaments has been limited by the lack of three-dimensional information of this large macromolecular assembly. Electron microscopy studies of myosin filaments have yielded common molecular staggers that occur in a variety of filament types (Lowey et al., 1969; Kendrick-Jones et al., 1971; Niederman and Pollard, 1975; Trybus and Lowey 1984; Trybus and Lowey, 1987; Cross et al., 1991; Atkinson and Stewart, 1992; Sohn et al., 1997). The prevailing structural model of the non-muscle myosin II minifilament described the limitations of the overall filament length, and the length of the bare-zone (Figure 5D)(Niederman and Pollard, 1975). Our results have led us to an alternative model that employs a consistent anti-parallel interaction, which leads to distinct geometrical features if the length of the mini-filament is constrained to twice the length of the monomer (Figure 5E). This highly schematic model for a minifilament utilizes two interactions (parallel-14.3 nm and anti-parallel-43 nm), similar to the model for smooth muscle myosin II (Figure 5E)(Cross et al., 1991). Smooth muscle myosin II forms large side-polar filaments that extend for long distances (Cross et al., 1991). The filament structure of non-muscle myosin II would likely inherently constrain the length of the minifilaments. Thus, we propose a three-dimensional, theoretical model for the zipper minifilament that could explain the size and character of these filaments (Figure 6).

Myosin tail domains pack tightly within the filament backbone using parallel and anti-parallel interactions. The simple coiled-coil nature of the myosin tail domains and the periodic structure of the minifilament make theoretical modeling of the minifilament structure tractable. Tail domains interact favorably with molecules staggered odd multiples of 14.3 nm (Figure 5, B and C). This places constraints on the placement of tail domains within the filament. It has been suggested that tail domains laterally pack within the filament backbone in a hexagonal array (Niederman and Pollard, 1975). Hexagonal packing, in which a tail contacts six interacting partners, is difficult to achieve due to unfavorable interaction constraints (Figure 6A; Figure 5, B and C). By contrast, tetragonal packing allows favorable tail-tail interactions, while distancing unfavorable interactions by diagonal positioning (Figure 6A).

The overall length of the mini-filament is determined by the inability of the terminal molecules to interact with anti-parallel contacts (Niederman and Pollard, 1975). We propose that early contacts within the filament set both the overall length, and the length of the bare-zone (Figure 6B). These contacts are comprised of the stable anti-parallel 395Å overlap, and a parallel 430Å staggered parallel interaction, which stabilizes two end-on-end tails and the overall length of the minifilament (Figure 6B). Interestingly, these contacts lead to the occupation of head positions at the each end of the head zone, and determine many of the observed filament features (Figure 6B). It should be noted that a distance of 35Å separates the end-on-end tail domains to yield synergistic parallel and anti-parallel interactions (Figure 6B). It is likely that the non-helical tailpiece occupies this space in the native filament.

Electrostatic calculations suggested that rotational effects on tail-tail interactions were negligible (data not shown). Thus, a tail domain may interact with multiple partners using identical molecular staggers. The model we propose here assembles the first 8 molecules in the center of the filament using only the 395Å (3 x 14.3 nm equivalent) anti-parallel overlap and the 430Å parallel stagger tail-tail interactions. This likely represents the most stable filament core possible. The next filament intermediate involves inter-tail domain contacts of an anti-parallel dimer with neighboring molecules, utilizing anti-parallel overlaps (1 x 14.3 nm and 5 x 14.3 nm equivalent) and a parallel offset of 14.3 nm, which are all energetically favorable (Figure 5, B and C; Figure 6C). Addition of the last anti-parallel dimer involves two parallel contacts of 14.3 nm and an anti-parallel overlap (5 x 14.3 nm equivalent)(Figure 6C).

We were able to build a three-dimensional model of the zipper minifilament utilizing, primarily the stable anti-parallel overlap (3 x 14.3nm equivalent), two less stable overlaps (1 x 14.3 nm and 5 x 14.3 nm equivalent), and two parallel molecular staggers (1 x 14.3 nm and 3 x 14.3 nm)(Figure 6D). Perhaps more importantly, by using tetragonal packing, we were able to avoid any unfavorable molecular staggers within the minifilament (Figure 6). All of the tail domain n-termini are solvent exposed, so that head and neck domains would be able to project from the filament backbone at these sites (Figure 6E). Interestingly, the filament geometry prevents the n-terminal portion of the tail domains to pack together tightly, which is electrostatically unfavorable (Figure 6, D and E; Figure 5, B and C).

The model we present here is consistent with all physical observations and provides a framework for understanding the detailed mechanism by which this fundamental cellular structure is generated. Several other slight variations of this model would satisfy the tail-tail interactions that we have described in this study. However, the general principles introduced by our structural model must be satisfied by any alternative model. Five total interactions between neighboring tail domains form the basis for non-muscle myosin bipolar minifilament formation.

## Materials and methods

### *Cloning, overexpression, and purification*

Zipper regions were subcloned using a plasmid containing the full-length Zipper B sequence that was kindly provided by Dan Kiehart (Su and Kiehart, 2001). Deletions were created using splicing by overlapping extension PCR. Zipper tail fragments were mutated using QuikChange$^{TM}$ Site Directed Mutagenesis Kit (Stratagene, La Jolla, CA) according to the manufacturer's instructions. All deletions and mutations were confirmed by DNA sequencing. Zipper regions were expressed in *E. coli* using the pET-19b derivative pBH vector (Peterson et al., 2004). Recombinant his-tagged fusion proteins were purified using Ni-NTA resin and standard protocols, which yielded >90% pure protein. Ion-exchange chromatography was used to further purify proteins if necessary. The Ni-NTA purified proteins were dialyzed extensively against salt-free buffer (10 mM Tris, pH 8.0; 1 mM DTT; 1 mM EDTA) at 4°C. Purity was established using SDS-PAGE.

### *Filament assembly assay*

The filament assembly assay was performed as previously described (Liu et al., 2008). Briefly, we incubated zipper tail constructs (10 μM) at a range of salt concentrations in assembly buffer (10 mM Tris-HCl, pH 8.0; 1 mM DTT; 1 mM EDTA) for 30 minutes at 4°C followed by centrifugation at 100,000 x *g* for 30 minutes. We then separated the soluble and insoluble phases and loaded equal volumes for analysis by SDS-PAGE. We used ImageJ (NIH) to determine relative protein amounts from scanned, coomassie brilliant blue stained gels.

### *Electron microscopy*

For paracrystal formation tail fragments (1 μM) were incubated in buffer (10 mM Tris-HCl, pH 8.0; 50mM NaCl, 1 mM DTT) with the addition of 2 mM or 10 mM $MgCl_2$ or $CaCl_2$. For negative staining 10 μl samples were applied to 300-mesh carbon stabilized copper grids coated with formvar (#01753-F; Ted Pella), that were render hydrophilic by glow discharge in a partial vacuum, for 30 seconds. The grids were then washed with 6 drops of the same buffer, and stained with 1–2% uranyl acetate for 30 seconds and dried. Electron micrographs were taken on a FEI Titan FEG-TEM electron microscope, at an acceleration voltage of 80 kV, with a Gatan 2K x 2K CCD for image capture.

### *Construction of zipper tail structural model and electrostatic calculations*

The structural model for the zipper tail domain was created by duplicating and aligning a repeatable subunit to generate a long, straight coiled-coil. The repeatable subunit was derived from the structure of the coiled-coil trigger site of the actin crosslinker I from *Dictyostelium discoideum* (Burkhard et al., 2000; 1D7M). We then mutated the sequence to the zipper tail sequence with skip residues removed to keep the heptad repeat in register. The residue sidechains were energy minimized to yield a feasible zipper tail domain structure.

We generated models of parallel or antiparallel myosin rod pairs (with the monomer model described above) using PyMol. The rods were placed 2 nm apart (center to center) at the desired overlap. To avoid steric clashes, we subjected amino acid side chains in the model to 20 cycles of conjugate gradient energy minimization using CNS. Charge states were assigned with pdb2pqr and electrostatic energies were calculated with APBS using a dielectric of 80.

# CHAPTER IV

# CONCLUDING REMARKS

Non-muscle myosin II generates contractile forces in non-muscle cells for fundamental cell biology features, such as maintenance of cell shape and cortical rigidity, and is necessary for complex behaviors like cell migration, organ morphogenesis, wound healing, and cytokinesis (Young et al., 1993; Edwards and Kiehart, 1996; Shelden and Knecht, 1996; Hickson et al., 2006; Martens and Radmacher, 2008; Pollard, 1981; Warrick and Spudich, 1987; Ridley et al., 2001; Bement et al., 1999; Glotzer, 2005; Robinson and Spudich, 2004). Myosin II is able to generate contraction by assembling into bipolar minifilaments that slide opposing actin filaments, which leads to a spatially shortened actin network. Myosin II activity in non-muscle cells is tightly regulated to ensure that contractile force is generated in regions of the cell where contraction is needed locally. This targeted activation of non-muscle myosin II is required for its physiological role of controlling cell shape during complex cellular processes. Unlike other isoforms of myosin II, non-muscle myosin II activity is targeted to cellular domains through the regulated formation of force-producing minifilaments (Egelhoff et al., 1993; Breckenridge et al., 2009). Filament assembly, regulation, and cellular localization of non-muscle myosin II are mediated by the unique tail domain (Sellers et al., 2000; Zang and Spudich, 1998; Liu et al., 2008). Much of what is known about the activity of the tail domain comes from studies of protozoan non-muscle myosin IIs, which are divergent from higher eukaryotes (Liu et al., 2008). The mechanisms of tail domain activity are unknown in higher eukaryotes.

In this dissertation, we used the *Drosophila* non-muscle myosin II heavy chain, also known as zipper, to investigate the role of the tail domain in forming bipolar filaments and targeting to cellular sites. We identified specific domains within the tail that mediated different activities of the tail domain. One of the most appreciated activities of the tail domain is mediating minifilament formation through electrostatic tail-tail interactions. It was previously shown that the carboxy-terminal 300 residues of the tail domain were required to form filaments (Su and Kiehart, 2001). We tested the ability of various tail fragments to oligomerize in a salt-dependent manner, in order to narrow down the region of the tail domain that was responsible for the formation of filaments. These experiments led to the identification of a 90-residue “assembly domain” (1849-1940) near the c-terminus of the coiled-coil tail that was necessary and sufficient for filament assembly. This domain displayed a unique positive charge profile, compared to the rest of the tail domain.

Likewise, we tested the ability of different tail fragments to localize within the cell in a cell cycle-dependent manner. Non-muscle myosin displays a complex localization pattern in cells. During interphase, myosin II localizes to the cytoplasm and the actin-rich cell cortex. As the cell begins cell division, myosin II depletes from the cortex and becomes cytoplasmic during metaphase. During anaphase, myosin II forms cortical patches, but depletes from the polar cortex, while enriching at the midzone during anaphase extension and chromosome separation. Myosin II becomes concentrated in a narrow band at the cleavage furrow that separates the resulting daughter cells during telophase. Distinct tail fragments were able to localize to the interphase cortex (1350-1865) and the cleavage furrow (1744-1969). Interestingly, targeting to the cleavage furrow requires the assembly domain, which is consistent with studies of *Dictyostelium* myosin, where filament assembly was necessary for cleavage furrow localization (Sabry et al., 1997). This indicates that the ability to form filaments is important for targeting of myosin II to certain cytoskeleton assemblies, but not the interphase cortex.

We next set out to understand how tail domains interacted with each other to produce a force-generating minifilament. Assembly domains, which have been discovered in all myosin II isoforms studied to date, are required and often sufficient for filament assembly (Nakasawa et al., 2005; Sohn et al., 1997; Nyitray et al., 1983; Cross and Vandekerckhove, 1986; Atkinson and Stewart, 1991; Cohen and Parry 1998; Ikebe et al., 2001; Rosenburg et al., 2008). These assembly domains are often small, and it is unclear how assembly domains interact to form filaments. Using deletion analysis and mutagenesis, we defined the critical elements within the assembly domain of zipper that are required for filament assembly. Positively charged residues and regions were critical for filament assembly; especially a short 15-residue segment (1880-1894) that likely forms a critical interaction surface. Structural modeling and electrostatic calculations described how two tail fragments interact with each other, and how these critical positive charge regions could make several less stable alternative interactions making the identification of complementary interaction surfaces difficult. We confirmed the modeling results with complementary mutagenesis and electron microscopic analysis of tails packing in a crystalline array with molecular staggers identified by the electrostatic calculations. Modeling of the entire tail domain led to the identification of specific electrostatic interactions, which explains the molecular packing observed in a variety of myosin II filaments (Lowey et al., 1969; Kendrick-Jones et al., 1971; Niederman and Pollard, 1975; Trybus and Lowey 1984; Trybus and Lowey, 1987; Cross et al., 1991; Atkinson and Stewart, 1992; Sohn et al., 1997). We were able to build a three-dimensional model of the zipper bipolar minifilament using the tail-tail interaction information garnered through structural modeling and electrostatic interaction calculations. To our knowledge, this structural model of the 8.58 MDa non-muscle myosin II bipolar filament is consistent with all physical observations and provides a framework for understanding the detailed mechanism by which this fundamental cellular structure is generated. Reconstructions of zipper filaments from electron microscopy would be useful to evaluate in detail the validity of this structural model.

This work has been important for identifying distinct domains within the coiled-coil tail of myosin II that mediate different activities like the formation of minifilaments and targeting to cellular sites. These studies have uniquely examined the interactions that lead to the assembly of non-muscle myosin II minifilament in unprecedented detail. However, there are still many outstanding questions left to investigate. I will briefly detail several areas of research that are left to be addressed in the future.

The tail domain of non-muscle myosin II not only mediates localization and filament assembly, but has also been implicated in the regulation of myosin activity (Sellers, 2000; Sellers and Knight, 2007). Regulation of non-muscle myosin II activity occurs by modulating the assembly state of myosin (Egelhoff et al., 1993; Breckenridge et al., 2009). Thus, it is not surprising that the tail domain plays a role in regulation of myosin activity. In higher eukaryotes, the activity of non-muscle myosin II is controlled by signal transduction pathways that alter the phosphorylation state of the regulatory light chain (RLC). When RLC in not phosphorylated, myosin II folds into a compact "off" state that requires the tail domain to fold back with two acute bends (Trybus and Lowey, 1984; Burgess et al., 2007). Recent electron microscopy studies suggest that segments of the tail interact to form a three-stranded bundle (Burgess et al., 2007). The tail likely utilizes intra-tail domain contacts that are similar to the inter-tail domain contacts we have described for the formation of filaments. This could explain the inability of this off state to interact with other molecules to form filaments.

It is currently unknown how the RLC, which binds in the neck domain, communicates with the tail to inhibit the activity of the assembly domain near the c-terminus of the molecule. In the extended, active conformation, approximately 150 nm of distance and nearly 1000 residues separate the RLC and the assembly domain. Therefore, allosteric communication between these domains must occur over a great distance. To understand how RLC and the tail domain interact to achieve regulation of non-muscle myosin II, we have developed an artificial construct that can be recombinantly expressed and purified for *in vitro* experiments. This experimentally tractable system will lead to important insights into the mechanism of non-muscle myosin II regulation.

We have generated a detailed structural model for the non-muscle myosin II bipolar minifilament. This model explains many of the molecular staggers observed in different types of myosin filaments such as the 14.3 nm axial stagger, 43 nm helical repeat, and the widely reported 43 nm anti-parallel overlap (Trybus and Lowey, 1984; Craig and Woodhead, 2006). These conserved parameters could be explained by the large amount of sequence conservation throughout the tail domain of different myosin II isoforms from a variety of organisms (Sohn et al., 1997; Nakasawa et al., 2005). Given this, it is unclear why different myosin II isoforms assembly into filaments of different sizes and shapes. Myosin II isoforms from striated muscle form large bipolar thick filaments. Non-muscle myosin II forms small bipolar minifilaments with a similar character, but a distinct size (Niederman and Pollard, 1975). Skeletal myosin II filaments contain 4 heads, cardiac myosin II contains 3 heads, and non-muscle myosin II contains 2 heads per axial interval (Offer et al., 2000; Woodhead et al., 2005; Zoghbi et al., 2008; Niederman and Pollard, 1975). Smooth muscle myosin II displays molecular staggers similar to other myosin II isoforms, but the filaments have a side-polar nature, forming a flattened sheet (Cross et al., 1991; Hodge et al., 1992; Xu et al., 2008). Currently, given the conserved sequence and conserved molecular staggers, it is unknown what the unique features contained within the tail domain of different myosin II isoforms lead to the unique characters of the resulting filaments that are formed.

Finally, we identified distinct domains for localizing to the interphase cortex and the cleavage furrow during cell division. These domains are part of the tail domain, which displays the same localization as full-length non-muscle myosin II. Actin binding is not required for localization, as expected since the head domain was not required for localization. The mechanisms these domains employ to target to cytoskeletal domains are unknown. Also, changes in the cortex or cell signaling lead to the depletion of myosin from the cortex. Defining the localization mechanisms of myosin II would deepen our understanding of contractile force regulation. To this end we began using *Drosophila* neuroblasts as a model for understanding regulated localization of myosin II. Neuroblasts are polarized cells that divide asymmetrically to yield daughter cells with distinct protein content and daughter cell size. During division, non-muscle myosin II depletes only from the apical, polar cortex at the onset of anaphase. Contraction accompanying chromosome separation leads to an asymmetric anaphase extension, which results in an asymmetry in daughter cell size. Genetic perturbations and imaging techniques in *Drosophila* will allow us to dissect signaling pathways that lead to asymmetric depletion of myosin.

# BIBLIOGRAPHY

## Chapter I

Aguado-Velasco, C., and Bretscher, M. S. (1997). Dictyostelium myosin II null mutant can still cap Con A receptors. Proc Natl Acad Sci U S A 94, 9684-9686.

Amos, L. A. (2008). Molecular motors: not quite like clockwork. Cell Mol Life Sci 65, 509-515.

Bement, W. M., Mandato, C. A., and Kirsch, M. N. (1999). Wound-induced assembly and closure of an actomyosin purse string in Xenopus oocytes. Curr Biol 9, 579-587.

Berg, J. S., Powell, B. C., and Cheney, R. E. (2001). A millennial myosin census. Mol Biol Cell 12, 780-794.

Breckenridge, M. T., Dulyaninova, N. G., and Egelhoff, T. T. (2009). Multiple regulatory steps control mammalian nonmuscle myosin II assembly in live cells. Mol Biol Cell 20, 338-347.

Bresnick, A. R. (1999). Molecular mechanisms of nonmuscle myosin-II regulation. Curr Opin Cell Biol 11, 26-33.

Burgess, S. A., Yu, S., Walker, M. L., Hawkins, R. J., Chalovich, J. M., and Knight, P. J. (2007). Structures of smooth muscle myosin and heavy meromyosin in the folded, shutdown state. J Mol Biol 372, 1165-1178.

Burkhard, P., Stetefeld, J., and Strelkov, S. V. (2001). Coiled coils: a highly versatile protein folding motif. Trends Cell Biol 11, 82-88.

Cheney, R. E., and Mooseker, M. S. (1992). Unconventional myosins. Curr Opin Cell Biol 4, 27-35.

Cheney, R. E., O'Shea, M. K., Heuser, J. E., Coelho, M. V., Wolenski, J. S., Espreafico, E. M., Forscher, P., Larson, R. E., and Mooseker, M. S. (1993). Brain myosin-V is a two-headed unconventional myosin with motor activity. Cell 75, 13-23.

Clarke, M., and Spudich, J. A. (1977). Nonmuscle contractile proteins: the role of actin and myosin in cell motility and shape determination. Annu Rev Biochem 46, 797-822.

Cooke, R. (2004). The sliding filament model: 1972-2004. J Gen Physiol 123, 643-656.

Craig, R., and Woodhead, J. L. (2006). Structure and function of myosin filaments. Curr Opin Struct Biol 16, 204-212.

Cremo, C. R., Wang, F., Facemyer, K., and Sellers, J. R. (2001). Phosphorylation-dependent regulation is absent in a nonmuscle heavy meromyosin construct with one complete head and one head lacking the motor domain. J Biol Chem 276, 41465-41472.

Cross, R. A., Citi, S., and Kendrick-Jones, J. (1988). How phosphorylation controls the self-assembly of vertebrate smooth and non-muscle myosins. Biochem Soc Trans 16, 501-503.

De La Cruz, E. M., and Ostap, E. M. (2004). Relating biochemistry and function in the myosin superfamily. Curr Opin Cell Biol 16, 61-67.

De Lozanne, A., and Spudich, J. A. (1987). Disruption of the Dictyostelium myosin heavy chain gene by homologous recombination. Science 236, 1086-1091.

Ding, H. L., Ryder, J. W., Stull, J. T., and Kamm, K. E. (2009). Signaling processes for initiating smooth muscle contraction upon neural stimulation. J Biol Chem.

Dominguez, R., Freyzon, Y., Trybus, K. M., and Cohen, C. (1998). Crystal structure of a vertebrate smooth muscle myosin motor domain and its complex with the essential light chain: visualization of the pre-power stroke state. Cell 94, 559-571.

Edwards, K. A., and Kiehart, D. P. (1996). Drosophila nonmuscle myosin II has multiple essential roles in imaginal disc and egg chamber morphogenesis. Development 122, 1499-1511.

Egelhoff, T. T., Brown, S. S., and Spudich, J. A. (1991). Spatial and temporal control of nonmuscle myosin localization: identification of a domain that is necessary for myosin filament disassembly in vivo. J Cell Biol 112, 677-688.

Egelhoff, T. T., Lee, R. J., and Spudich, J. A. (1993). Dictyostelium myosin heavy chain phosphorylation sites regulate myosin filament assembly and localization in vivo. Cell 75, 363-371.

Espindola, F. S., Suter, D. M., Partata, L. B., Cao, T., Wolenski, J. S., Cheney, R. E., King, S. M., and Mooseker, M. S. (2000). The light chain composition of chicken brain myosin-Va: calmodulin, myosin-II essential light chains, and 8-kDa dynein light chain/PIN. Cell Motil Cytoskeleton 47, 269-281.

Franke, J. D., Montague, R. A., and Kiehart, D. P. (2005). Nonmuscle myosin II generates forces that transmit tension and drive contraction in multiple tissues during dorsal closure. Curr Biol 15, 2208-2221.

Ganitkevich, V., Hasse, V., and Pfitzer, G. (2002). Ca2+-dependent and Ca2+-independent regulation of smooth muscle contraction. J Muscle Res Cell Motil 23, 47-52.

Geeves, M. A., and Holmes, K. C. (1999). Structural mechanism of muscle contraction. Annu Rev Biochem 68, 687-728.

Glotzer, M. (2005). The molecular requirements for cytokinesis. Science 307, 1735-1739.

Gordon, A. M., Homsher, E., and Regnier, M. (2000). Regulation of contraction in striated muscle. Physiol Rev 80, 853-924.

Greene, L. E., Sellers, J. R., Eisenberg, E., and Adelstein, R. S. (1983). Binding of gizzard smooth muscle myosin subfragment 1 to actin in the presence and absence of adenosine 5'-triphosphate. Biochemistry 22, 530-535.

Guilford, W. H., Dupuis, D. E., Kennedy, G., Wu, J., Patlak, J. B., and Warshaw, D. M. (1997). Smooth muscle and skeletal muscle myosins produce similar unitary forces and displacements in the laser trap. Biophys J 72, 1006-1021.

Hackney, D. D. (1992). Kinesin and myosin ATPases: variations on a theme. Philos Trans R Soc Lond B Biol Sci 336, 13-17; discussion 17-18.

Hickson, G. R., Echard, A., and O'Farrell, P. H. (2006). Rho-kinase controls cell shape changes during cytokinesis. Curr Biol 16, 359-370.

Horowitz, A., Trybus, K. M., Bowman, D. S., and Fay, F. S. (1994). Antibodies probe for folded monomeric myosin in relaxed and contracted smooth muscle. J Cell Biol 126, 1195-1200.

Hostetter, D., Rice, S., Dean, S., Altman, D., McMahon, P. M., Sutton, S., Tripathy, A., and Spudich, J. A. (2004). Dictyostelium myosin bipolar thick filament formation: importance of charge and specific domains of the myosin rod. PLoS Biol 2, e356.

Houdusse, A., Kalabokis, V. N., Himmel, D., Szent-Gyorgyi, A. G., and Cohen, C. (1999). Atomic structure of scallop myosin subfragment S1 complexed with MgADP: a novel conformation of the myosin head. Cell 97, 459-470.

Howard, J., and Spudich, J. A. (1996). Is the lever arm of myosin a molecular elastic element? Proc Natl Acad Sci U S A 93, 4462-4464.

Huxley, A. F. (2000). Cross-bridge action: present views, prospects, and unknowns. J Biomech 33, 1189-1195.

Johnston, G. C., Prendergast, J. A., and Singer, R. A. (1991). The Saccharomyces cerevisiae MYO2 gene encodes an essential myosin for vectorial transport of vesicles. J Cell Biol 113, 539-551.

Jordan, P., and Karess, R. (1997). Myosin light chain-activating phosphorylation sites are required for oogenesis in Drosophila. J Cell Biol 139, 1805-1819.

Kee, Y. S., and Robinson, D. N. (2008). Motor proteins: myosin mechanosensors. Curr Biol 18, R860-862.

Knecht, D. A., and Loomis, W. F. (1987). Antisense RNA inactivation of myosin heavy chain gene expression in Dictyostelium discoideum. Science 236, 1081-1086.

Knecht, D. A., and Loomis, W. F. (1988). Developmental consequences of the lack of myosin heavy chain in Dictyostelium discoideum. Dev Biol 128, 178-184.

Koide, H., Kinoshita, T., Tanaka, Y., Tanaka, S., Nagura, N., Meyer zu Horste, G., Miyagi, A., and Ando, T. (2006). Identification of the single specific IQ motif of myosin V from which calmodulin dissociates in the presence of Ca2+. Biochemistry 45, 11598-11604.

Komatsu, S., Yano, T., Shibata, M., Tuft, R. A., and Ikebe, M. (2000). Effects of the regulatory light chain phosphorylation of myosin II on mitosis and cytokinesis of mammalian cells. J Biol Chem 275, 34512-34520.

Konishi, K., Kojima, S., Katoh, T., Yazawa, M., Kato, K., Fujiwara, K., and Onishi, H. (2001). Two new modes of smooth muscle myosin regulation by the interaction between the two regulatory light chains, and by the S2 domain. J Biochem 129, 365-372.

Kovacs, M., Thirumurugan, K., Knight, P. J., and Sellers, J. R. (2007). Load-dependent mechanism of nonmuscle myosin 2. Proc Natl Acad Sci U S A 104, 9994-9999.

Krementsov, D. N., Krementsova, E. B., and Trybus, K. M. (2004). Myosin V: regulation by calcium, calmodulin, and the tail domain. J Cell Biol 164, 877-886.

Kubalek, E. W., Uyeda, T. Q., and Spudich, J. A. (1992). A Dictyostelium myosin II lacking a proximal 58-kDa portion of the tail is functional in vitro and in vivo. Mol Biol Cell 3, 1455-1462.

Li, X. D., Jung, H. S., Mabuchi, K., Craig, R., and Ikebe, M. (2006). The globular tail domain of myosin Va functions as an inhibitor of the myosin Va motor. J Biol Chem 281, 21789-21798.

Li, X. D., Mabuchi, K., Ikebe, R., and Ikebe, M. (2004). Ca2+-induced activation of ATPase activity of myosin Va is accompanied with a large conformational change. Biochem Biophys Res Commun 315, 538-545.

Liu, J., Taylor, D. W., Krementsova, E. B., Trybus, K. M., and Taylor, K. A. (2006). Three-dimensional structure of the myosin V inhibited state by cryoelectron tomography. Nature 442, 208-211.

Liu, J., Wendt, T., Taylor, D., and Taylor, K. (2003). Refined model of the 10S conformation of smooth muscle myosin by cryo-electron microscopy 3D image reconstruction. J Mol Biol 329, 963-972.

Lu, H., Krementsova, E. B., and Trybus, K. M. (2006). Regulation of myosin V processivity by calcium at the single molecule level. J Biol Chem 281, 31987-31994.

Lupas, A. (1996). Coiled coils: new structures and new functions. Trends Biochem Sci 21, 375-382.

Manstein, D. J., and Hunt, D. M. (1995). Overexpression of myosin motor domains in Dictyostelium: screening of transformants and purification of the affinity tagged protein. J Muscle Res Cell Motil 16, 325-332.

Manstein, D. J., Ruppel, K. M., and Spudich, J. A. (1989a). Expression and characterization of a functional myosin head fragment in Dictyostelium discoideum. Science 246, 656-658.

Manstein, D. J., Titus, M. A., De Lozanne, A., and Spudich, J. A. (1989b). Gene replacement in Dictyostelium: generation of myosin null mutants. Embo J 8, 923-932.

Marston, S. B., and Taylor, E. W. (1980). Comparison of the myosin and actomyosin ATPase mechanisms of the four types of vertebrate muscles. J Mol Biol 139, 573-600.

Martens, J. C., and Radmacher, M. (2008). Softening of the actin cytoskeleton by inhibition of myosin II. Pflugers Arch 456, 95-100.

McLachlan, A. D., and Karn, J. (1982). Periodic charge distributions in the myosin rod amino acid sequence match cross-bridge spacings in muscle. Nature 299, 226-231.

Mehta, A. D., Rock, R. S., Rief, M., Spudich, J. A., Mooseker, M. S., and Cheney, R. E. (1999). Myosin-V is a processive actin-based motor. Nature 400, 590-593.

Mercer, J. A., Seperack, P. K., Strobel, M. C., Copeland, N. G., and Jenkins, N. A. (1991). Novel myosin heavy chain encoded by murine dilute coat colour locus. Nature 349, 709-713.

Nagasaki, A., Itoh, G., Yumura, S., and Uyeda, T. Q. (2002). Novel myosin heavy chain kinase involved in disassembly of myosin II filaments and efficient cleavage in mitotic dictyostelium cells. Mol Biol Cell 13, 4333-4342.

Nguyen, H., and Higuchi, H. (2005). Motility of myosin V regulated by the dissociation of single calmodulin. Nat Struct Mol Biol 12, 127-132.

Nock, S., Liang, W., Warrick, H. M., and Spudich, J. A. (2000). Mutational analysis of phosphorylation sites in the Dictyostelium myosin II tail: disruption of myosin function by a single charge change. FEBS Lett 466, 267-272.

O'Halloran, T. J., Ravid, S., and Spudich, J. A. (1990). Expression of Dictyostelium myosin tail segments in Escherichia coli: domains required for assembly and phosphorylation. J Cell Biol 110, 63-70.

Olivares, A. O., Chang, W., Mooseker, M. S., Hackney, D. D., and De La Cruz, E. M. (2006). The tail domain of myosin Va modulates actin binding to one head. J Biol Chem 281, 31326-31336.

Onishi, H., and Wakabayashi, T. (1982). Electron microscopic studies of myosin molecules from chicken gizzard muscle I: the formation of the intramolecular loop in the myosin tail. J Biochem 92, 871-879.

Parry, D. A. (1981). Structure of rabbit skeletal myosin. Analysis of the amino acid sequences of two fragments from the rod region. J Mol Biol 153, 459-464.

Pasternak, C., Spudich, J. A., and Elson, E. L. (1989). Capping of surface receptors and concomitant cortical tension are generated by conventional myosin. Nature 341, 549-551.

Peters, D. J., Knecht, D. A., Loomis, W. F., De Lozanne, A., Spudich, J., and Van Haastert, P. J. (1988). Signal transduction, chemotaxis, and cell aggregation in Dictyostelium discoideum cells without myosin heavy chain. Dev Biol 128, 158-163.

Pollard, T. D. (1981). Cytoplasmic contractile proteins. J Cell Biol 91, 156s-165s.

Pollard, T. D. (2000). Reflections on a quarter century of research on contractile systems. Trends Biochem Sci 25, 607-611.

Purcell, T. J., Sweeney, H. L., and Spudich, J. A. (2005). A force-dependent state controls the coordination of processive myosin V. Proc Natl Acad Sci U S A 102, 13873-13878.

Rayment, I. (1996). Kinesin and myosin: molecular motors with similar engines. Structure 4, 501-504.

Rayment, I., Rypniewski, W. R., Schmidt-Base, K., Smith, R., Tomchick, D. R., Benning, M. M., Winkelmann, D. A., Wesenberg, G., and Holden, H. M. (1993). Three-dimensional structure of myosin subfragment-1: a molecular motor. Science 261, 50-58.

Reck-Peterson, S. L., Provance, D. W., Jr., Mooseker, M. S., and Mercer, J. A. (2000). Class V myosins. Biochim Biophys Acta 1496, 36-51.

Rhoads, A. R., and Friedberg, F. (1997). Sequence motifs for calmodulin recognition. Faseb J 11, 331-340.

Ridley, A. J. (2001). Rho GTPases and cell migration. J Cell Sci 114, 2713-2722.

Rief, M., Rock, R. S., Mehta, A. D., Mooseker, M. S., Cheney, R. E., and Spudich, J. A. (2000). Myosin-V stepping kinetics: a molecular model for processivity. Proc Natl Acad Sci U S A 97, 9482-9486.

Robinson, D. N., and Spudich, J. A. (2004). Mechanics and regulation of cytokinesis. Curr Opin Cell Biol 16, 182-188.

Sabry, J. H., Moores, S. L., Ryan, S., Zang, J. H., and Spudich, J. A. (1997). Myosin heavy chain phosphorylation sites regulate myosin localization during cytokinesis in live cells. Mol Biol Cell 8, 2605-2615.

Sakamoto, T., Yildez, A., Selvin, P. R., and Sellers, J. R. (2005). Step-size is determined by neck length in myosin V. Biochemistry 44, 16203-16210.

Schott, D. H., Collins, R. N., and Bretscher, A. (2002). Secretory vesicle transport velocity in living cells depends on the myosin-V lever arm length. J Cell Biol 156, 35-39.

Sellers, J. R. (2000). Myosins: a diverse superfamily. Biochim Biophys Acta 1496, 3-22.

Sellers, J. R., and Knight, P. J. (2007). Folding and regulation in myosins II and V. J Muscle Res Cell Motil 28, 363-370.

Sellers, J. R., Pato, M. D., and Adelstein, R. S. (1981). Reversible phosphorylation of smooth muscle myosin, heavy meromyosin, and platelet myosin. J Biol Chem 256, 13137-13142.

Seow, C. Y. (2005). Myosin filament assembly in an ever-changing myofilament lattice of smooth muscle. Am J Physiol Cell Physiol 289, C1363-1368.

Shelden, E., and Knecht, D. A. (1996). Dictyostelium cell shape generation requires myosin II. Cell Motil Cytoskeleton 35, 59-67.

Shu, S., Lee, R. J., LeBlanc-Straceski, J. M., and Uyeda, T. Q. (1999). Role of myosin II tail sequences in its function and localization at the cleavage furrow in Dictyostelium. J Cell Sci 112 (Pt 13), 2195-2201.

Somlyo, A. V., Butler, T. M., Bond, M., and Somlyo, A. P. (1981). Myosin filaments have non-phosphorylated light chains in relaxed smooth muscle. Nature 294, 567-569.

Sweeney, H. L., Chen, L. Q., and Trybus, K. M. (2000). Regulation of asymmetric smooth muscle myosin II molecules. J Biol Chem 275, 41273-41277.

Sweeney, H. L., and Stull, J. T. (1990). Alteration of cross-bridge kinetics by myosin light chain phosphorylation in rabbit skeletal muscle: implications for regulation of actin-myosin interaction. Proc Natl Acad Sci U S A 87, 414-418.

Tan, J. L., Ravid, S., and Spudich, J. A. (1992). Control of nonmuscle myosins by phosphorylation. Annu Rev Biochem 61, 721-759.

Taylor, K. A. (2007). Regulation and recycling of myosin V. Curr Opin Cell Biol 19, 67-74.

Thirumurugan, K., Sakamoto, T., Hammer, J. A., 3rd, Sellers, J. R., and Knight, P. J. (2006). The cargo-binding domain regulates structure and activity of myosin 5. Nature 442, 212-215.

Thompson, R. F., and Langford, G. M. (2002). Myosin superfamily evolutionary history. Anat Rec 268, 276-289.

Trybus, K. M. (1989). Filamentous smooth muscle myosin is regulated by phosphorylation. J Cell Biol 109, 2887-2894.

Trybus, K. M. (1994). Role of myosin light chains. J Muscle Res Cell Motil 15, 587-594.

Trybus, K. M. (2008). Myosin V from head to tail. Cell Mol Life Sci 65, 1378-1389.

Trybus, K. M., Freyzon, Y., Faust, L. Z., and Sweeney, H. L. (1997). Spare the rod, spoil the regulation: necessity for a myosin rod. Proc Natl Acad Sci U S A 94, 48-52.

Trybus, K. M., Gushchin, M. I., Lui, H., Hazelwood, L., Krementsova, E. B., Volkmann, N., and Hanein, D. (2007). Effect of calcium on calmodulin bound to the IQ motifs of myosin V. J Biol Chem 282, 23316-23325.

Trybus, K. M., and Henry, L. (1989). Monoclonal antibodies detect and stabilize conformational states of smooth muscle myosin. J Cell Biol 109, 2879-2886.

Trybus, K. M., Huiatt, T. W., and Lowey, S. (1982). A bent monomeric conformation of myosin from smooth muscle. Proc Natl Acad Sci U S A 79, 6151-6155.

Trybus, K. M., and Lowey, S. (1984). Conformational states of smooth muscle myosin. Effects of light chain phosphorylation and ionic strength. J Biol Chem 259, 8564-8571.

Uyeda, T. Q., Abramson, P. D., and Spudich, J. A. (1996). The neck region of the myosin motor domain acts as a lever arm to generate movement. Proc Natl Acad Sci U S A 93, 4459-4464.

Vale, R. D., and Milligan, R. A. (2000). The way things move: looking under the hood of molecular motor proteins. Science 288, 88-95.

Veigel, C., Schmitz, S., Wang, F., and Sellers, J. R. (2005). Load-dependent kinetics of myosin-V can explain its high processivity. Nat Cell Biol 7, 861-869.

Vilfan, A. (2005). Elastic lever-arm model for myosin V. Biophys J 88, 3792-3805.

Wang, F., Chen, L., Arcucci, O., Harvey, E. V., Bowers, B., Xu, Y., Hammer, J. A., 3rd, and Sellers, J. R. (2000). Effect of ADP and ionic strength on the kinetic and motile properties of recombinant mouse myosin V. J Biol Chem 275, 4329-4335.

Wang, F., Kovacs, M., Hu, A., Limouze, J., Harvey, E. V., and Sellers, J. R. (2003). Kinetic mechanism of non-muscle myosin IIB: functional adaptations for tension generation and maintenance. J Biol Chem 278, 27439-27448.

Wang, F., Thirumurugan, K., Stafford, W. F., Hammer, J. A., 3rd, Knight, P. J., and Sellers, J. R. (2004). Regulated conformation of myosin V. J Biol Chem 279, 2333-2336.

Warrick, H. M., and Spudich, J. A. (1987). Myosin structure and function in cell motility. Annu Rev Cell Biol 3, 379-421.

Wendt, T., Taylor, D., Messier, T., Trybus, K. M., and Taylor, K. A. (1999). Visualization of head-head interactions in the inhibited state of smooth muscle myosin. J Cell Biol 147, 1385-1390.

Wendt, T., Taylor, D., Trybus, K. M., and Taylor, K. (2001). Three-dimensional image reconstruction of dephosphorylated smooth muscle heavy meromyosin reveals asymmetry in the interaction between myosin heads and placement of subfragment 2. Proc Natl Acad Sci U S A 98, 4361-4366.

Xu, X. S., Kuspa, A., Fuller, D., Loomis, W. F., and Knecht, D. A. (1996). Cell-cell adhesion prevents mutant cells lacking myosin II from penetrating aggregation streams of Dictyostelium. Dev Biol 175, 218-226.

Yamakita, Y., Yamashiro, S., and Matsumura, F. (1994). In vivo phosphorylation of regulatory light chain of myosin II during mitosis of cultured cells. J Cell Biol 124, 129-137.

Young, P. E., Richman, A. M., Ketchum, A. S., and Kiehart, D. P. (1993). Morphogenesis in Drosophila requires nonmuscle myosin heavy chain function. Genes Dev 7, 29-41.

Zang, J. H., Cavet, G., Sabry, J. H., Wagner, P., Moores, S. L., and Spudich, J. A. (1997). On the role of myosin-II in cytokinesis: division of Dictyostelium cells under adhesive and nonadhesive conditions. Mol Biol Cell 8, 2617-2629.

## Chapter II

1. Glotzer, M. (2005) *Science* **307**, 1735-1739

2. Robinson, D. N., and Spudich, J. A. (2004) *Curr Opin Cell Biol* **16**, 182-188

3. Goldman, Y. (2000) *Cell* **93**, 1-4

4. Pollard, T. D. (1981) *J. Cell Biol.* **91**, 156-165

5. Peng, C. Y., Manning, L., Albertson, R., and Doe, C. Q. (2000) *Nature* **408**, 596-600

6. Ohshiro, T., Yagami, T., Zhang, C., and Matsuzaki, F. (2000) *Nature* **408**, 593-596

7. Barros, C. S., Phelps, C. B., and Brand, A. H. (2003) *Dev Cell* **5**, 829-840

8. Guo, S., and Kemphues, K. J. (1996) *Nature* **382**, 455-458

9. Betschinger, J., and Knoblich, J. A. (2004) *Curr Biol* **14**, R674-685

10. O'Halloran, T. J., Ravid, S., and Spudich, J. A. (1990) *J Cell Biol* **110**, 63-70

11. Lee, R. J., Egelhoff, T. T., and Spudich, J. A. (1994) *J Cell Sci* **107** (Pt 10), 2875-2886

12. Shoffner, J. D., and De Lozanne, A. (1996) *Biochem Biophys Res Commun* **218**, 860-864

13. Hostetter, D., Rice, S., Dean, S., Altman, D., McMahon, P. M., Sutton, S., Tripathy, A., and Spudich, J. A. (2004) *PLoS Biol* 2, e356

14. Turbedsky, K., and Pollard, T. D. (2005) *J Mol Biol* **345**, 351-361

15. Nakasawa, T., Takahashi, M., Matsuzawa, F., Aikawa, S., Togashi, Y., Saitoh, T., Yamagishi, A., and Yazawa, M. (2005) *Biochemistry* **44**, 174-183

16. Sohn, R.L., Vikstrom, K.L., Strauss, M., Cohen, C., Szent-Gyorgyi, A. G. and Leinwand, L. A. (1997*) J. Mol. Biol.* **266**, 317-330

17. Liang, W., Warrick, H. M., and Spudich, J. A. (1999) *J Cell Biol* **147**, 1039-1048

18. Yumura, S., Yoshida, M., Betapudi, V., Licate, L. S., Iwadate, Y., Nagasaki, A., Uyeda, T. Q., and Egelhoff, T. T. (2005) *Mol Biol Cell* **16**, 4256-4266

19. Su, Z., and Kiehart, D. P. (2001) *Biochemistry* **40**, 3606-3614

20. Even-Faitelson, L., and Ravid, S. (2006) *Mol Biol Cell* **17**, 2869-2881

21. Severson, A. F., and Bowerman, B. (2003) *J Cell Biol* **161**, 21-26

22. Nance, J., Munro, E. M., and Priess, J. R. (2003) *Development* **130**, 5339-5350

23. Munro, E., Nance, J., and Priess, J. R. (2004) *Dev Cell* **7**, 413-424

24. Zang, J. H., and Spudich, J. A. (1998) *Proc Natl Acad Sci U S A* **95**, 13652-13657

25. Edwards, K. A., and Kiehart, D. P. (1996) *Development* **122**, 1499-1511

26. Wheatley, S., Kulkarni, S., and Karess, R. (1995) *Development* **121**, 1937-1946

27. Royou, A., Sullivan, W., and Karess, R. (2002) *J Cell Biol* **158**, 127-137

28. Royou, A., Field, C., Sisson, J. C., Sullivan, W., and Karess, R. (2004) *Mol Biol Cell* **15**, 838-850

29. Young, P. E., Richman, A. M., Ketchum, A. S., and Kiehart, D. P. (1993) *Genes Dev* **7**, 29-41

30. Peterson, F. C., Penkert, R. R., Volkman, B. F., and Prehoda, K. E. (2004) *Mol Cell* **13**, 665-676

31. Ikebe, M., Komatsu, S., Woodhead, J. L., Mabuchi, K., Ikebe, R., Saito, J., Craig, R., and Higashihara, M. (2001) *J. Biol. Chem.* **276**, 30293-30300

32. Frank, S., Lustig, A., Schulthess, T., Engel, J. and Kammerer, R. A. (2000*) J. Biol. Chem.* **275**, 11672-11677

33. Atkinson, S.J., Stewart M. (1992) *J Mol Biol* **226**, 7-13

34. Yumura, S. (2001) *J Cell Biol* **154**, 137-146

35. Dean, S. O., Rogers, S. L., Stuurman, N., Vale, R. D., and Spudich, J. A. (2005) *Proc Natl Acad Sci U S A* **102**, 13473-13478

36. Dean, S. and Spudich, J. A. (2006) *PLoS Biol* 1, e131

37. Murakami, N., Singh, S. S., Chauhan, V. P., and Elzinga, M. (1995) *Biochemistry* **34**, 16046-16055

38. Strand, D., Jakobs, R., Merdes, G., Neumann, B., Kalmes, A., Heid, H. W., Husmann, I., and Mechler, B. M. (1994) *J Cell Biol* **127**, 1361-1373

## Chapter III

Atkinson, S. J., and Stewart, M. (1991). Expression in Escherichia coli of fragments of the coiled-coil rod domain of rabbit myosin: influence of different regions of the molecule on aggregation and paracrystal formation. J Cell Sci 99 (Pt 4), 823-836.

Atkinson, S. J., and Stewart, M. (1992). Molecular interactions in myosin assembly. Role of the 28-residue charge repeat in the rod. J Mol Biol 226, 7-13.

Barylko, B., Dobrowolski, Z., and Karasinski, J. (1989). The assembly of the rod portion of brain myosin. Eur J Cell Biol 48, 264-270.

Bennett, P. M. (1981). The structure of spindle-shaped paracrystals of light meromyosin. J Mol Biol 146, 201-221.

Brown, J. H., Kim, K. H., Jun, G., Greenfield, N. J., Dominguez, R., Volkmann, N., Hitchcock-DeGregori, S. E., and Cohen, C. (2001). Deciphering the design of the tropomyosin molecule. Proc Natl Acad Sci U S A 98, 8496-8501.

Burkhard, P., Kammerer, R. A., Steinmetz, M. O., Bourenkov, G. P., and Aebi, U. (2000). The coiled-coil trigger site of the rod domain of cortexillin I unveils a distinct network of interhelical and intrahelical salt bridges. Structure 8, 223-230.

Burkhard, P., Stetefeld, J., and Strelkov, S. V. (2001). Coiled coils: a highly versatile protein folding motif. Trends Cell Biol 11, 82-88.

Chowrashi, P. K., and Pepe, F. A. (1977). Light meromyosin paracrystal formation. J Cell Biol 74, 136-152.

Cohen, C., and Parry, D. A. (1998). A conserved C-terminal assembly region in paramyosin and myosin rods. J Struct Biol 122, 180-187.

Craig, R., and Woodhead, J. L. (2006). Structure and function of myosin filaments. Curr Opin Struct Biol 16, 204-212.

Cross, R. A., Geeves, M. A., and Kendrick-Jones, J. (1991). A nucleation--elongation mechanism for the self-assembly of side polar sheets of smooth muscle myosin. Embo J 10, 747-756.

Cross, R. A., and Vandekerckhove, J. (1986). Solubility-determining domain of smooth muscle myosin rod. FEBS Lett 200, 355-360.

Glotzer, M. (2005). The molecular requirements for cytokinesis. Science 307, 1735-1739.

Hickson, G. R., Echard, A., and O'Farrell, P. H. (2006). Rho-kinase controls cell shape changes during cytokinesis. Curr Biol 16, 359-370.

Hodge, T., and Cope, M. J. (2000). A myosin family tree. J Cell Sci 113 Pt 19, 3353-3354.

Hodge, T. P., Cross, R., and Kendrick-Jones, J. (1992). Role of the COOH-terminal nonhelical tailpiece in the assembly of a vertebrate nonmuscle myosin rod. J Cell Biol 118, 1085-1095.

Hostetter, D., Rice, S., Dean, S., Altman, D., McMahon, P. M., Sutton, S., Tripathy, A., and Spudich, J. A. (2004). Dictyostelium myosin bipolar thick filament formation: importance of charge and specific domains of the myosin rod. PLoS Biol 2, e356.

Ikebe, M., Komatsu, S., Woodhead, J. L., Mabuchi, K., Ikebe, R., Saito, J., Craig, R., and Higashihara, M. (2001). The tip of the coiled-coil rod determines the filament formation of smooth muscle and nonmuscle myosin. J Biol Chem 276, 30293-30300.

Kendrick-Jones, J., Szent-Gyorgyi, A. S., and Cohen, C. (1971). Segments from vertebrate smooth muscle myosin rods. J Mol Biol 59, 527-529.

Kiehart, D. P., and Feghali, R. (1986). Cytoplasmic myosin from Drosophila melanogaster. J Cell Biol 103, 1517-1525.

Lee, R. J., Egelhoff, T. T., and Spudich, J. A. (1994). Molecular genetic truncation analysis of filament assembly and phosphorylation domains of Dictyostelium myosin heavy chain. J Cell Sci 107 (Pt 10), 2875-2886.

Liu, S. L., Fewkes, N., Ricketson, D., Penkert, R. R., and Prehoda, K. E. (2008). Filament-dependent and -independent localization modes of Drosophila non-muscle myosin II. J Biol Chem 283, 380-387.

Lowey, S., Slayter, H. S., Weeds, A. G., and Baker, H. (1969). Substructure of the myosin molecule. I. Subfragments of myosin by enzymic degradation. J Mol Biol 42, 1-29.

Lupas, A. (1996). Coiled coils: new structures and new functions. Trends Biochem Sci 21, 375-382.

Martens, J. C., and Radmacher, M. (2008). Softening of the actin cytoskeleton by inhibition of myosin II. Pflugers Arch 456, 95-100.

McLachlan, A. D., and Karn, J. (1982). Periodic charge distributions in the myosin rod amino acid sequence match cross-bridge spacings in muscle. Nature 299, 226-231.

McLachlan, A. D., and Stewart, M. (1975). Tropomyosin coiled-coil interactions: evidence for an unstaggered structure. J Mol Biol 98, 293-304.

Nakasawa, T., Takahashi, M., Matsuzawa, F., Aikawa, S., Togashi, Y., Saitoh, T., Yamagishi, A., and Yazawa, M. (2005). Critical regions for assembly of vertebrate nonmuscle myosin II. Biochemistry 44, 174-183.

Niederman, R., and Pollard, T. D. (1975). Human platelet myosin. II. In vitro assembly and structure of myosin filaments. J Cell Biol 67, 72-92.

Nyitray, L., Mocz, G., Szilagyi, L., Balint, M., Lu, R. C., Wong, A., and Gergely, J. (1983). The proteolytic substructure of light meromyosin. Localization of a region responsible for the low ionic strength insolubility of myosin. J Biol Chem 258, 13213-13220.

O'Halloran, T. J., Ravid, S., and Spudich, J. A. (1990). Expression of Dictyostelium myosin tail segments in Escherichia coli: domains required for assembly and phosphorylation. J Cell Biol 110, 63-70.

Offer, G. (1990). Skip residues correlate with bends in the myosin tail. J Mol Biol 216, 213-218.

Onishi, H., and Wakabayashi, T. (1984). Electron microscopic studies on myosin molecules from chicken gizzard muscle III. Myosin dimers. J Biochem 95, 903-905.

Parry, D. A. (1981). Structure of rabbit skeletal myosin. Analysis of the amino acid sequences of two fragments from the rod region. J Mol Biol 153, 459-464.

Peterson, F. C., Penkert, R. R., Volkman, B. F., and Prehoda, K. E. (2004). Cdc42 regulates the Par-6 PDZ domain through an allosteric CRIB-PDZ transition. Mol Cell 13, 665-676.

Pollard, T. D. (1981). Cytoplasmic contractile proteins. J Cell Biol 91, 156s-165s.

Ridley, A. J. (2001). Rho GTPases and cell migration. J Cell Sci 114, 2713-2722.

Robinson, D. N., and Spudich, J. A. (2004). Mechanics and regulation of cytokinesis. Curr Opin Cell Biol 16, 182-188.

Rosenberg, M., Straussman, R., Ben-Ya'acov, A., Ronen, D., and Ravid, S. (2008). MHC-IIB filament assembly and cellular localization are governed by the rod net charge. PLoS ONE 3, e1496.

Shelden, E., and Knecht, D. A. (1996). Dictyostelium cell shape generation requires myosin II. Cell Motil Cytoskeleton 35, 59-67.

Shoffner, J. D., and De Lozanne, A. (1996). Sequences in the myosin II tail required for self-association. Biochem Biophys Res Commun 218, 860-864.

Sinard, J. H., and Pollard, T. D. (1990). Acanthamoeba myosin-II minifilaments assemble on a millisecond time scale with rate constants greater than those expected for a diffusion limited reaction. J Biol Chem 265, 3654-3660.

Sinard, J. H., Stafford, W. F., and Pollard, T. D. (1989). The mechanism of assembly of Acanthamoeba myosin-II minifilaments: minifilaments assemble by three successive dimerization steps. J Cell Biol 109, 1537-1547.

Small, J. V., and Squire, J. M. (1972). Structural basis of contraction in vertebrate smooth muscle. J Mol Biol 67, 117-149.

Sohn, R. L., Vikstrom, K. L., Strauss, M., Cohen, C., Szent-Gyorgyi, A. G., and Leinwand, L. A. (1997). A 29 residue region of the sarcomeric myosin rod is necessary for filament formation. J Mol Biol 266, 317-330.

Straussman, R., Squire, J. M., Ben-Ya'acov, A., and Ravid, S. (2005). Skip residues and charge interactions in myosin II coiled-coils: implications for molecular packing. J Mol Biol 353, 613-628.

Su, Z., and Kiehart, D. P. (2001). Protein kinase C phosphorylates nonmuscle myosin-II heavy chain from Drosophila but regulation of myosin function by this enzyme is not required for viability in flies. Biochemistry 40, 3606-3614.

Trybus, K. M., and Lowey, S. (1984). Conformational states of smooth muscle myosin. Effects of light chain phosphorylation and ionic strength. J Biol Chem 259, 8564-8571.

Trybus, K. M., and Lowey, S. (1987). Assembly of smooth muscle myosin minifilaments: effects of phosphorylation and nucleotide binding. J Cell Biol 105, 3007-3019.

Turbedsky, K., and Pollard, T. D. (2005). Assembly of Acanthamoeba myosin-II minifilaments. Definition of C-terminal residues required to form coiled-coils, dimers, and octamers. J Mol Biol 345, 351-361.

Woodhead, J. L., Zhao, F. Q., Craig, R., Egelman, E. H., Alamo, L., and Padron, R. (2005). Atomic model of a myosin filament in the relaxed state. Nature 436, 1195-1199.

Young, P. E., Richman, A. M., Ketchum, A. S., and Kiehart, D. P. (1993). Morphogenesis in Drosophila requires nonmuscle myosin heavy chain function. Genes Dev 7, 29-41.

Zoghbi, M. E., Woodhead, J. L., Moss, R. L., and Craig, R. (2008). Three-dimensional structure of vertebrate cardiac muscle myosin filaments. Proc Natl Acad Sci U S A 105, 2386-2390.

## Chapter IV

Atkinson, S. J., and Stewart, M. (1991). Expression in Escherichia coli of fragments of the coiled-coil rod domain of rabbit myosin: influence of different regions of the molecule on aggregation and paracrystal formation. J Cell Sci 99 (Pt 4), 823-836.

Atkinson, S. J., and Stewart, M. (1992). Molecular interactions in myosin assembly. Role of the 28-residue charge repeat in the rod. J Mol Biol 226, 7-13.

Bement, W. M., Mandato, C. A., and Kirsch, M. N. (1999). Wound-induced assembly and closure of an actomyosin purse string in Xenopus oocytes. Curr Biol 9, 579-587.

Breckenridge, M. T., Dulyaninova, N. G., and Egelhoff, T. T. (2009). Multiple regulatory steps control mammalian nonmuscle myosin II assembly in live cells. Mol Biol Cell 20, 338-347.

Burgess, S. A., Yu, S., Walker, M. L., Hawkins, R. J., Chalovich, J. M., and Knight, P. J. (2007). Structures of smooth muscle myosin and heavy meromyosin in the folded, shutdown state. J Mol Biol 372, 1165-1178.

Cohen, C., and Parry, D. A. (1998). A conserved C-terminal assembly region in paramyosin and myosin rods. J Struct Biol 122, 180-187.

Craig, R., and Woodhead, J. L. (2006). Structure and function of myosin filaments. Curr Opin Struct Biol 16, 204-212.

Cross, R. A., Geeves, M. A., and Kendrick-Jones, J. (1991). A nucleation--elongation mechanism for the self-assembly of side polar sheets of smooth muscle myosin. Embo J 10, 747-756.

Cross, R. A., and Vandekerckhove, J. (1986). Solubility-determining domain of smooth muscle myosin rod. FEBS Lett 200, 355-360.

Edwards, K. A., and Kiehart, D. P. (1996). Drosophila nonmuscle myosin II has multiple essential roles in imaginal disc and egg chamber morphogenesis. Development 122, 1499-1511.

Egelhoff, T. T., Lee, R. J., and Spudich, J. A. (1993). Dictyostelium myosin heavy chain phosphorylation sites regulate myosin filament assembly and localization in vivo. Cell 75, 363-371.

Glotzer, M. (2005). The molecular requirements for cytokinesis. Science 307, 1735-1739.

Hickson, G. R., Echard, A., and O'Farrell, P. H. (2006). Rho-kinase controls cell shape changes during cytokinesis. Curr Biol 16, 359-370.

Hodge, T. P., Cross, R., and Kendrick-Jones, J. (1992). Role of the COOH-terminal nonhelical tailpiece in the assembly of a vertebrate nonmuscle myosin rod. J Cell Biol 118, 1085-1095.

Ikebe, M., Komatsu, S., Woodhead, J. L., Mabuchi, K., Ikebe, R., Saito, J., Craig, R., and Higashihara, M. (2001). The tip of the coiled-coil rod determines the filament formation of smooth muscle and nonmuscle myosin. J Biol Chem 276, 30293-30300.

Kendrick-Jones, J., Szent-Gyorgyi, A. S., and Cohen, C. (1971). Segments from vertebrate smooth muscle myosin rods. J Mol Biol 59, 527-529.

Liu, S. L., Fewkes, N., Ricketson, D., Penkert, R. R., and Prehoda, K. E. (2008). Filament-dependent and -independent localization modes of Drosophila non-muscle myosin II. J Biol Chem 283, 380-387.

Lowey, S., Slayter, H. S., Weeds, A. G., and Baker, H. (1969). Substructure of the myosin molecule. I. Subfragments of myosin by enzymic degradation. J Mol Biol 42, 1-29.

Martens, J. C., and Radmacher, M. (2008). Softening of the actin cytoskeleton by inhibition of myosin II. Pflugers Arch 456, 95-100.

Nakasawa, T., Takahashi, M., Matsuzawa, F., Aikawa, S., Togashi, Y., Saitoh, T., Yamagishi, A., and Yazawa, M. (2005). Critical regions for assembly of vertebrate nonmuscle myosin II. Biochemistry 44, 174-183.

Niederman, R., and Pollard, T. D. (1975). Human platelet myosin. II. In vitro assembly and structure of myosin filaments. J Cell Biol 67, 72-92.

Nyitray, L., Mocz, G., Szilagyi, L., Balint, M., Lu, R. C., Wong, A., and Gergely, J. (1983). The proteolytic substructure of light meromyosin. Localization of a region responsible for the low ionic strength insolubility of myosin. J Biol Chem 258, 13213-13220.

Offer, G. (1990). Skip residues correlate with bends in the myosin tail. J Mol Biol 216, 213-218.

Pollard, T. D. (1981). Cytoplasmic contractile proteins. J Cell Biol 91, 156s-165s.

Ridley, A. J. (2001). Rho GTPases and cell migration. J Cell Sci 114, 2713-2722.

Robinson, D. N., and Spudich, J. A. (2004). Mechanics and regulation of cytokinesis. Curr Opin Cell Biol 16, 182-188.

Rosenberg, M., Straussman, R., Ben-Ya'acov, A., Ronen, D., and Ravid, S. (2008). MHC-IIB filament assembly and cellular localization are governed by the rod net charge. PLoS ONE 3, e1496.

Sellers, J. R. (2000). Myosins: a diverse superfamily. Biochim Biophys Acta 1496, 3-22.

Sellers, J. R., and Knight, P. J. (2007). Folding and regulation in myosins II and V. J Muscle Res Cell Motil 28, 363-370.

Shelden, E., and Knecht, D. A. (1996). Dictyostelium cell shape generation requires myosin II. Cell Motil Cytoskeleton 35, 59-67.

Sohn, R. L., Vikstrom, K. L., Strauss, M., Cohen, C., Szent-Gyorgyi, A. G., and Leinwand, L. A. (1997). A 29 residue region of the sarcomeric myosin rod is necessary for filament formation. J Mol Biol 266, 317-330.

Su, Z., and Kiehart, D. P. (2001). Protein kinase C phosphorylates nonmuscle myosin-II heavy chain from Drosophila but regulation of myosin function by this enzyme is not required for viability in flies. Biochemistry 40, 3606-3614.

Trybus, K. M., and Lowey, S. (1984). Conformational states of smooth muscle myosin. Effects of light chain phosphorylation and ionic strength. J Biol Chem 259, 8564-8571.

Trybus, K. M., and Lowey, S. (1987). Assembly of smooth muscle myosin minifilaments: effects of phosphorylation and nucleotide binding. J Cell Biol 105, 3007-3019.

Warrick, H. M., and Spudich, J. A. (1987). Myosin structure and function in cell motility. Annu Rev Cell Biol 3, 379-421.

Woodhead, J. L., Zhao, F. Q., Craig, R., Egelman, E. H., Alamo, L., and Padron, R. (2005). Atomic model of a myosin filament in the relaxed state. Nature 436, 1195-1199.

Young, P. E., Richman, A. M., Ketchum, A. S., and Kiehart, D. P. (1993). Morphogenesis in Drosophila requires nonmuscle myosin heavy chain function. Genes Dev 7, 29-41.

Zang, J. H., and Spudich, J. A. (1998). Myosin II localization during cytokinesis occurs by a mechanism that does not require its motor domain. Proc Natl Acad Sci U S A 95, 13652-13657.

Zoghbi, M. E., Woodhead, J. L., Moss, R. L., and Craig, R. (2008). Three-dimensional structure of vertebrate cardiac muscle myosin filaments. Proc Natl Acad Sci U S A 105, 2386-2390.